Aus der
Kinderklinik und Kinderpoliklinik im Dr. von Haunerschen Kinderspital
Klinikum der Ludwig-Maximilians-Universität München

The role of the CD200/CD200 receptor axis on CAR T cells against paediatric acute lymphoblastic B-lineage leukaemia

Dissertation
zum Erwerb des Doktorgrades der Medizin
an der Medizinischen Fakultät der
Ludwig-Maximilians-Universität München

vorgelegt von

Wyona Claire Mate
aus
München

Jahr

2025

Mit Genehmigung der Medizinischen Fakultät der
Ludwig-Maximilians-Universität zu München

Erstes Gutachten:	*Prof. Dr. Tobias Feuchtinger*
Zweites Gutachten:	*Prof. Dr. Sebastian Kobold*
Drittes Gutachten:	*Prof. Dr. Tobias Herold*

Dekan: Prof. Dr. med. Thomas Gudermann

Tag der mündlichen Prüfung: 27.11.2025

Für meine Liebsten

„Die Normalität ist eine gepflasterte Straße: man kann gut darauf gehen - doch es wachsen keine Blumen auf ihr.“ – Vincent van Gogh

Abstract

Acute lymphoblastic leukaemia represents the most frequent malignancy in childhood. Despite impressive progress in the treatment of this disease, the long-term outcome for children suffering from primary therapy failure or relapse is still unsatisfying. Over the past few years, chimeric antigen receptor (CAR) T cells have proven to be as an auspicious approach in the fight of primary refractory or relapsed paediatric leukaemia. But even though CAR T cells archived high initial responds rates, most patients missed long-term remissions, making CAR T cells perfectible. It is known that cancer cells have the potential to create an immunosuppressive micromilieu by interacting with their environment. The immunoregulatory CD200/CD200 receptor (CD200R) axis is considered to play a crucial role in this interaction. As CD200 is abundantly expressed on leukaemic blasts, we aimed to investigate the implications of CD200 expressing acute B cell lymphoblastic leukaemia on immune cells. Therefore, we performed co-culture experiments of leukaemic cells lines and different immune cells including T cells, CAR T cells, macrophages and dendritic cells. We found that CD200 on B cell leukaemic blasts directly inhibit T cell and CAR T cell functionality *in vitro* depending on CD200R density and level of activation. Additionally, we developed two potent attempts of overcoming CD200 induced CAR T cell impairment: CD200R knock-out CAR T cells and CD200R-CD28 fusion receptor CAR T cells. All in all, we gained better understanding of the CD200-mediated interaction between leukaemic blasts and immune cells allowing us to enhance CAR T cell therapy for primary refractory or relapsed acute lymphoblastic leukaemia.

Table of content

Table of figures

Table index

List of abbreviations

Table 1: List of abbreviations

Abbreviation	Name
ALL	Acute lymphoblastic leukaemia
AML	Acute myeloid leukaemia
APC	Antigen-presenting cell
B-ALL	B cell precursor ALL
BiTE	Bi-specific T cell engager Blinatumomab.
CAR	Chimeric antigen receptor
CD	Cluster of differentiation
CD200R	CD200 receptor
CLL	Chronic lymphocytic leukaemia
$_{CR}CD200R^{KO}$	T cells with CD200R knock-out
$_{CR}$Control	CRISPR/Cas9 control T cells
CRISPR	Clustered Regularly Interspaced Short Palindromic Repeats
CRS	Cytokine release syndrome
CTLA-4	Cytotoxic T-lymphocyte-associated protein 4
DC	Dendritic cells
DMSO	Dimethyl sulfoxide
DNA	Deoxyribonucleic acid
E:T ratio	Effector to target ratio
EC	Extracellular
EGF	Epidermal growth factor
EMA	European Medicines Agency
FACS	Fluorescence-activated cell sorting
FasL	Fas ligand
FC	Fold change
FDA	Food and Drug Administration
FSB	Fetal bovine serum
GMP	Good manufacturing practice
HEPES	Hydroxyethyl piperazineethanesulfonic acid
HLA-DR	Human leukocyte antigen – DR isotype
HSA	Human serum albumin
IC	Intracellular
IDO	indoleamine 2,3-dioxygenase
IFN-γ	Interferon gamma
IL	Interleukin
ITAM	immunoreceptor tyrosine-based activation motif
LAG-3	Lymphocyte-activation gene 3
LME	Leukaemia associated macrophages
LPS	Lipopolysaccharides
MDS	myelodysplastic syndrome
MDSC	Myeloid derived suppressor cells
MFI	Median fluorescent intensity
MLR	Mixed lymphocyte reactions
Mϕ	Macrophages
n	Number of independent experiments
NK cell	Natural killer cell
NK T cells	Natural killer T cells

Abbreviation	Name
PBMC	Peripheral blood mononuclear cell
PBS	Phosphate buffer saline
PCR	Polymerase chain reaction
PD-1	Programmed cell death 1
PD-L1	Programmed cell death ligand 1
RNP	Ribonucleoprotein
RPMI	Roswell Park Memorial Institute
$_{RV}$19-BBz	Conventional second generation CAR T cells
$_{RV}$19-BBz$_{CR}$CD200R^{KO}	Second generation CAR T cells with CD200R knock-out
$_{RV}$19-BBz$_{CR}$Control	CRISPR/Cas9 control second generation CAR T cells
$_{RV}$19-BBz$_{RV}$CD200R-CD28	Second generation CAR T cell with CD200R-CD28 fusion receptor
$_{RV}$19-BBz$_{RV}$CD200R-Iso4^{OE}	Second generation CAR T cells with CD200R isoform 4 overexpression
$_{RV}$19-z	Conventional first generation CAR T cells
$_{RV}$19-z$_{RV}$CD200R-CD28	First generation CAR T cell with CD200R-CD28 fusion receptor
$_{RV}$CD200R-Iso1^{OE}	T cells with CD200R isoform 1 overexpression
$_{RV}$CD200R-Iso4^{OE}	T cells with CD200R isoform 4 overexpression
ScFv	Single chain variable fragment
SD	Standard deviation
SEB	Staphylococcus enterotoxin B
SSC	Side scatter
TAM	Tumour associated macrophages
T_{CM}	Central memory T cells
T_{EFF}	Effector T cells
T_{EM}	Effector memory T cells
Th1	Type 1 T helper cell
Th2	Type 2 T helper cell
TIM-3	T-cell immunoglobulin and mucin domain 3
TM	Transmembrane
TME	Tumour microenvironment
T_N	Naïve T cells
TNF-α	Tumour necrosis factor alpha
Treg	Regulatory T cells
T_{SCM}	Stem cell-like memory
VEGF	Vascular endothelial growth factor
VH	Variable heavy chain
VL	Variable light chain
WT	Wild type

Nomenclature

Genetic modified T cells are named after the following method:

i. Method of genetic modification in abbreviation in subscript in front of the modified protein.
   - rv: retroviral transduction
   - cr: CRISPR/ Cas9 mediated

ii. Type of modification in abbreviation as superscript behind the modified protein.
   - OE: overexpression
   - KO: knock-out

iii. Underscore is used to separate different modifications. The chronological sequence of the modifications is noted.

1 Introduction

1.1 Acute lymphoblastic leukaemia

Acute lymphoblastic leukaemia (ALL) is the most prevalent cancer in childhood, accounting for around 25 % of all malignancies [1, 2]. 98 % of all ALL cases have their origin in a mutation of precursor cells of the lymphoid cell line [1]. Depending on the affected cell line, ALL is differentiated into B or T cell ALL, which occur in a ratio of 85 to 15 [3]. The mutation results in an uncontrolled growth of immature lymphoblastic cells (blasts), which displace the normal haematopoiesis in the bone marrow and infiltrate the peripheral blood and extramedullary organs. The consequences are anaemia, unusual susceptibility for bleeding and immunodeficiency. Untreated, acute lymphoblastic leukaemia is lethal within months [3, 4]. Fortunately, constant progress in therapy increased the survival probabilities steadily from around 10 % in the 1960s up to 90 % nowadays [1, 5]. The standard therapy of ALL include intensive, modern polychemotherapy, which can be escalated by cranial radiation and/ or stem cell transplantation [6].

In contrast to these encouraging results, up to 20 % of paediatric ALL patients are primary refractory to standard therapy or relapse after successful initial treatment [7-9]. Despite escalated therapy, the prognosis for those children is still bad and gets worse with each subsequent relapse [9, 10]. All in all, only around one third of these children can be cured [10-13] (Figure 1). Due to the large number of cases, ALL is associated with more deaths than any other malignancy in childhood [1]. These low survival probabilities highlight that conventional treatment options are exhausted at this stage of disease. New therapeutic alternatives are therefore urgently needed for the treatment of relapsing and refractory ALL. At this point, targeted immunotherapy represents a novel and promising approach. For instance, T cells expressing a chimeric antigen receptor (CAR) have already shown great success in numerous studies in the treatment of severely pre-treated patients [14]. In 2017, the anti-CD19 CAR tisagenlecleucel was approved by the United States Food and Drug Administration (FDA) for the therapy of relapsed or refractory paediatric B-ALL patients, being the first drug ever for gene therapy in the United States [15]. The approval of the European Medicines Agency (EMA) for the European market followed in 2018 [16].

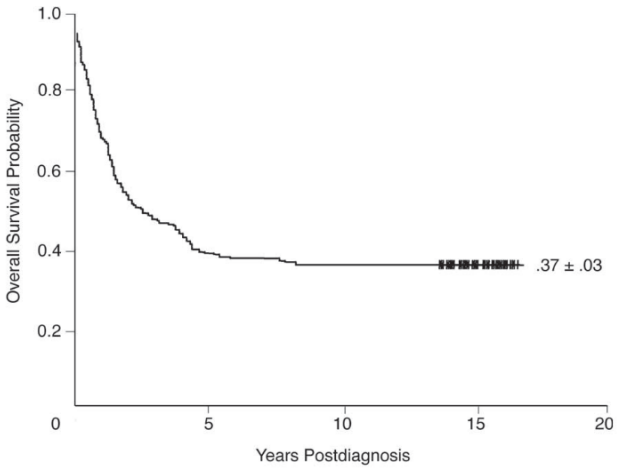

Figure 1: Overall survival probability after first relapse
37 % of 207 children with first relapse of ALL, enrolled in a multicentre trial, archived long term survival after risk-adapted therapy. Figure adapted from Einsiedel et al., 2005 with permission of the publisher.

1.2 CAR T cell therapy

The basic idea behind CAR T cell therapy is to redirect the patient's own T cells against tumour cells by equipping them with an antigen specific receptor (Figure 2). Therefore, peripheral blood mononuclear cells (PBMCs) are extracted from the patient's blood and T cells are isolated. In a next step, the expression of a recombinant receptor – the CAR– is induced by retro- or lentiviral transduction. At the end, the final CAR T cell product is intravenously reinfused into the patient [17, 18].

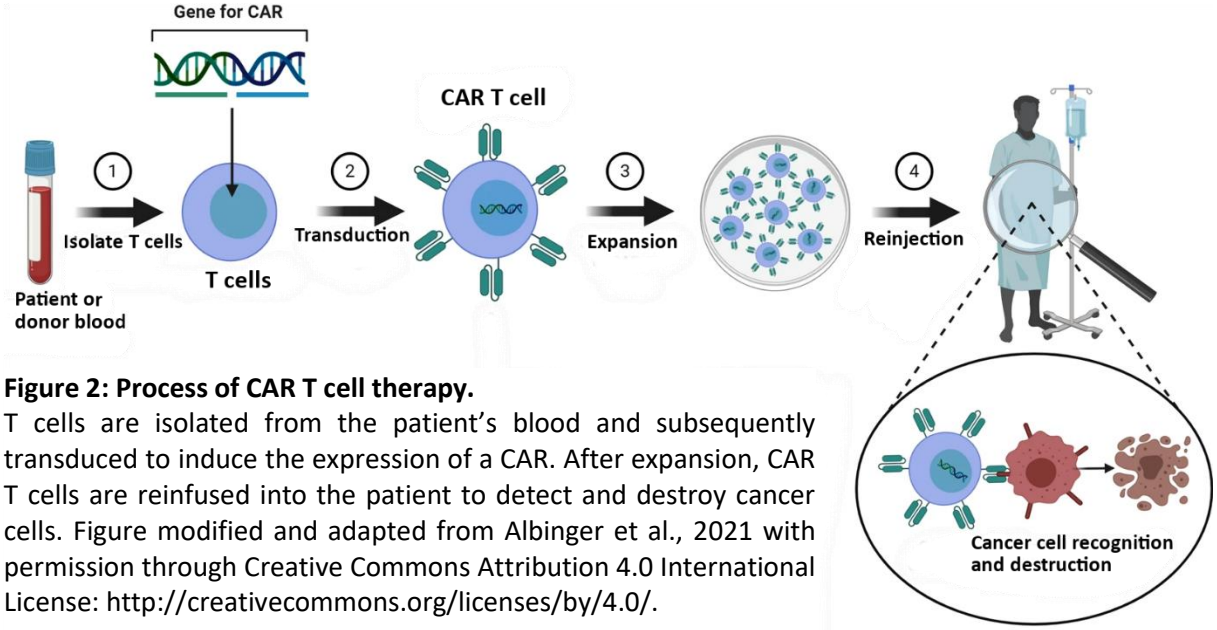

Figure 2: Process of CAR T cell therapy.
T cells are isolated from the patient's blood and subsequently transduced to induce the expression of a CAR. After expansion, CAR T cells are reinfused into the patient to detect and destroy cancer cells. Figure modified and adapted from Albinger et al., 2021 with permission through Creative Commons Attribution 4.0 International License: http://creativecommons.org/licenses/by/4.0/.

CARs possess an extracellular chimeric single chain variable fragment (scFv) as antigen-binding domain (Figure 3). The scFv is reminiscent of the variable regions of a monoclonal antibody. It consists of a variable light (VL) and heavy (VH) chain linked together resulting in antigen-specificity. The extracellular domain is connected by a hinge region to a transmembrane and intracellular T cell activating signalling domain. While first generation CARs only have CD3ζ as intracellular signalling domain, second and third generation CARs have additional costimulatory molecules, such as 4-1BB or CD28, which lead to increased T cell activation [19-21]. Engagement of the CAR with its specific antigen leads to activation and thus to proliferation and differentiation of

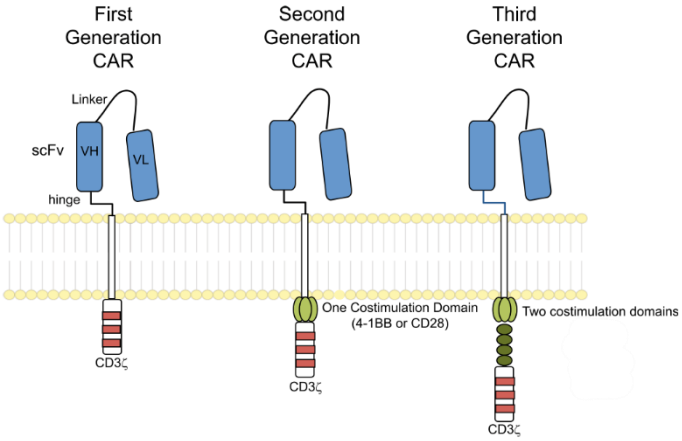

Figure 3: Chimeric antigen receptor design.
CARs consist of an extracellular binding domain, a transmembrane and an intracellular domain. Depending on the number of intracellular co-stimulatory molecules, different generation of CARs are distinguished. Figure adapted from Maus et al., 2014 with permission of the publisher.

the T cell. For anti-tumour therapy CARs directed against tumour-specific surface proteins are used. Various advantages, such as independence from major histocompatibility complex, increased reservoir of potential targets, and tumour specificity make CAR T cells particularly attractive as a new therapeutic approach [19-21].

Studies have shown encouraging results using CD19-specific CAR T cells in the therapy of refractory or relapsing paediatric B-ALL. CD19 is a surface molecule specifically found on B cells and their pre-cursors. It represents the target antigen for the majority of CAR T cell studies. Anagnostou et al. analysed 23 clinical trials in a meta-analysis and revealed that 81 % of all paediatric patients suffering from refractory or relapsing B-ALL achieved complete remission after anti-CD19 CAR T cell therapy. Despite high initial respond rates, a large proportion of children developed another relapse of the underlying disease [14]. For instance, Maude et al. and Gardner et al. reported initial complete remission of 90 % and 93 %, whereas the progression free survival after one year of CAR T cell therapy was at 47 % and 51 % [22, 23]. These findings emphasise that further studies are needed to improve the durability of CAR T cell-induced remissions.

1.3 Tumour escape mechanisms under CAR T cell therapy

1.3.1 CD19 negative relapse

Failure of anti-CD19 CAR T cell therapy can be mainly divided into CD19 negative or positive relapse [24]. CD19 negative relapse is characterised by loss or downregulation of CD19. Alternative splicing and mutations of the CD19 gene as well as lineage switch of B-ALL into a myeloid cell line are found as underlying mechanisms for anti-CD19 CAR T cell resistance [25-29]. Consequently, new targets for CAR T cells are under evaluation. Anti-CD22 CAR T cells proved to be safe and were able to induce high remission rates in B-ALL [30, 31]. Other efforts include the generation of dual targeting CAR T cells, like the bi-specific CD19/CD22 CAR or the co-infusion of anti-CD19 CAR T cells and anti-CD22 CAR T cells to overcome antigen escape [32, 33]. But Fry et al. showed that relapses because of antigen downregulation following CAR T cell therapies occurred for CD22 as well as for CD19 [30]. Thus, it is debatable if multi-specific targeting is the definitive solution for antigen escape [29, 34].

1.3.2 CD19 positive relapse

CD19 positive relapse is associated with early dysfunction and loss of anti-CD19 CAR T cells. Prolonged persistence is crucial for long-term tumour surveillance [22, 23, 34]. Gardner et al. found out that the loss of functional CAR T cells enhanced the risk for CD19 positive leukaemic relapse [23]. It is discussed that issues in the manufacturing process, quality of T cells, CAR design and initial phenotype of CAR T cells have impact on CAR T cell functionality [24].

1.3.3 Direct and indirect immunosuppressive effects through leukaemic cells

In addition to the aspects already mentioned, direct or indirect immunosuppressive effects through leukaemic cells might lead to leukaemic relapse (Figure 4) [35]. Under physiological conditions the interaction of stimulatory and inhibitory ligands through receptors on immune cells, called checkpoints, ensures balance between inflammation and immunosuppression. This is essential for an effective immune response against pathogens while minimizing collateral tissue damage. Cancer cells, like non-small cell lung cancer and ovarian cancer, are able to mimic this physiological regulation to escape the immune system [36-39]. This pathology is exploited for the design of new strategies in cancer therapy. Drugs against the checkpoints programmed death protein 1 (PD-1) and cytotoxic T-lymphocyte-associated protein 4 (CTLA-4) are already in clinical use and show impressive results by increasing T cell activity. For example, the CTLA-4 antibody ipilimumab enables long-term survival in stage IV melanoma for the first time [40].

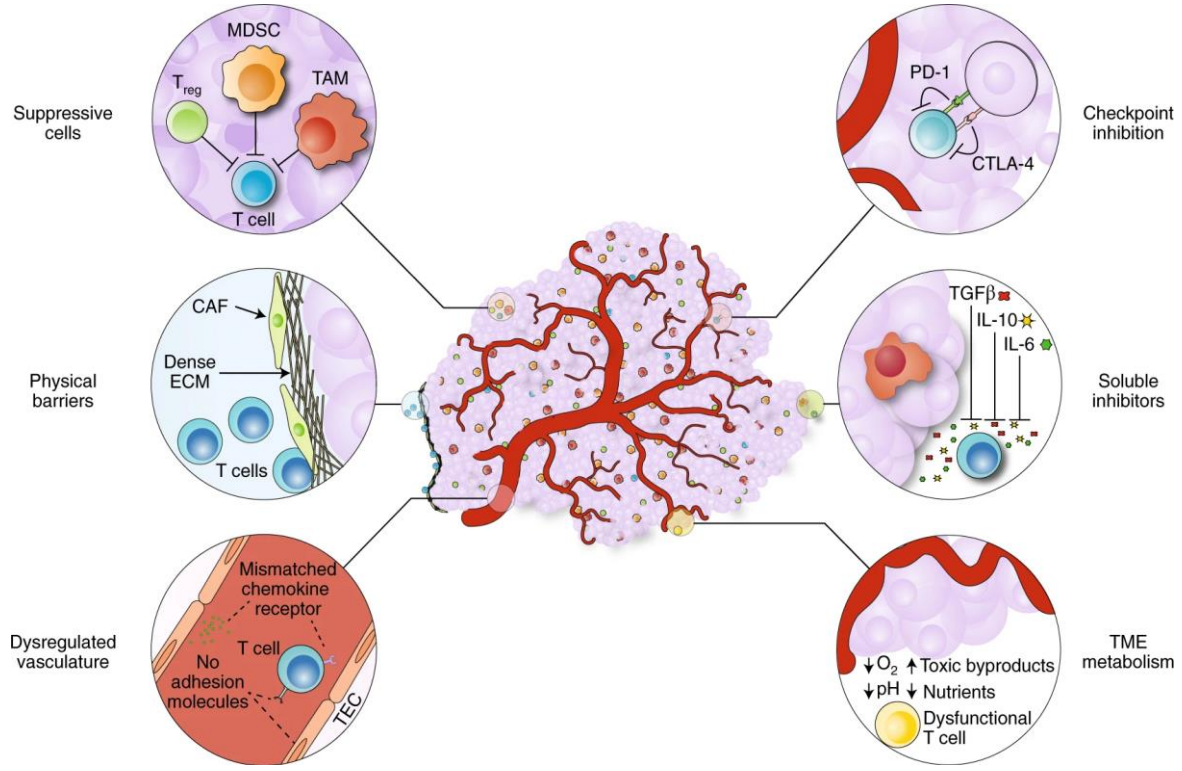

Figure 4: Mechanism of tumour escape

Tumour cells are able to create a tumour growth supporting micromilieu through the induction of suppressive bystander cells, like Treg cells, MDSC and TAMs, which inhibit T cell activation. T cell effector function can be further suppressed by the expression of checkpoint receptors (e.g., PD-1 and CTLA-4) or the release of soluble molecules (e.g., TGF-β, IL-10 and IL-6). T cell recruitment can be obstructed by physical barriers and dysregulated blood vessels. In addition, cancer cells can form an unfavourable metabolic milieu for T cells. Figure adapted from Labanieh et al., 2018 with permission of the publisher.

Apart from interaction with T cells, cancer cells are also able to communicate with other cells through the expression of stimulatory and inhibitory molecules and the release of different cytokines. Within the tumour microenvironment (TME) cancer cells can interact with blood

vessels, bystander cells including macrophages, dendritic cells (DCs) and fibroblasts, as well as soluble molecules and the extracellular matrix. Thus, cancer cells have the potential to create a milieu which acts immunosuppressive and supports tumour growth [41, 42].

Dendritic cells are crucial for an effective anti-tumour response in solid cancers [43]. DCs represents a heterogenic group of antigen-presenting cells, which collect, process and present antigens to T cells. Thus, DCs can induce peripheral immune tolerance against endogenous tissues or activate T cells against exogenous antigens [44]. In context of cancer, DCs are able to recruit and prime anti-tumour T cells by presenting tumour-specific antigens. But the immunostimulatory capacity of DCs can be diminished and even lead to immunotolerance in the TME through the interference of DC recruitment, activation and phenotype. For example, different cancer cells can inhibit DC maturation by secreting soluble factors, like interleukin 6, and thus induce tolerogenic DCs [43, 45, 46].

Macrophages represent important cells of the innate immune system. They are involved in phagocytosis of apoptotic cells and pathogens, wound repair and induction of inflammation or immunosuppression. In addition, through the presentation of processed antigens to T cells they play a role in the adaptive immune system [47]. Macrophages display high plasticity and various forms of phenotypes, in terms of biochemistry, morphology and function, depending on the local microenvironment. Thus, macrophages have the potential to adapt to changing circumstances [48, 49]. Macrophages are divided into M1 and M2 macrophages according to their reaction to external stimuli [50]. Because M1 macrophages induce a strong type 1 T helper cell (Th1) response, they are considered to support inflammation, anti-tumour response and pathogen elimination. In contrast, M2 macrophages are regarded to promote anti-inflammatory responses and tissue repair [51]. Macrophages represent a crucial element of the TME. Recruited and affected by the TME, they are important for tumour progression, migration and angiogenesis through the secretion of different growth factors like vascular endothelial growth factor (VEGF) and epidermal growth factor (EGF) [52-55]. Tumour-associated macrophages (TAMs) are related to a M2-like immunosuppressive phenotype [56, 57]. M2-like TAMs are associated with diminished T cell activation and poorer prognosis in various cancer identities, for example breast cancer or AML [53, 54, 58].

For leukaemia, the mechanisms of tumour escape are yet to be clarified, especially in terms of paediatric B-ALL. Leukaemic cells are considered to reprogram the bone marrow's and the blood's micromilieu into an immunosuppressive leukaemic microenvironment (LME), which support leukaemic endurance [59, 60]. Feucht et al. showed that the expression pattern of signal molecules on paediatric B-ALL blasts differs significantly from that of healthy B cells. Thus, leukaemic blasts, like other malignancies, have the capability to evade detection by T cells through the expression of inhibitory checkpoint molecules [61].

1.4 The CD200/CD200R axis

CAR T cells, like normal T cells, are affected by cancer cells or their microenvironment [62]. It is indispensable to rule out the exact impact of leukaemic blasts on CAR T cells to improve CAR T cell therapy and to ensure long-term benefit. Here we investigate the induction of a leukaemic microenvironment through the immunoregulatory axis of CD200/CD200 receptor.

CD200 is a type 1 transmembrane glycoprotein consisting of extracellular, transmembrane and a short cytoplasmic domain with no known signalling motifs [63, 64]. It is found on hematopoietic cells, like B and T cells, as well as on tissue cells, like thymocytes, kidney glomeruli, neurons, the syncytiotrophoblast and endothelial cells [65]. In contrast to this wide distribution, the expression of the corresponding CD200 receptor (CD200R) is limited to myeloid cells, like macrophages and dendritic cells, NK cells, B cells and T cells [66]. CD200R is a type 1 transmembrane glycoprotein. It contains two V/C2 configurated immunoglobulin fold-family domains, which are linked through a transmembrane domain to a cytoplasmatic domain. In the intracellular domain three tyrosine residues, one of which includes a NPXY motif but no ITAMs, could be found [67]. The CD200R gene consists of nine exons, which can be differently arranged through alternative splicing, resulting in four isoforms. Isoform 4 represents the full-length transmembrane glycoprotein, while isoform 1 is shortened by skipping exon 2. Additionally, for each isoform a truncated soluble form, isoform 2 and 3, exist. Until now, the impact of exon 2 is unknown. Different binding activities for isoform 1 and 4 are discussed, but need further investigations [67].

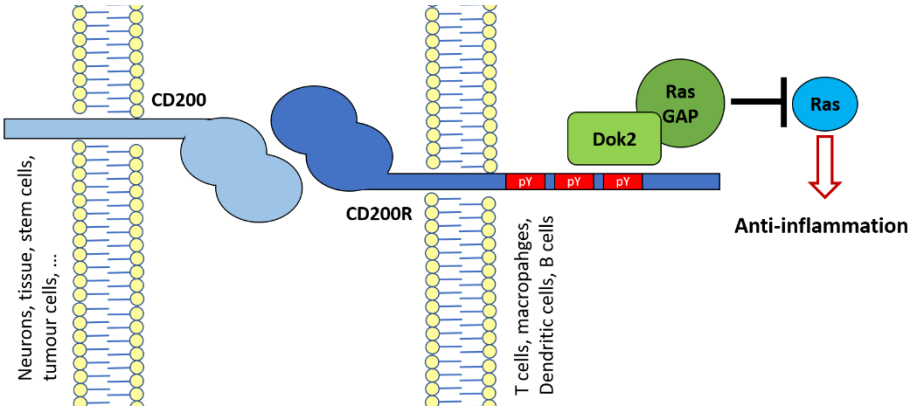

Figure 5: Distribution and signalling pathway of the CD200/CD200R axis
Engagement of CD200 and CD200R lead to the recruitment of Dok2 and RasGAP to the intracellular domain of CD200R, which result in anti-inflammatory effects. Figure redrawn and modified from Rygiel et al., 2012.

CD200 exclusively binds CD200R (Figure 5) [68]. In myeloid cells, engagement of receptor and ligand lead to recruitment of Dok2 and RasGAP and thereby to inhibition of the Ras/MAPK signal pathway [69]. For lymphoid cells, the intracellular signalling pathway is yet to be clarified. All in all, the CD200/CD200R axis results in inhibition of myeloid and lymphocyte activation, indicating that it works as a checkpoint molecule.

It is believed that immunologically privileged cells use CD200 to protect themselves from excessive immune response [65]. Experiments showed that CD200 lacking mice had a higher susceptibility to develop autoimmune illnesses like autoimmune encephalitis, collagen-induced arthritis [70] and autoimmune uveoretinitis [71]. Other studies found CD200 and CD200R downregulated in brains of patients suffering from Alzheimer's disease, linking deficiency of the CD200/CD200R axis to enhanced inflammation and disease progression [72].

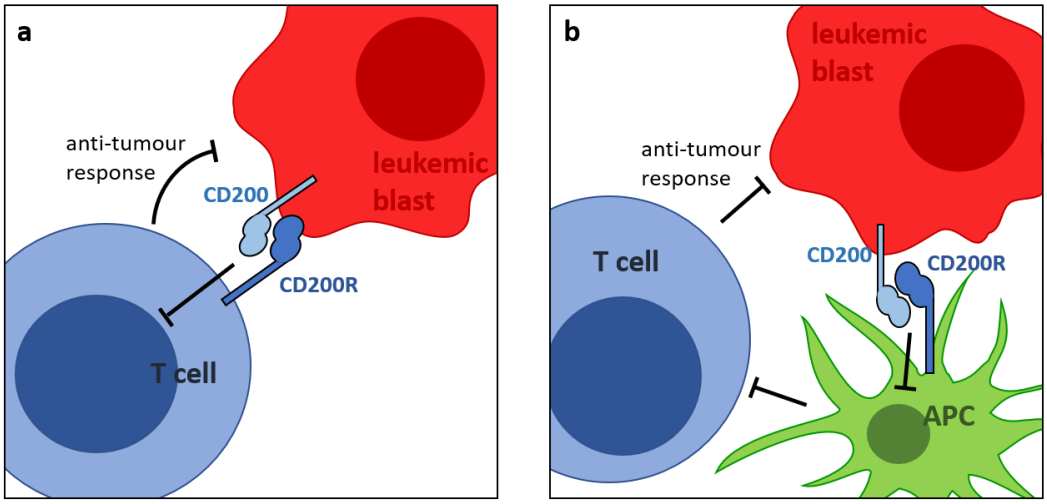

Figure 6: Inhibitory ways of the CD200/CD200R axis
It is yet unclear if inhibition of anti-tumour response mediated by CD200 is driven by **a** direct interaction between leukemic blasts and T cells, or because of **b** indirect affection of CD200R expressing APCs, which themselves inhibit T cell function.

CD200/CD200R is also in the centre of researchers' attention in the context of immune oncology. CD200 is overexpressed in multiple cancer identities, such as B cell chronic lymphocytic leukaemia (B-CLL), ovarian cancer, melanoma, acute myeloid leukaemia (AML), and B-ALL [61, 73-76]. It is associated with poor prognosis as well as reduced overall survival in diseases like myelodysplastic syndrome (MDS) and AML [77-79]. Various studies have shown that CD200 expression on cancer cells support an immunosuppressive tumour microenvironment. It decreases activation and changes the cytokine profile of the myeloid lineage and T cells [70, 80, 81]. Further, it induces anti-inflammatory DCs, which diminish T cell function [82, 83]. CD200 suppresses memory T cell function in AML, switches the Th1 cytokine profile of T helper cells into anti-inflammatory type 2 T helper cell response (Th2) in CLL and is associated with increased frequencies of regulatory, immunosuppressive T cells [74, 84, 85]. Until now, most studies addressing the impact on CD200 in tumour growth were conducted in mixed lymphocyte reactions (MLR). As myeloid cells as well as T cells carry the CD200R, it remains unclear if the pro-tumour effect of CD200 is driven by tumour - T cell or tumour - myeloid cell interaction (Figure 6) [86].

Knowledge of the role of the CD200/C200R axis in paediatric B-ALL is very limited. CD200 is expressed in 95 % of all precursor B-ALL blasts [87]. Blaeschke et al. showed that CD200 leads to decreased T cell activation. Further, CD200 on ALL induced TIM-3^{+}CD4^{+} bone marrow T cells, which were associated with a 7.1-fold increased risk of developing a relapse [88].

The inhibitory axis of CD200/CD200R represents an auspicious therapeutic target. The anti-CD200 checkpoint inhibitor samalizumab achieved promising results in a phase I study. It proved to be safe and decreased tumour load in most patients with advanced CLL [89]. In 2021, NSG mice engrafted with low risk CD200^{+} ALL showed extended survival after treatment with the monoclonal antibody TTI-CD200 [90]. Furthermore, the expression of a CD200R-CD28 fusion receptor on tumour-specific T cells leads to an increased T cell activation in AML [91].

B-ALL blasts abundantly express the immunoinhibitory molecule CD200. Thus, interfering the CD200/CD200R axis is a promising approach for innovative immunotherapeutic approaches.

2 Aim of the study

Although 90 % of all children suffering from ALL can be cured nowadays, relapsing or refractory ALL is responsible for more deaths than any other malignancy in childhood [1, 5]. T cells equipped with a chimeric antigen receptor (CAR) are capable of killing tumour cells through specific binding. CAR T cells have emerged as a promising approach in the fight of paediatric acute lymphoblastic leukaemia, but many patients subsequently relapse [14, 23]. The development of resistance to CAR T cell therapy is governed by plenty of intrinsic and leukaemic microenvironmental factors [35]. For example, through the expression of immunoregulatory molecules on their surface leukaemic blasts can specifically evade immunosurveillance [38].

Here we focus on the immunoregulatory checkpoint axis of CD200/CD200R. CD200 is a glycoprotein found abundantly expressed on B-ALL blasts [61, 87] and it is considered to inhibit anti-tumour response [73]. Its receptor is found on T cells as well as on APCs [66]. This study aims to elucidate the impact of CD200 expressing paediatric B-ALL blasts on the functionality of T cells and CAR T cells, addressing the questions if and to what extend T cells and CAR T cells are affected by the CD200/CD200R axis. Further, to clarify if CD200 mediated immunoregulation results from blast – T cell or blast – APC interaction, macrophages and dendritic cells were included into experiments. To investigate the role of CD200R on T cells and CAR T cells within the CD200/CD200R axis, overexpression of CD200R will be performed. Moreover, as an attempt of overcoming CD200 induced immune evasion, we test a CD200R knock-out and a CD200R-CD28 fusion receptor on CAR T cells.

Conclusively, this study aims to gain better understanding of blast – CAR T cell interaction in order to enhance CAR T cell therapy for refractory and relapsing B-ALL to pave the way for durable remissions.

3 Material

3.1 Equipment and software

Table 2: Equipment and software

Parts of this section were adapted from Antonia Apfelbeck, 2022 [92] and from Larissa Deisenberger, 2022 [93] with permission of the authors, as identical equipment and software were used within the work group.

Equipment/ Software	Name, Manufacturer
Autoclaves	VX-55, VX-150, DX-65, Systec, Linden, Germany
Cell counting auxiliaries	Cell Counting Chamber Neubauer, Chamber Depth 0.1 mm, Paul Marienfeld, Lauda-Königshofen, Germany
Centrifuges	Multifuge X3R and Mini Centrifuge Fresco 17, Heraeus, Hanau, Germany
Cleaner Box	UVC/T-M-AR, DNA-/RNA UV-cleaner box, Biosan, Riga, Latvia
Cooling units	Cooler (4 °C) Comfort No Frost, Liebherr, Biberach an der Riß, Germany
	Cryogenic Freezer MVE 600 Series, Chart, Luxemburg
	Freezer (-20 °C) Premium No Frost, Liebherr, Biberach an der Riß, Germany
	Freezer (-86 °C) HERAfreeze HFC Series, Heraeus, Hanau, Germany
	Freezer (-86 °C) HERAfreeze HFU T Series, Heraeus, Hanau, Germany
	Thermo Scientific Cryo 200 liquid nitrogen dewar, Thermo Fisher Scientific, Waltham, Massachusetts, USA
Electroporator	Nucleofector® II, Amaxa Biosystems GmbH, Cologne, Germany
Flow cytometer	BD FACSAria III, BD, Franklin Lakes, New Jersey, USA
	BD LSRFortessa Cell Analyzer, BD, Franklin Lakes, New Jersey, USA
	MACSQuant Analyzer 10, Miltenyi Biotec, Bergisch Gladbach, Germany
Freezing container	Nalgene Mr. Frosty, Thermo Fisher Scientific, Waltham, Massachusetts, USA
Gel Imager	Gel iX20 Imager, Intas Science Imaging, Göttingen, Germany
Heat block	Eppendorf ThermoMixer comfort, Eppendorf, Hamburg, Germany
Incubator	HERAcell 240, 150i CO_2 Incubator, Thermo Fisher, Waltham, Massachusetts, USA
Laminar flow hood	HERAsafe, Thermo Fisher, Waltham, Massachusetts, USA
	Uniflow KR130, Uniequip, Planegg, Germany
Magnetic cell separator	MACS MultiStand, Miltenyi Biotec, Bergisch Gladbach, Germany
	MidiMACS Separator, Miltenyi Biotec, Bergisch Gladbach, Germany
	QuadroMACS Separator, Miltenyi Biotec, Bergisch Gladbach, Germany
Microscope	Axiovert 25, Carls Zeiss Microscopy, Jena, Germany
	Leica DM IL, Leica Microsysteme, Wetzlar, Germany
Pipettes (electrical)	Easypet 3, Eppendorf, Hamburg, Germany Pipetboy 2, Integra Biosciences, Biebertal, Germany

Equipment/ Software	Name, Manufacturer
Pipettes (manual)	2.5 µl, 20 µl, 200 µl, 1000 µl Eppendorf Research, Eppendorf, Hamburg, Germany
Power Supply	Biorad Power Pac 200, Biorad, Hercules, California, USA
Scale	R 200 D, Sartorius AG, Göttingen, Germany
Software	BD FACSDiva Version 6, BD Biosciences, San Jose, California, USA
	FlowJo 10.0.7r2, Ashland, Oregon, USA
	GraphPad PRISM 7.0, La Jolla, California, USA
	LEGENDplex™ Data Analysis Software, Biolegend, San Diego, California, USA
	MACSQuantify, Miltenyi Biotec, Bergisch Gladbach, Germany
	Microsoft Office 2016, Redmond, Washington, USA
	TIDE, Bas van Steensel lab and Desktop Genetics Ltd., London, UK
Spectrophotometer	Nanodrop ND-1000 spectrophotometer, Nanodrop Technologies, Wilmington, Delaware, USA
Thermocycler	peqSTAR 96 Universal Gradient, Isogen, Utrecht, Netherlands
Vacuum pump	Vakuumsytem BVC 21 NT, Vacuubrand, Wertheim, Germany
Water bath	LAUDA Aqualine AL 18, LAUDA-Brinkmann, Delran, New Jersey, USA

3.2 Chemical reagents

Table 3: Chemical reagents

Parts of this section were adapted from Antonia Apfelbeck, 2022 [92] and from Larissa Deisenberger, 2022 [93] with permission of the authors, as identical chemical reagents were used within the work group.

Solution/ Medium/ Serum	Order number	Manufacturer
100 bp DNA Ladder Ready to Load	01-11-00050	Solis BioDyne, Tartu, Estonia
Agarose	50004	Seakem Le Agarose, DMA, Rockland, Maine, USA
Albiomin 5 % infusion solution human albumin (HSA)	623 050	Biotest, Dreieich, Germany
Albumin Fraction V (BSA)	8076.3	Carl Roth GmbH + Co.KG , Karlsruhe, Germany
Biocoll separating solution	L6115	Biochrom, Berlin, Germany
BLINCYTO® (Blinatumomab)	-	Amgen, Thousand Oaks, California, USA
Brefeldin A	5936	Sigma-Aldrich, Steinheim, Germany
Cas9 Nuclease	-	MacroLab, Stanley Hall, California, USA
CellTrace Violet Proliferation Kit	C34557	Invitrogen, Thermo Fisher Scientific, Life Technologies Cooperation, Eugene, Oregon, USA
Compensation beads	130-097-900 130-104-693	MACS Comp Bead Kit anti mouse/anti REA, Miltenyi Biotec, Bergisch Gladbach, Germany

Solution/ Medium/ Serum	Order number	Manufacturer
	552843	BD Biosciences, San Diego, California, USA
CRISPR-cas9 CD200R crRNA	-	Integrated DNA Technologies, Inc., Skokie, Illinois, USA
CRISPR-cas9 Negative Control crRNA	1072544	Integrated DNA Technologies, Inc., Skokie, Illinois, USA
CRISPR-cas9 tracrRNA	1073191	Integrated DNA Technologies, Inc., Skokie, Illinois, USA
Dimethylsulfoxid (DMSO)	4720.4	Carl Roth, Karlsruhe, Germany
	D5879	Honeywell, Seelze, Germany
DMEM medium with 1% L-glutamin	FG1445	Bio-sell, Nürnberg, Germany
DNA Clean & Conentrator -5	D4014	Zymo Research, Irvine, California, USA
DNA Gel Loading Dye (6X)	R0611	Thermo Fisher Scientific, Waltham, Massachusetts, USA
Dulbeccos phosphate buffer saline (PBS)	14190-250	Gibco, Life Technologies, Darmstadt, Germany
EasySep™ Human T Cell Enrichment Kit	19051	Stemmcell Technologies, Vancouver, British Columbia, Canada
Electroporation Enhancer (400µM)	1075916	Integrated DNA Technologies, Inc. , Skokie, Illinois, USA
Ethidium bromide	2218.1	Roth, Karlsruhe, Germany
Fc Blocking Reagent	130-059-901	Miltenyi Biotec, Bergisch Gladbach, Germany
Fetal Bovine Serum (FBS)	F0804	Sigma-Aldrich CHEMIE, Steinheim, Germany
Fix & Perm Cell Permeabilization Kit	GAS004	Life Technologies, Frederick, Maryland, USA
HEPES-Buffer (1 M)	L 1613	Biochrom, Berlin, Germany
Human AB serum	Human AB serum was kindly provided by Prof. R. Lotfi, University Hospital Ulm, Institute for Transfusion Medicine and German Red Cross Blood Services Baden-Württemberg—Hessen, Institute for Clinical Transfusion Medicine and Immunogenetics, both from Ulm, Germany	
Human CD8/NK Panel LEGENDplex™ Multiplex Assay	740267	Biolegend, San Diego, California, USA
IFN-γ	-	Boehringer Ingelheim Pharma GmbH & Co. KG, Ingelheim am Rhein, Germany
IL-7, IL-15 (human, premium grade)	130-95-363 130-095-764	Miltenyi Biotec, Bergisch Gladbach, Germany
Interleukin 4	200-04	Peprotech, Cranbury, New Jersey, USA
Interleukin 4	200-04	Peprotech, Cranbury, New Jersey, USA
KAPA HiFi HotStart ReadyMix	7958935001	Roche, Basel, Schweiz

Solution/ Medium/ Serum	Order number	Manufacturer
L-Glutamine 200 mM	K 0283	Biochrom, Berlin, Germany
Lipopolysaccharide	L 2654	Sigma-Aldrich CHEMIE, Steinheim, Germany
Lympho Spin Medium	SKU 60-00092-11	pluriSelect Life Science, Leipzig, Germany
MicroBeads (CD4, CD8, CD14, CD56)	130-045-101 130-045-201 130-050-201 130-050-401	Miltenyi Biotec, Bergisch Gladbach, Germany
Penicillin/ streptomycin	15140-122	Gibco, Life Technologies, Darmstadt, Germany
Protamine sulfate	P3369	Sigma-Aldrich CHEMIE, Steinheim, Germany
Q5 High-Fidelity DNA Polymerase	M0491S	New England BioLabs, Frankfurt am Main, Germany
QIAamp DNA Mini Kit	51306	QIAGEN, Hilden, Germany
Recombinant human M-CSF, GM-CSF	300-25, 300-03	Peprotech, Cranbury, New Jersey, USA
RetroNectin Reagent	T100A	Takara, Saint-Germain-en-Laye, France
RPMI 1640 Medium with 1 % L-glutamin	880170-12	Lonza, Basel, Switzerland
Sodium pyruvate	11360-039	Gibco, Life Technologies, Darmstadt, Germany
Stapyhlococcal enterotoxin B	4881	Sigma-Aldrich CHEMIE, Steinheim, Germany
T cell TransAct, human	130-111-160	Miltenyi Biotec, Bergisch Gladbach, Germany
TAE Buffer	A4686	TAE buffer (50x), Applichem, Darmstadt, Germany
TexMACS GMP Medium	170-076-307	Miltenyi Biotec, Bergisch Gladbach, Germany
TexMACS Medium research grade	130-097-196	Miltenyi Biotec, Bergisch Gladbach, Germany
TransIT-293 Transfection Reagent	Mirumir270 4	Mirus Bio LLC, Madison, Wisconsin, USA
Trypan blue	15250-061	Gibco, Life Technologies, Darmstadt, Germany
Versene Solution	15040066	Gibco, Life Technologies, Darmstadt, Germany

3.3 Consumables

Table 4: Consumables

Parts of this section were adapted from Antonia Apfelbeck, 2022 [92] with permission of the author, as identical consumables were used within the work group.

Consumable	Order number	Name, Manufacturer
Cannula	851.638.235	Safety-Multifly-Needle, Sarstedt, Nümbrecht, Germany

Consumable	Order number	Name, Manufacturer
Cell culture dish	664 160	Cellstar Greiner Labortechnik, Kremsmünster, Austria
Cell culture flasks with ventilation caps	83.3910.002 83.3911.002 83.3912.002	T25, T75, T175, Sarstedt, Nümbrecht, Germany
Cell culture multiwell plates	657160	6 well, Cellstar Greiner Labortechnik, Kremsmünster, Austria
	3524 3548	24 well, 48 well, Costar Corning Incorporated, Corning, New York, USA
	10212811 163320	96 well flat button, 96 well round button, Nunclon Delta Surface, Thermo Fisher Scientific, Waltham, Massachusetts, USA
	83.3925	96 well round button, Sarstedt, Nümbrecht, Germany
Cell scraper	83.3950	Cell scraper 2-position blade size S, Sarstedt, Nümbrecht, Germany
Compresses	18507	Gauze Compresses 10 x 10 cm, Nobamed Paul Danz, Wetter, Germany
Cover slips	C10143263NR1	Menzel-Gläser 20 x 20 mm, Gerhard Menzel, Braunschweig, Germany
FACS buffers and solutions	130-092-747, 130-092-748, 130-092-749	Running Buffer, Storage Solution, Washing Solution, Miltenyi Biotec, Bergisch Gladbach, Germany
	340345, 340346, 342003	FACS clean/rinse/flow, Becton, Dickinson and Company (BD), Franklin Lakes, New Jersey, USA
FACS tubes	352235	5 ml Polystyrene Round Bottom Tube with cell strainer snap cap, Falcon, Corning Science, Taumaulipas, Mexico
Freezing tubes	72.379	Cryo Pure Gefäß 1.8 ml, Sarstedt, Nümbrecht, Germany
Magnetic separation columns	130-042-401, 130-042-901	LS Columns, LD Columns, Miltenyi Biotec, Bergisch Gladbach, Germany
Pasteur pipettes	747720	Glass Pasteur Pipettes 230 mm, Brand, Wertheim, Germany
Pipette tips	70.1130.217, 70.760.213, 70.760.212, 70.762.211	0.1-2.5 µl, 10 µl, 20 µl, 100 µl, 2-200 µl, 1000 µl, Sarstedt, Nümbrecht, Germany
Reaction vessels	4440100	50 ml, Orange Scientific, Braine-l'Alleud, Belgium
	62.554.502	15 ml, Sarstedt, Nümbrecht, Germany
	72.690.550	1.5 ml, Sarstedt, Nümbrecht, Germany
Safety gloves	9209817	Vaso Nitril Blue, B. Braun Melsungen, Melsungen, Germany
Serological pipettes	86.1685.001 86.1253.001 86.1254.001	5 ml, 10 ml, 25ml Serological Pipette, Sarstedt, Nümbrecht, Germany
Skin disinfectant	975512 306650	Sterilium Classic Pure, Sterilium Virugard, Hartmann, Heidenheim, Germany
Sterile filters	SE2M229104, SE2M230104	0.2µm, 0.45µm, Carl Roth, Karlsruhe, Germany

Consumable	Order number	Name, Manufacturer
Surface disinfectant	CLN-1006.5000	Ethanol 80 % MEK/Bitrex, CLN, Niederhummel, Germany
Syringe	309658	3ml, Becton, Dickinson and Company (BD), Franklin Lakes, New Jersey, USA
	4606728V	10ml, B. Braun Melsungen, Melsungen, Germany
	4617509F	50ml, Omnifix, B. Braun Melsungen, Melsungen, Germany

3.4 Composition

Table 5: Composition

Description	Ingredient	End concentration
Dendritic cell medium	GM-CSF	1000 U/ml
	HEPES-Buffer (1 M)	1 %
	human AB Serum	10 %
	IL-4	500 U/ml
	RPMI 1640 Medium with 1 % L-glutamin	Ad 50ml
Electroporation Buffer M	KCL	5 mM
	Mannitol	50 mM
	$MgCl_2$	15 mM
	Na_2HOP_4/NaH_2PO_4	120 mM
Leukaemic cell line medium	Fetal Bovine Serum	10 %
	RPMI 1640 Medium with 1 % L-glutamin	Ad 500 ml
Macrophage medium	DMEM medium with 1 % L-glutamin	Ad 500 ml
	Fetal bovine serum	20 %
	HEPES-Buffer (1 M)	1 %
	M-CSF	50 ng/ml
	Penicillin/ streptomycin	1 %
	Sodium-pyruvat	1 %
T cell medium	Human AB serum	2.5 %
	IL-15	12.5 ng/ml
	IL-7	12.5 ng/ml
	TexMACS Medium research grade	Ad 500 ml

3.5 FACS antibodies

Table 6: FACS antibodies

Parts of this section were adapted from Antonia Apfelbeck, 2022 [92] and from Larissa Deisenberger, 2022 [93] with permission of the authors, as identical FACS antibodies were used within the work group.

Fluro-chrome	Antigen	Clone	Order number	Manufacturer
7AAD	Viability		420404	Biolegend, San Diego, California, USA
AF647	CD200R	OX108	MCA2282A647	Bio-Rad Laboratories, Hercules, California, USA
APC	CD14	TÜK4	130-115-559	Miltenyi Biotec, Bergisch Gladbach, Germany
APC Cy 7	HLA-DR	L243	307618	Biolegend, San Diego, California, USA
APC-Vio770	CD8	REA734	130-110-681	Miltenyi Biotec, Bergisch Gladbach, Germany

Fluro-chrome	Antigen	Clone	Order number	Manufacturer
BB515	CCR6	11A9	564479	Becton, Dickinson and Company (BD), Franklin Lakes, New Jersey, USA
BUV395	CD4	L200	564107	Becton, Dickinson and Company (BD), Franklin Lakes, New Jersey, USA
BUV395	CD80	L307.4	565210	Becton, Dickinson and Company (BD), Franklin Lakes, New Jersey, USA
BUV496	CD8	RPA-T8	564804	Becton, Dickinson and Company (BD), Franklin Lakes, New Jersey, USA
BUV496	CD19	SJ25C1	564655	Becton, Dickinson and Company (BD), Franklin Lakes, New Jersey, USA
BUV737	CD3	UCHT1	564307	Becton, Dickinson and Company (BD), Franklin Lakes, New Jersey, USA
BUV737	CD56	NCAM16.2	564447	Becton, Dickinson and Company (BD), Franklin Lakes, New Jersey, USA
BV421	CD56	HCD56	318328	Biolegend, San Diego, California, USA
BV421	CD137	4B4-1	309820	Biolegend, San Diego, California, USA
BV421	CD200	MRC OX-104	564114	Becton, Dickinson and Company (BD), Franklin Lakes, New Jersey, USA
BV421	CD274	29E.2A3	329714	Biolegend, San Diego, California, USA
BV421	CCR4	L291H4	359413	Biolegend, San Diego, California, USA
BV510	CD25	M-A251	563352	Becton, Dickinson and Company (BD), Franklin Lakes, New Jersey, USA
BV510	CD163	GHI/61	333628	Biolegend, San Diego, California, USA
BV650	CD62L	FN50	563835	Becton, Dickinson and Company (BD), Franklin Lakes, New Jersey, USA
BV650	CD86	IT2.2	305428	Biolegend, San Diego, California, USA
BV785	CD132	6H6	306032	Biolegend, San Diego, California, USA
BV786	CD127	HIL-7R-M21	563324	Becton, Dickinson and Company (BD), Franklin Lakes, New Jersey, USA
eFLour 780	Viability dye		65-0865-14	eBioscience, Thermo Fisher Scientific, Waltham, Massachusetts, USA
FITC	CD14	M5E2	301804	Biolegend, San Diego, California, USA
FITC	Anti c-myc	14D3	130-116-485	Miltenyi Biotec, Bergisch Gladbach, Germany
FITC	Lineage Cocktail	UCHT1, HCD14, HIB19, 2H7, HCD56	348701	Biolegend, San Diego, California, USA
FITC	CTLA-4	14D3	11-1529-42	eBioscience, Thermo Fisher Scientific,Waltham, Massachusetts, USA
Pacific Blue	TNF-α	MAb11	502920	Biolegend, San Diego, California, USA
PE	CD19	LT19	130-113-169	Miltenyi Biotec, Bergisch Gladbach, Germany
PE	CD25	REA570	130-113-286	Miltenyi Biotec, Bergisch Gladbach, Germany
PE	CD45RO	UCHL1	304206	Biolegend, San Diego, California, USA

Fluro-chrome	Antigen	Clone	Order number	Manufacturer
PE	IFN-γ	25723.11	340452	Becton, Dickinson and Company (BD), Franklin Lakes, New Jersey, USA
PE Cy5	CD206	15-2	321108	Biolegend, San Diego, California, USA
PE-CF594	CXCR3	1C6/CXCR3	562451	Becton, Dickinson and Company (BD), Franklin Lakes, New Jersey, USA
PE-Vio770	CD3	REA613	130-113-140	Miltenyi Biotec, Bergisch Gladbach, Germany
PE-Vio770	CD11c	MJ4-27G12	130-114-107	Miltenyi Biotec, Bergisch Gladbach, Germany
PE-Vio770	CD19	REA675	130-113-647	Miltenyi Biotec, Bergisch Gladbach, Germany
PE-Vio770	CD69	REA824	130-112-615	Miltenyi Biotec, Bergisch Gladbach, Germany
PE-Vio770	CD95	DX2	130-104-199	Miltenyi Biotec, Bergisch Gladbach, Germany
VioBlue	CD62L	145/15	130-098-699	Miltenyi Biotec, Bergisch Gladbach, Germany
VioGreen	CD4	REA623	130-113-230	Miltenyi Biotec, Bergisch Gladbach, Germany

4 Methods

Sections 4.1.1, 4.1.2, 4.1.5, 4.1.7, 4.1.8.1, 4.2.1, 4.4.3, 4.4.5, 4.4.6 and 4.5 were adapted from MD thesis of Antonia Apfelbeck: Generation and Characterization of CD19 CAR T cells with PD 1_CD28 fusion receptor (Ludwig-Maximilian-University, 2022 Munich [92]). Section 4.1.6 was adapted from MD thesis of Larissa Deisenberger: CRISPR/Cas9-mediated generation and characterization of glucocorticoid-resistant virus-specific T cells (Ludwig-Maximilian-University, 2022 Munich [93]). Sections 4.4.2 and 4.4.4 were adapted from MD thesis of Eva Ortner: Induction of T-cell attack against ALL through a TIM-3-CD28 fusion receptor (Ludwig-Maximilian-University, 2023 Munich [94]). Although the methods were identical to the previous MD thesis mentioned above, the experiments shown in this thesis were totally unique and apart from the previous MD thesis in terms of scientific questions, samples and results.

4.1 Cell generation

4.1.1 PBMC isolation

Isolation of peripheral blood mononuclear cells (PBMCs) was performed as described in Apfelbeck, 2022 [92] via density gradient centrifugation. For this, 60 – 100 ml heperin blood of healthy donors who had given written informed consent before blood draw was used. Heparin blood diluted 1:2 with PBS was carefully layered on 15 ml Biocoll and then centrifugated at 800 g for 20 minutes without brake. PBMCs were aspirated subsequently.

4.1.2 T cell isolation and activation

T cells were isolated and activated according to Apfelbeck, 2022 [92]. Therefore, T cells were isolated from PBMCs either by CD4 and CD8 MicroBeads or by using EasySepTM Human T cell enrichment kit based on manufacturer's specifications. T cells were cultured in TexMACS™ Medium + 2.5 % human AB serum + 12.5 ng/ml interleukins 7 and 15. For further transduction

or CRISPR/Cas9 mediated knock-out, isolated T cells were activated with T Cell TransAct according to manufacturer's information and washed one or two days afterwards.

4.1.3 Monocytes derived macrophages

PBMCs were isolated according to 4.1.1. For macrophage generation, PBMCs were cultured in 10 cm dishes in a concentration of 2 – 4 x10^6/ml in DMEM supplemented with 20 % fetal bovine serum (FBS), 1 % HEPES 1 M, 1 % L-glutamin, 1 % sodium-pyruvat and 1 % penicillin/ streptomycin. To direct monocytes into macrophage differentiation, PBMCs were cultured in the presence of 50 ng/ml M-CSF. To remove non-adherent cells, medium and cytokines were changed every two or three days within the differentiation period of eight days. Differentiation of monocytes to macrophages was controlled regularly by light microscope. On day eight, Versene solution was used for non-enzymatic dissociation of macrophages after washing with PBS. Macrophages were subsequently scratched from dish surface by using cell scraper and seeded for experiments. Success of macrophage generation was evaluated by flow cytometry.

4.1.4 Monocytes derived dendritic cells

PBMCs were isolated according to 4.1.1, followed by monocyte enrichment using CD14 MicroBeads according to the manufacturer's information. Subsequently, monocytes were cultured in RPMI 1640 medium supplemented with 10 % human AB Serum, 1 % L-glutamin and 1 % HEPES 1 M in presence of 500 U/ml interleukin 4 and 1000 U/ml GM-CSF. Cells were cultured for five days. New cytokines were added every two days. Differentiation of monocytes to dendritic cells was controlled regularly by light microscope. Success of dendritic cell generation was evaluated by flow cytometry.

4.1.5 Retroviral transduction of T cells

4.1.5.1 Virus generation

Viruses for retroviral transduction were generated as previously described in Apfelbeck, 2022 [92].

"Producer cells (293Vec-RD114 cells) were previously generated for all constructs according to published literature [95, 96]. Untransduced producer cells were kindly provided by Manuel Caruso, BioVec Pharma, Québec, Canada.

Virus was harvested by aspirating supernatant of 293VEC-RD114 cells. Supernatant was filtered with a 0.45 µm filter, frozen and stored at -80 °C.

For verification of the constructs a PCR followed by Sanger sequencing was performed. Therefore, genomic DNA of transduced producer cells was isolated with the QIAamp DNA Mini Kit according to the manufacturer's information. For PCR, isolated genomic DNA was amplified using Q5 High-Fidelity DNA Polymerase according to the supplier's information" [92].

The setting for the thermocycler is shown in Table 7: Thermocycler settings for virus generation

Table 7: Thermocycler settings for virus generation.

Step	Number of cycles	Temperature [°C]	Time [s]
Initial denaturation	1	98	30
Denaturation	35	98	10
Annealing		60	20
Elongation		72	80
Final elongation	1	72	80

To purify the PCR product, DNA Clean and Concentrator kit was used as specified by the manufacturer. Subsequently, Sanger sequencing (Genewiz) of the purified PCR product was performed. Primer (see Supp. 1.1) and construct sequences (see Supp. 2) are shown in the supplements.

4.1.5.2 Retroviral transduction

Retroviral transduction of T cells was performed two days after T cell isolation and activation (see 4.1.2) as described in Apfelbeck, 2022 [92]: "24 well plates were coated with 2.5 µg RetroNectin reagent per well either overnight at 4 °C or for 2 hours at 37 °C. Plates were blocked with 2 % Albumin Fraction V in PBS for 30 minutes and afterwards washed with a 1:40 dilution of HEPES 1 M in PBS. 1 ml of thawed virus supernatant was centrifuged on coated wells at 3000 g for 90 minutes at 32 °C. Supernatants were discarded and 1 x10^6 T cells in 1 ml TexMACS™ medium supplemented with 2.5 % human AB serum and 12.5 ng/ml interleukins 7 and 15 were added per well. For untransduced control, same amount of T cells was added in untreated wells. Plates were centrifuged at 450 g for 10 minutes at 32 °C" [92]. After one or two days, T cells were washed to eliminate virus.

4.1.6 CD200R knock-out of T cells

4.1.6.1 CRISPR/Cas9 mediated knock-out of CD200R on T cells

CD200R knock-out was performed as described in Deisenberger, 2022 [93]. Knock-out of CD200R was performed two days after T cell activation or 24 hours after retroviral transduction of T cells using CRISPR/ Cas9 system. For the ribonucleoprotein (RNP) complex, a 1:1 mix of 80 µM CD200R-crRNA and 80µM tracrRNA was heated for 5 min at 95 °C and subsequently mixed with 40µM Cas9 enzyme in a ratio of 5:1. 20 µM electroporation enhancer was added. Up to 1x10^6 cells were resuspended in 100 µl of electroporation buffer M and mixed with 10.4 µl of the pre-incubated RNP complex. T cells underwent electroporation using Amaxa nucleofector with program t-023 according to manufacturer's instructions. T cells were then seeded in pre-warmed TexMACS™ medium in a 24 well plate at a concentration of 1 x10^6

cells/ml. T cells which underwent the same procedure but were mixed with a non-targeting negative control crRNA served as control group.

4.1.6.2 Evaluation of CD200R knock-out

Evaluation of CD200R knock-pout was adapted from Deisenberger, 2022 [93]. CD200R knock-out was verified on DNA level by PCR followed by Sanger sequencing. Therefore, isolation of the genomic DNA of CD200R knock-out, knock-out control and untransduced T cells was performed using the QIAamp DNA Mini Kit according to the supplier's information. The DNA was amplified by PCR using KAPA HiFi HotStart ReadyMix as specified by the manufacturer's information. The setting of the thermocycler is shown in Table 8. The PCR product was subsequently purified using DNA Clean and Concentrator kit as specified by the manufacturer and sent for Sanger sequencing (Genewiz).

Table 8: Thermocycler settings for evaluation of CD200R knock-out.

Step	Number of cycles	Temperature [°C]	Time [s]
Initial denaturation	1	95	180
Denaturation	35	98	20
Annealing		60	15
Elongation		72	20
Final elongation	1	72	60

Knock-out rates were determined using the TIDE Analysis tool offered by Brikman et. al [97]. "In brief, raw data files of Sanger sequencing and a crRNA sequence were uploaded, and a test sample was aligned to a control sample. By comparing the sequences after the expected cut site of the crRNA the tool gave information about deletions and insertions (InDels) around the cut site. The sum of all InDel frequencies was determined as […] knock-out rate on DNA level" [93]. Primers used for PCR and Sanger sequencing are shown in the supplements (see Supp. 1.2).

4.1.7 Expansion of transduced or electroporated T cells

This section was adapted from Apfelbeck, 2022 [92]. During the expansion process, T cells were cultured in TexMACS™ Medium + 2.5 % human AB serum + 12.5 ng/ml interleukins 7 and 15. Fresh medium was added to the cell culture every second or third day. To evaluate expansion rate and viability, T cells were diluted with trypan blue and assessed under light microscope every second or third day. Viability was defined as ratio between vital cell count and total cell count. On day twelve after transduction or day eleven after electroporation, a part of the cells was harvested and frozen as described in 4.5. The other part was used for characterisation and functional tests as described in 4.3 and 4.4.

4.1.8 Target cell lines

4.1.8.1 Transduction of target cell line

Transduction of CD200 in target cell line was performed as described in Apfelbeck, 2022 [92]. As target cell line Nalm6 cells were used:

CD200_pMP71 “and helper plasmids MLV env (pALF-10A1-env) and MLV gag/ pol (pcDNA3.1-MLV-g/ p) were transfected into HEK 293T cells using TransIT-293 Transfection Reagent according to the supplier’s information. Helper plasmids were kindly provided by Sebastian Kobold, Department of Clinical Pharmacology, Ludwig-Maximilian-University of Munich. Vector map of pcDNA3.1-MLV-g/ p is shown in the supplements (see Supp. 3.2) and pALF-10A1 is described in Stitz et al [98]. Vector pMP71 was kindly provided by Christopher Baum, Department of Experimental Hematology, Hannover Medical School, and a vector map is shown in the supplements (see Supp. 3.1). After 48 hours, viral supernatant was harvested and used for transduction of [Nalm6 cells]. 24-well plates were coated with 2.5 µg RetroNectin Reagent overnight at 4 °C. Plates were blocked with 2 % Albumin Fraction V in PBS for 30 minutes and washed with a 1:40 dilution of HEPES 1 M in PBS. Virus supernatant was centrifuged at 500 g for 5 minutes at 32 °C and filtered with a 0.45 µm filter. 1 ml of virus supernatant was centrifuged on coated wells at 3000 g for 90 minutes at 32 °C. Supernatant was discarded and $1x10^6$ [Nalm6 cells] in RPMI + 10 % fetal bovine serum (FBS) + 1 % penicillin streptomycin + 1 % L-glutamine were added per well. 4 µg of protamine sulfate and 1 % HEPES 1 M were added. On day 2 after transduction, cells were washed to remove virus. Cells were sorted for [$CD19^+$/ $CD200^+$ Nalm6 cells] at a FACSAria III and cultured in RPMI + 10 % fetal bovine serum (FBS) + 1 % penicillin/ streptomycin + 1 % L-glutamine” [92].

4.1.8.2 CD200 induction assay

Nalm6 wildtype (WT) cells were stimulated with 20 ng IFN-γ and 20 ng TNF-α. CD200 expression on Nalm6 cells was subsequently evaluated after 2, 4, 8, 24 and 48 hours using flow cytometry.

4.2 Flow cytometry

4.2.1 Antibody staining

This method was adapted from Apfelbeck, 2022 [92]: For flow cytometry staining, antibodies were titrated before application. Cells were stained for 10 minutes at 4 °C and washed once with PBS + 1 % fetal bovine serum (FBS). For samples containing macrophages or dendritic cells, Fc receptor block was used as specified by supplier's manual. Measurements were carried out with a MACSQuant Analyzer 10 or BD LSRFortessa Cell Analyzer.

4.2.2 Gating strategy

Flow cytometry data was analysed using FlowJo 10 software. A general gating strategy was established (Figure 7a). First, forward (FSC) versus side scatter (SSC) was used to discriminate between different cell populations and debris, followed by FSC-area (FSC-A) against FSC-height (FSC-H) to exclude doublets from single cells. Next, viability dyes (7-AAD, APC eFluor780) were used to eliminate dead or apoptotic cells. Among the living cells different lineage marker were utilized to discriminate between cell populations. T helper cells were defined as $CD3^+/CD4^+$ and cytotoxic T cells as $CD3^+/CD8^+$. Genetic modified T cells were subsequently gated based on their respective expression of CD200R or c-myc (see Table 9, Figure 7b). Macrophages were defined as $CD14^+$/ HLA-DR^+ and dendritic cells as $CD14^-$/ HLA-DR^+/ $CD11c^+$/ $CD123^-$. After the population of interest was identified, cells were examined for the expression of certain extracellular and intracellular markers.

Table 9: Gating strategy for different T cell conditions.

T cell condition	Gate c-myc	Gate CD200R
unmodified T cells	No staining	Bulk
untransduced T cells		
$_{CR}$Control T cells		
$_{RV}$CD200R-Iso1^{OE} T cells	No staining	Positive fraction
$_{RV}$CD200R-Iso4^{OE} T cells		
$_{CR}$CD200R^{KO} T cells	No staining	Negative fraction
$_{RV}$19-z CAR T cells	Positive fraction	Bulk
$_{RV}$19-BBz CAR T cells		
$_{RV}$19-BBz$_{CR}$Control CAR T cells		
$_{RV}$19-z$_{RV}$CD200R-CD28 CAR T cells		
$_{RV}$19-BBz$_{RV}$CD200R-CD28 CAR T cells		
$_{RV}$19-BBz$_{RV}$CD200R-Iso4^{OE} CAR T cells	Double positive	
$_{RV}$19-BBz$_{CR}$CD200R^{KO} CAR T cells	Positive fraction	Negative fraction

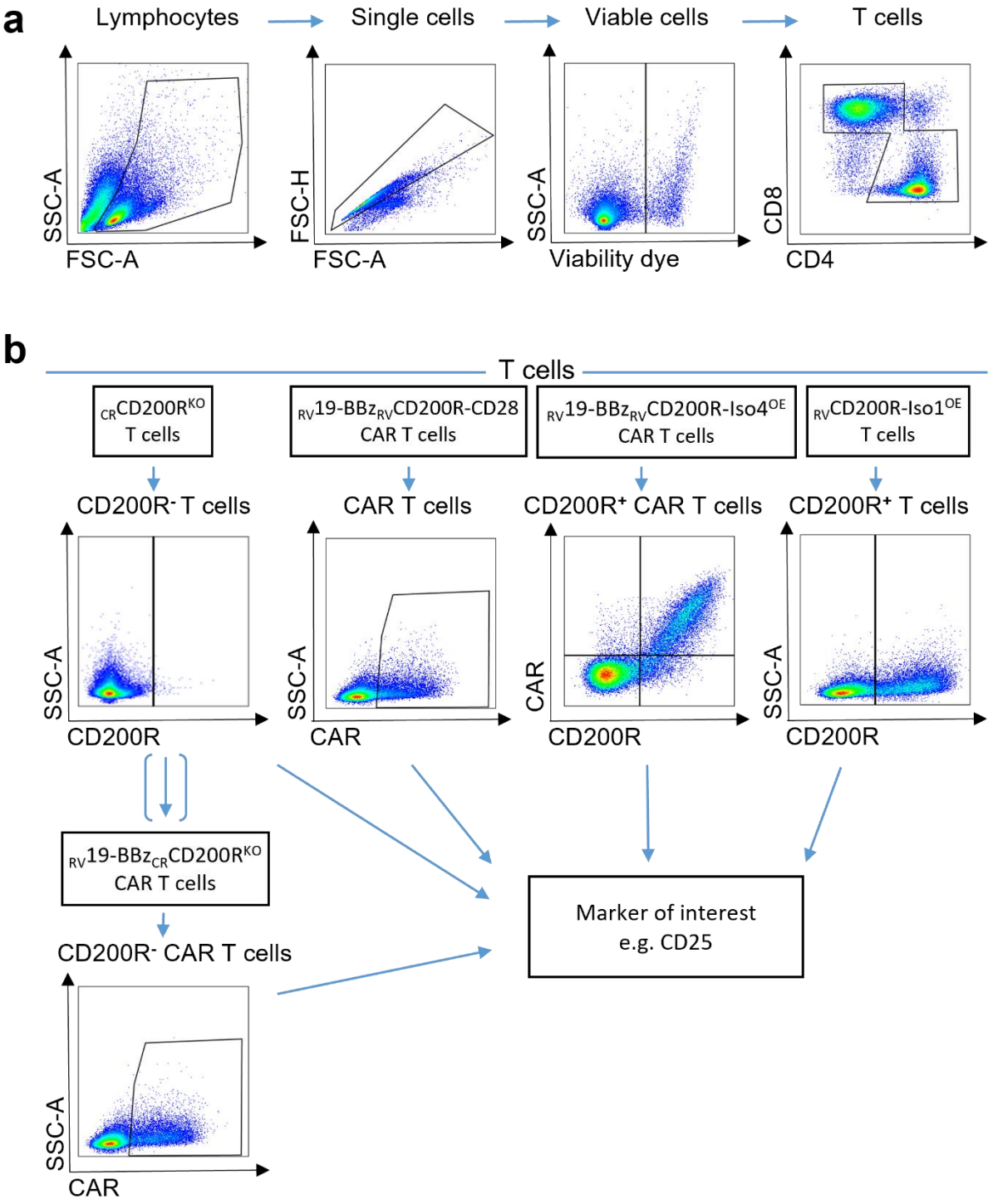

Figure 7: Representative gating strategy for different T cell conditions.
a Common gating strategy for all T cell conditions. T cells were gradually gated for lymphocytes, single cells, viable cells and $CD4^+$/$CD8^+$ T cells. **b** Depending on the T cell condition, T cells were subsequently gated based on their respective expression of CD200R or for the CAR. Here, the gating strategy is exemplary shown for $_{CR}CD200R^{KO}$, $_{RV}19\text{-}BBz_{CR}CD200R^{KO}$, $_{RV}19\text{-}BBz_{RV}CD200R\text{-}CD28$, $_{RV}19\text{-}BBz_{RV}CD200R\text{-}Iso4^{OE}$ and $_{RV}CD200R\text{-}Iso1^{OE}$ T cells.

4.3 Characterisation

For characterisation of the final T cell product, transduction rate, cellular composition and phenotype was analysed by flow cytometry. Transduction rate of T cells was determined by pre-gating on CD200R and/ or c-myc-positive cells. Cellular composition was analysed by staining for CD3, CD4, CD8, CD56, CD19 and CD14. Phenotype of the T cells was evaluated by expression of CD62L, CD45RO and CD95 according to [99, 100]: Naïve T cells were defined as $CD62L^+$/ $CD95^-$/ $CD45RO^-$, stem cell-like memory T cells as $CD62L^+$/ $CD95^+$/ $CD45RO^-$, central memory T cells as $CD62L^+$/ $CD95^+$/ $CD45RO^+$, effector memory T cells as $CD62L^-$/ $CD95^+$/ $CD45RO^+$ and effector T cells as $CD62L^-$/ $CD95^+$/ $CD45RO^-$.

4.4 Functionality assays

Results of functionality assays are compared in the results section as follows: Value of co-culture with Nalm6 WT cells vs. value of co-culture with Nalm6 CD200.

4.4.1 Co-culture of effector cells, target cells and APCs

APCs were seeded overnight in a concentration of $3x10^5$/ml in their respective medium. Subsequently, Nalm6 WT or Nalm6 CD200 cells were added in different E:T ratios. After six hours, freshly isolated T cells from the same donor were added. Co-culture experiments were performed in presence or absence of 4 ng/ml blinatumomab. Functionality assays were performed in singlets or technical duplicates. Experiments were measured on MACSQuant Analyzer 10 or on BD LSRFortessa Cell Analyzer.

4.4.2 Co-culture of effector cells and target cells

This section was adapted from Ortner, 2023 [94]. Thawed or fresh T cells were co-cultured with target cell lines in TexMACS™ GMP medium. Effects of Nalm6 WT and Nalm6 CD200 target cell lines on T cells were compared. Co-culture experiments with T cells were performed in presence or absence of 2 ng/ml blinatumomab. For experiments using CAR T cells, transduction rate was evaluated by FITC c-myc single stain prior to co-culture. Untransduced cells were added to adjust all conditions to the lowest transduction rate within the donor. Effector count was calculated based on the number of CAR positive T cells. All functionality assays were conducted in technical duplicates. Experiments were measured using MACSQuant Analyzer 10.

4.4.3 Intracellular cytokine stain (ICS)

The method of intracellular cytokine stain was adapted from Apfelbeck, 2022 [92]. Cells were co-cultured in an effector to target (to APC) ratio of 1:1(:1) as described in 4.4.1 and 4.4.2. After 24 hours 10 µg/ml Brefeldin A was added to the co-cultures. Cells were incubated for another 2 hours before stimulation was stopped with cold PBS and T cells were washed. For identification of T cell subsets, T cells were stained extracellularly for CD3, CD4, CD8 and CD200R. In addition, CAR T cells were stained for c-myc. Macrophages were stained for CD14

and HLA-DR. Intracellular stain for IFN-γ and TNF-α was conducted with FIX & PERM cell Fixation & Permeabilization Kit as specified by the manufacturer.

For positive controls, T cells and macrophages cultured without target cells were stimulated 2 hours before addition of Brefeldin A. T cells were stimulated with 10 µg/ml staphylococcus enterotoxin B (SEB) and macrophages were stimulated with 1 µg/ml lipopolysaccharide (LPS). For negative controls, T cells and macrophages were cultured without target cells.

4.4.4 Activation assay

Activation was measured according to Ortner, 2023 [94]. Cells were co-cultured (see 4.4.1 and 4.4.2) for 24 or 48 hours as specified in the figure legends in an effector to target (to APC) ratio of 1:1(:1). Untransduced T cells cultured without target cells and stimulated with 10 µg/ml SEB served as positive controls. For negative controls, T cells were cultured without target cells.

After co-culture, T cells were stained for CD3, CD4, CD8, CD200R and for the activation markers CD25, CD69 and CD137. In addition, CAR T cells were stained for c-myc.

4.4.5 Cytotoxicity assay

This section was adapted from Apfelbeck, 2022 [92]. For cytotoxicity measurement, T cells were depleted using CD56 MicroBeads based on manufacturer's specifications to remove NK T cells. Target cells were labelled with CellTrace Violet Cell Proliferation Kit according to supplier's information. Cells were then co-cultured for 48 hours as described in 4.4.1 and 4.4.2. 1:1, 0.1:1 and 0.01:1 effector to target ratios were used. For experiments including APCs, 1:1:1, 0.2:1:1 and 0.04:1:1 effector to target to APC ratios were applied. "Absolute cell count of CellTrace Violet positive cells was measured and killing rate was calculated with following formula: 100 - (100/ targets only*targets left in co-culture). "Targets only" describes target cell lines without co-cultured effector cells and were used as reference" [92].

4.4.6 Proliferation assay

Proliferation assay was performed according to Apfelbeck, 2022 [92]. T cells were first labelled using CellTrace Violet Cell Proliferation Kit according to supplier's information. Cells were then co-cultured (see 4.4.1 and 4.4.2) for 48 or 72 hours as specified in the figure legends in an effector to target (to APC) ratio of 1:1(:1) For positive control, T cells without target cells were stimulated with 10 µg/ml SEB. For negative controls, T cells were cultured without target cells.

After co-culture, cells were stained for CD19, CD3, CD4, CD8, and CD200R. In addition, CAR T cells were stained for c-myc.

Fold changes of proliferation were calculated as ratio of the percentage of proliferating T cells co-cultured with Nalm6 CD200 cells to the percentage of proliferating T cells co-cultured with Nalm6 WT cells to make values more comparable.

4.4.7 T helper subset assay

Cells were co-cultured for 72 hours (see 4.4.1 and 4.4.2) in an effector to target to APC ratio of 1:1:1. T cells cultured without target cells were used as control. After 72 hours T cells were stained for CCR6, CXCR3, CD127, CD25, CCR4, as well as CD3, CD4 and CD8. T cells were considered as Th1 cells if $CCR4^-$/ $CCR6^-$/ $CD25^-$/ $CXCR3^+$ and as Th2 cells if $CCR4^+$/ $CCR6^-$/ $CD25^-$/ $CXCR3^-$.

4.4.8 Macrophage polarization assay

Cells were co-cultured (see 4.4.1) for 72 hours in an effector to target to macrophage ratio of 1:1:1. Macrophages cultured without target and effector cells were used as negative controls. M1 and M2 polarised macrophages served as controls. Therefore, macrophages were stimulated for 48 hours with 100 U/µl GM-CSF, 20 ng/ml IFN-γ and 50 ng/ml LPS to induce M1 polarisation and with 1 µg/ml interleukin 4 and 1 µg/ml M-CSF to induce M2 polarisation according to the protocol of Benner et al. [101]. After 72 hours of co-culture, macrophages were stained for the polarisation markers CD206, CD200R, CD86, CD163, CD274, CD80. CD14, HLA-DR, CD3, CD56 and CD19 were used to identify macrophage population.

4.4.9 Dendritic cell maturation assay

Cells were co-cultured (see 4.4.1) for 72 hours in an effector to target to dendritic cell ratio of 1:1:1. Dendritic cells cultured without target and effector cells were used as negative controls. After 72 hours, dendritic cells were stained for the maturation and differentiation markers CD80, CD83, CD86, CD274 and CD200R. CD11c, HLA-DR and CD123 were used as linage markers to identify dendritic cell population.

4.4.10 LEGENDplex assay

Cells were co-cultured (see 4.4.1) for 48 hours in an effector to target to macrophage ratio of 1:1:1. T cells and macrophages cultured in absence of other cells were used as controls. Supernatant of the different conditions were tested for interleukin (IL) 2, IL-4, IL-6, IL-10, IL-17a, IL-27, TNF-α, INF-γ, sFas, sFasL, granzyme A and B, perforin and granulysin by using LEGENDplex™ according to supplier's manual.

4.5 General cell culture

All cells were cultured as described in Apfelbeck, 2022 [92].

Cell lines were cultured at 37°C with 5% CO_2 in RPMI + 10 % fetal bovine serum (FBS) + 1 % penicillin/streptomycin + 1 % L-glutamine and splitted regularly in a 1:10 ratio. The identity of cell lines was controlled by FACS analysis on a regular basis.

All other cells were cultured at 37°C with 5% CO_2 in their respective medium.

For preservation, cell lines and primary T cells were frozen at -80°C and afterwards transferred to liquid nitrogen (-179°). For protection during freezing, cell lines were transferred to RPMI

+ 20% fetal bovine serum (FBS) + 1% penicillin/streptomycin + 1% L-glutamine containing 10 % dimethyl sulfoxide (DMSO) and primary T cells were transferred to 5 % human serum albumin (HSA) containing 10 % DMSO.

For conducting experiments, cells were thawed quickly in a warm water bath, transferred to prewarmed RMPI medium, washed once and then cultured in TexMACS^{TM} or RPMI medium.

4.6 Statistical analysis

Statistics were conducted with GraphPad Prism 7. Paired or unpaired Student's t test or RM one-way ANOVA was used for analysis of statistical differences between experimental conditions. Differences were defined as significant (*) at a p-value of < 0.05, very significant (**) at a p-value of < 0.01 and extremely significant (*** and ****) at a p-value of < 0.001 and < 0.0001.

5 Results

5.1 Selective transduction of CD200 in target cells

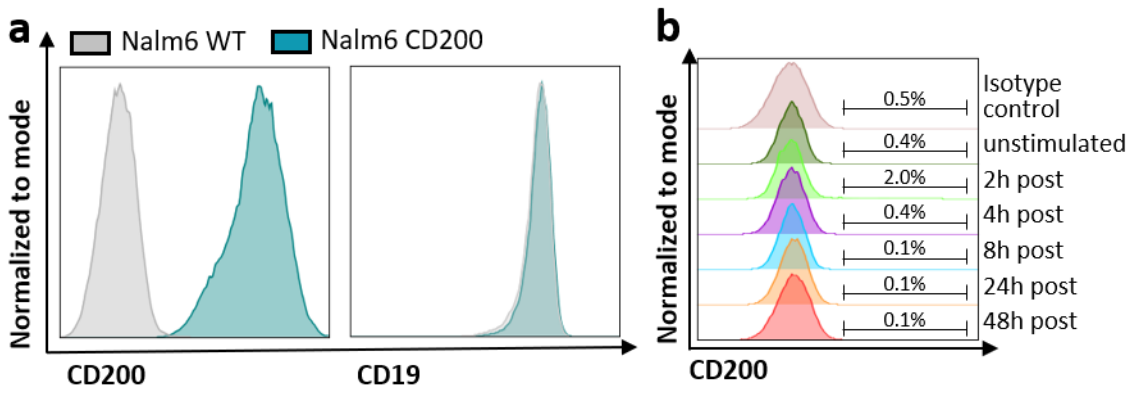

Figure 8: CD200 expression of Nalm6 target cell line.
Nalm6 WT and Nalm6 CD200 cells were characterized using flow cytometry-based analysis. **a** Representative overlay histogram (n ≥ 10) for CD200 and CD19 expression on Nalm6 WT and Nalm6 CD200 cells. **b** Nalm6 WT cells were stimulated with IFN-γ and TNF-α to induce CD200 expression. Representative overlay histogram (n = 2) of CD200 expression on Nalm6 WT cells over time is shown. The results were compared to the unstimulated control and isotype control. WT = Wild type. IFN-γ = Interferon gamma. TNF-α = Tumor necrosis factor alpha.

To investigate the role of CD200 in leukaemia – T cell interaction, the B cell precursor cell line Nalm6 was retrovirally transduced with CD200 to generate Nalm6 CD200 expressing target cells (Nalm6 CD200). While Nalm6 wildtype (WT) cells are CD200 negative, all Nalm6 CD200 cells show high CD200 expression (Figure 8a). Additionally, both target cell lines have comparable expression levels of CD19. CD200 induction test of Nalm6 WT cells was performed to test if CD200 expression is inducible in presence of cytokines secreted by activated T cells. Thus, Nalm6 WT cells were stimulated with IFN-γ and TNF-α and stained for CD200 at indicated time points up to two days after stimulation (Figure 8b). Nalm6 WT cells showed no upregulation of CD200 upon stimulation after 2, 4, 8, 24 and 48 hours (ranging from 0.1 – 2.0 %), when compared to unstimulated Nalm6 WT cells (0.4 ± 0.1 %). Nalm6 WT and Nalm6 CD200 cells were used as models for ALL blasts for the upcoming experiments.

5.2 CD200 on leukaemia binds CD200R on macrophages without inducing M1/M2 polarisation

To study the effect of CD200 expressing ALL blasts through CD200R on macrophages, monocyte derived macrophages were co-cultured with Nalm6 WT or Nalm6 CD200 cells. Expression of different surface antigens and cytokine release of macrophages were assessed using flow cytometry. Macrophages were generated and prepared for co-culture experiments as described in the methods section.

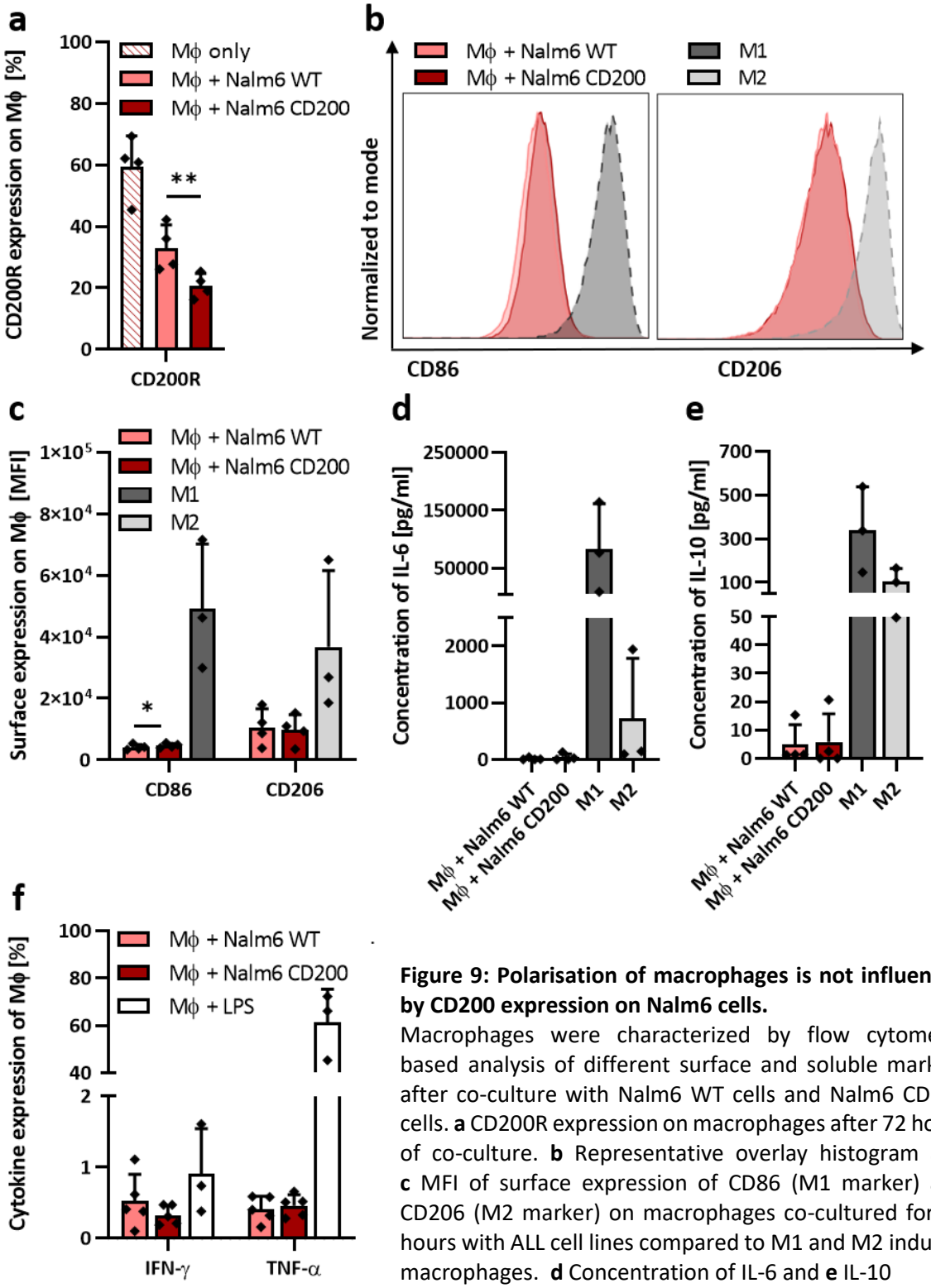

Figure 9: Polarisation of macrophages is not influenced by CD200 expression on Nalm6 cells.
Macrophages were characterized by flow cytometry based analysis of different surface and soluble markers after co-culture with Nalm6 WT cells and Nalm6 CD200 cells. **a** CD200R expression on macrophages after 72 hours of co-culture. **b** Representative overlay histogram and **c** MFI of surface expression of CD86 (M1 marker) and CD206 (M2 marker) on macrophages co-cultured for 72 hours with ALL cell lines compared to M1 and M2 induced macrophages. **d** Concentration of IL-6 and **e** IL-10 detected in the supernatant after 48 hours of co-culture. Values below detection minimum were define as 1E-10. **f** Percentage of IFN-γ and TNF-α secretion of macrophages after 24 hours of co-cultures measured by intracellular cytokine staining compared to LPS control. Data represent the mean ± SD of four donors performed in singlets. P-values were determined using paired Student's t-test. WT = Wild type. IL = Interleukin. IFN-γ = Interferon gamma. MΦ = Macrophages. TNF-α = Tumour necrosis factor alpha. LPS = Lipopolysaccharides

First, CD200R expression on macrophages was measured using flow cytometry (Figure 9a). Before co-culture, macrophages showed a mean expression of CD200R of 59.4 ± 10.1 %. Macrophages co-cultured with Nalm6 WT cells displayed a mean CD200R expression of 33.0 ± 7.5 %, while CD200 expression on Nalm6 cells further significantly decreased CD200R levels to 20.7 ± 4.0 % ($p = 0.0070$). We next compared polarisation of macrophages (Figure 9b). M1 or M2 induced macrophages served as controls. CD86 and CD80 were chosen as M1, and CD206 and CD163 as M2 macrophage markers [56, 102]. Macrophages co-cultured with Nalm6 WT or Nalm6 CD200 cells for 72 hours shared a comparable profile of CD86 and CD206 expression. Mean fluorescence intensity (MFI) of CD86 and CD206 was utilized as indicator for surface expression to quantify results (Figure 9c). Macrophages co-cultured with Nalm6 WT or Nalm6 CD200 cells displayed low polarisation with a MFI of 4161.8 ± 886.6 vs. 4700.3 ± 716.3 for CD86, and a MFI of 10653.0 ± 5963.2 vs. 9786.0 ± 4868.8 for CD206. M1 polarized macrophages showed a MFI of 49261.0 ± 20988.6 for CD86 and M2 polarized macrophages exhibited a MFI of 36832.7 ± 24773.5 for CD206. Macrophages co-cultured with Nalm6 CD200 cells showed a minor but significant difference in CD86 expression, when compared to Nalm6 WT cells ($p = 0.0194$). Comparable results regarding CD80 and CD163 expression were found (data not shown). To assess functionality of macrophages, supernatant of macrophages co-cultured with Nalm6 cells as well as M1 and M2 induced macrophages were harvested after 48 hours and used for cytokine detection by LEGENDplex™ (Figure 9d). While M1 and M2 induced macrophages secreted high concentrations of interleukin 6 (IL-6) (83634.4 ± 77684.0 pg/ml and 727.0 ± 1054.2 pg/ml), macrophages co-cultured with Nalm6 WT or Nalm6 CD200 cells secreted less than 130 pg/ml, with no significant differences in absence or presence of CD200. For interleukin 10 (IL-10) a similar pattern was observed (Figure 9e). M1 and M2 macrophages revealed IL-10 expression (340.2 ± 196.8 pg/ml and 105.0 ± 57.6 pg/ml), while macrophages co-cultured with Nalm6 WT or Nalm6 CD200 cells showed low IL-10 concentrations (4.9 ± 7.0 pg/ml vs. 5.8 ± 10.0 pg/ml). Additionally, macrophages were stained intracellularly for IFN-γ and TNF-α after 24 hours of co-culture (Figure 9f). As positive control, macrophages were stimulated with lipopolysaccharide (LPS). Macrophages co-cultured with Nalm6 WT or Nalm6 CD200 cells showed low expression of IFN-γ (0.5 ± 0.4 % vs. 0.3 ± 0.1 %) and TNF-α (0.4 ± 0.2 % vs. 0.5 ± 0.2 %). In contrast, 0.9 ± 0.6 % and 61.2 ± 14.1 % of LPS stimulated macrophages still expressed low levels of IFN-γ, but TNF-α was strongly increased (0.9 ± 0.6 % and 61.2 ± 14.1 %).

Taken together, macrophages showed high initial CD200R expression, which decreased in presence of CD200. Polarisation analysis revealed a comparable pattern for macrophages upon contact with Nalm6 WT or Nalm6 CD200 cells. Additionally, cytokine production of macrophages co-cultured with Nalm6 cells was limited and showed no differences relating to the cell line.

5.3 CD200 on leukaemia binds CD200R on dendritic cells without inducing maturation

Next, the interaction between DCs and CD200 expressing ALL blasts was investigated. Thus, monocytes derived DCs were co-cultured with Nalm6 WT or Nalm6 CD200 cells. Expression of several surface antigens on DCs were assessed using flow cytometry.

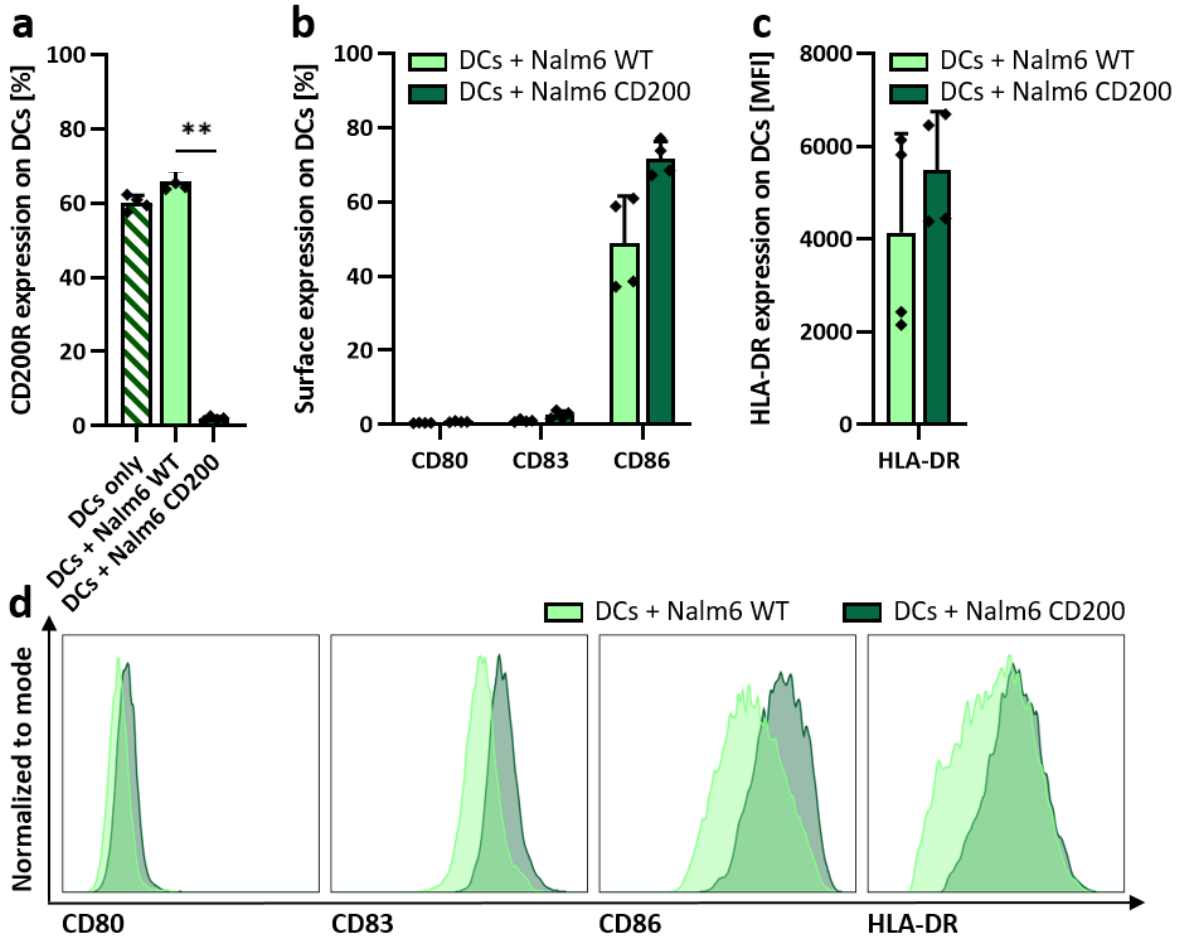

Figure 10: CD200 expressing Nalm6 cells do not alter maturation status of dendritic cells.
Dendritic cells were characterized by flow cytometry based analysis of different surface marker after 72 hours of co-culture with Nalm6 WT or Nalm6 CD200 cells. **a** Percentage of CD200R positive dendritic cells. **b** Percentage, **c** MFI and **d** representative overlay histogram of surface expression of the maturation markers CD80, CD83 CD86 and HLA-DR. Data represent the mean ± SD of two donors performed in duplicates. P-values were determined using paired Student's t-test. WT = Wild type. DC = Dendritic cells. HLA-DR = Human leukocyte antigen - DR isotype. MFI = Median fluorescent intensity.

First, CD200R expression on DCs after co-culture with leukaemic cells for 72 hours was assessed using flow cytometry (Figure 10a). DCs showed a mean CD200R baseline expression of 60.0 ± 2.1 %, which was not altered in presence of Nalm6 WT cells (65.9 ± 2.9 %). Compared to Nalm6 WT cells, co-culture with Nalm6 CD200 cells led to a strong significant decrease of CD200R levels in DCs (2.0 ± 0.6 %; p = 0.0021). Next, DCs were examined for maturation status by staining for CD80, CD83, CD86 and HLA-DR surface expression to uncover potential

alterations in presence of CD200. DCs co-cultured with Nalm6 WT or Nalm6 CD200 cells showed similar surface expression of CD80 (0.5 ± 0.1 % vs. 0.8 ± 0.2%, p = 0.0631), CD83 (1.0 ± 0.3 % vs. 2.6 ± 1.1 %, p = 0.0284) and CD86 (48.9 ± 12.7 % vs. 71.7 ± 4.6, p = 0.076) after 72 hours (Figure 10b, d). Additionally, DCs co-cultured with Nalm6 WT or Nalm6 CD200 cells displayed similar MFIs in HLA-DR expression (4133.5 ± 2135.0 vs. 5490.8 ± 1252.1) (Figure 10c, d).

Taken together, DCs showed high initial CD200R expression, which decreased in presence of CD200. Maturation profile of DCs was comparable after contact with Nalm6 WT or Nalm6 CD200 cells.

5.4 Macrophages modulate T cell functionality in presence of CD200 on ALL

Next, co-culture experiments of T cells and ALL cell lines were conducted in the presence of macrophages, addressing the questions if CD200 affect T cell function and which role macrophages play thereby. Thus, macrophages and T cells were generated from the same donor and prepared for co-culture experiments as described in the methods. The bi-specific T cell engager blinatumomab was supplemented to co-cultures, enabling an interaction between T cells and $CD19^+$ target cells. Activation, cytokine expression, proliferation, T helper cell subsets and cytotoxicity of T cells were analysed using flow cytometry.

Activation of T cells was measured after 24 hours of co-culture by staining for CD25 and CD69 (Figure 11a, b). T cells co-cultured with Nalm6 WT cells showed a mean expression of 36.3 ± 3.0 % for CD25 and 43.0 ± 3.8 % for CD69, which was slightly decreased in the presence of CD200 (CD25: 28.3 ± 6.8 %; CD69: 34.2 ± 6.9 %). Addition of macrophages resulted in a general increased expression of T cell activation marker. T cells co-cultured with Nalm6 CD200 cells showed a significantly diminished expression of CD25 and CD69, when compared to co-cultures with Nalm6 WT cells (CD25: 57.4 ± 5.7 % vs. 33.4 ± 9.9 %, p = 0.0285; CD69: 80.4 ± 12.5 % vs. 59.3 ± 23.2 %, p = 0.0248). These data are consistent with analysis of CD137 expression on T cells (data not shown). Further, cytokine release of T cells was investigated by intracellular staining for IFN-γ after 24 hours of co-culture (Figure 11c). T cells co-cultured with Nalm6 WT cells displayed a mean IFN-γ expression of 3.5 ± 1.3 %, while in presence of CD200 on Nalm6 cells IFN-γ expression was significantly reduced (2.6 ± 1.0 %, p = 0.0297). A similar picture could be seen in presence of macrophages (6.2 ± 0.8 % vs. 4.6 ± 0.9 %, p = 0.0122). Addition of macrophages led to general increase in T cell cytokine release. Next, proliferation of T cells was assessed after 72 hours of co-culture (Figure 11d). 55.8 ± 9.1 % of T cells started to proliferate upon contact with Nalm6 WT cells, whereas addition of Nalm6 CD200 cells resulted in a significantly reduced proliferation of 39.9 ± 4.2 % (p = 0.0301).

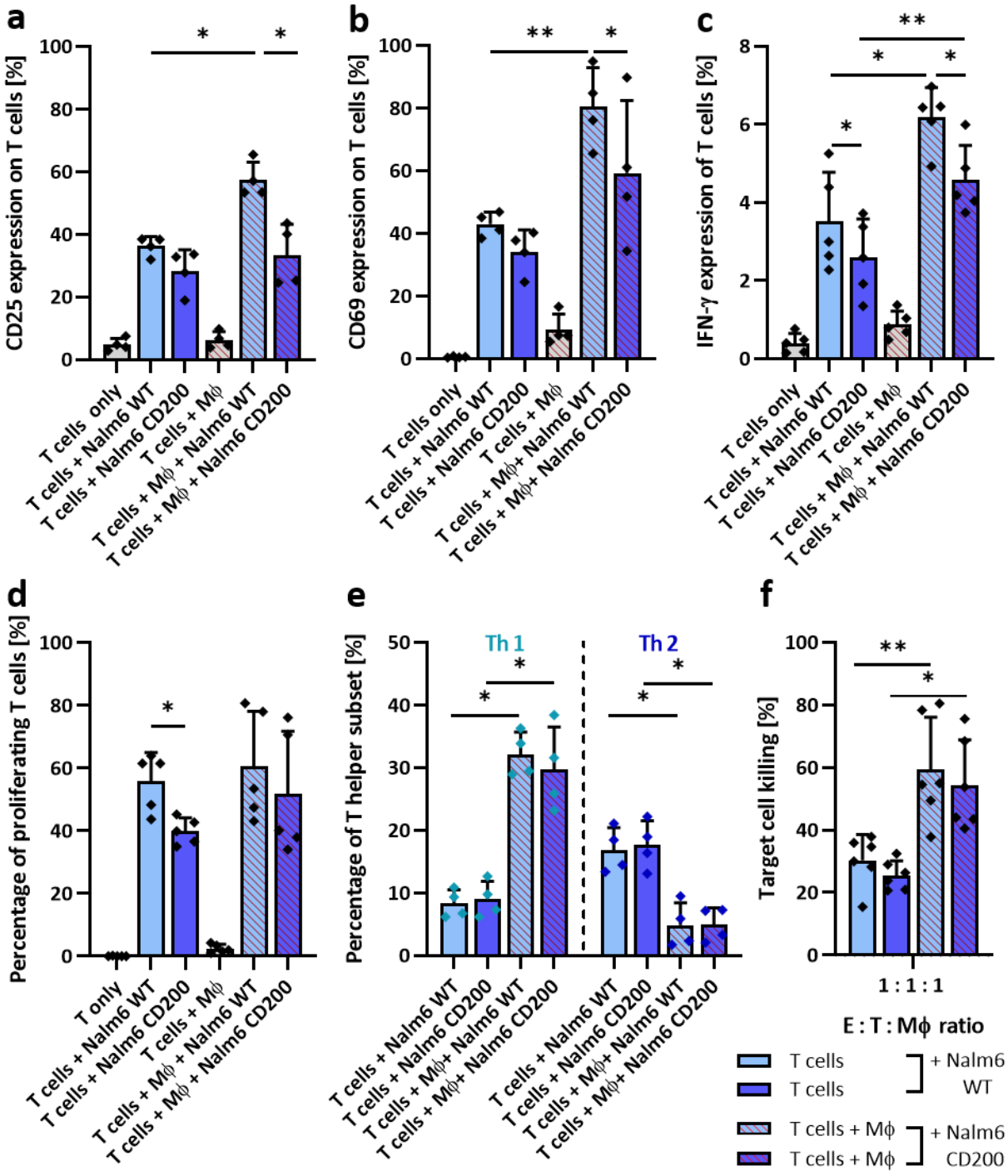

Figure 11: CD200 on ALL leads to reduced T cell functionality mediated through BiTE, which can be modulated by macrophages.

Functionality of T cells were assessed by flow cytometry based analysis of activation markers, cytokines, proliferative capacity, T helper cell subset and cytotoxicity of T cells co-cultured with Nalm6 WT or Nalm6 CD200 target cells in presence or absence of MΦ. Co-cultures were performed in presence of blinatumomab. **a** Percentage of CD25 and **b** CD69 expression on T cells after 24 hours of co-culture. **c** IFN-γ expression of T cells co-cultured for 24 hours measured by intracellular staining. **d** Percentage of proliferating T cells after 72 hours of co-culture. **e** Percentage of Th1 and Th2 cells after 72 hours of co-culture. **f** Cytotoxicity of T cells at an E:T:MΦ ratio of 1:1:1 after 48 hours. Data represent the mean ± SD of ≥ three donors performed in (a, b, c, d, e) singlets or (f) duplicates. P-values were determined using RM one way ANOVA. WT = Wild type. IFN-γ = Interferon gamma. TNF-α = Tumour necrosis factor alpha. MΦ = Macrophages. BiTE = Bi-specific T cell engager blinatumomab.

Upon supplementing the co-cultures with macrophages, T cells co-cultured with Nalm6 WT or Nalm6 CD200 cells shared a similar proliferation profile (60.6 ± 17.6 % vs. 51.8 ± 19.9 %, p = 0.0616). Next, T helper cell subsets were determined (Figure 11e). T cells co-cultured with Nalm6 WT or Nalm6 CD200 cells revealed comparable percentages of Th1 (8.3 ± 2.2 % vs. 9.0 ± 2.9 %) or Th2 T helper cells (16.9 ± 3.6 % vs. 17.7 ± 3.9 %). Although presence of macrophages led to different levels of Th1 und Th2 T cells in general, no differences in co-cultures with Nalm6 WT or Nalm6 CD200 cells regarding Th1 (32.2 ± 3.5 % vs. 29.8 ± 6.7 %) or Th2 (4.9 ± 3.6 % vs. 5.0 ± 2.7 %) levels could be seen. Lastly, cytotoxicity of T cells co-cultured with target cell lines in presence or absence of macrophages was determined after 48 hours (Figure 11f). Killing of target cells was calculated as described in the methods. All T cells showed a dose-dependent killing. At an effector to target to macrophage (E:T:M) ratio of 1:1:1, T cells killed 30.4 ± 8.2 % of Nalm6 WT cells and 25.5 ± 4.6 % Nalm6 CD200 cells. After the addition of macrophages, T cells killed significantly more target cells (59.3 ± 16.8 % of Nalm6 WT cells and 54.3 ± 14.6 % of Nalm6 CD200 cells).

Collectively, CD200 on leukaemic blasts resulted in reduced function in terms of activation, cytokine release, proliferation and cytotoxicity. The presence of macrophages led to general enhanced T cell functionality and more pronounced effects of CD200.

5.5 CD200 on ALL reduces T cell functionality independent of presence of dendritic cells mediated through BiTE

To rule out the role of DCs within CD200 mediated dysfunction in T cells, co-culture experiments of T cells, DCs and target cells were performed analogically to prior experiments with macrophages.

Activation of T cells was investigated by flow cytometry stain for CD25 and CD137 after 24 hours of co-culture. T cells showed high CD25 expression upon contact with Nalm6 WT cells, which was significantly lower in presence of CD200 (63.5 ± 2.2 % vs. 50.9 ± 1.7 %, p = 0.0039) (Figure 12a). A similar picture could be seen, when DC were added to the co-culture (63.0 ± 9.2 % vs. 39.2 ± 2.9 %, p = 0.0208). Moreover, T cells co-cultured with Nalm6 CD200 showed a further significant decrease in CD25 expression, when DCs were present (p = 0.0226). Comparable results were observed for CD137 (Figure 12b). T cells co-cultured with Nalm6 WT cells displayed a CD137 expression of 57.0 ± 2.4 %, while co-culture with Nalm6 CD200 cells significantly reduced CD137 levels to 47.6 ± 3.3 % (p = 0.0032). Likewise, CD200 induced a significant reduction of CD137 expression on T cells presence of DCs (65.7 ± 0.8 % vs. 49.8 ± 6.4 %, p = 0.0492). Upon contact with Nalm6 WT cells, T cells displayed a slightly enhanced (p = 0.0105) CD137 expression after addition of DCs. Next, cytokine expression was analysed in $CD8^+$ T cells after 24 hours of co-culture (Figure 12c, d). T cells co-cultured with Nalm6 WT or Nalm6 CD200 cells showed a mean expression of 5.4 ± 2.4 % vs. 4.0 ± 1.2 % for IFN-γ, and 8.6 ± 2.0 % vs. 6.6 ± 1.7 % for TNF-α.

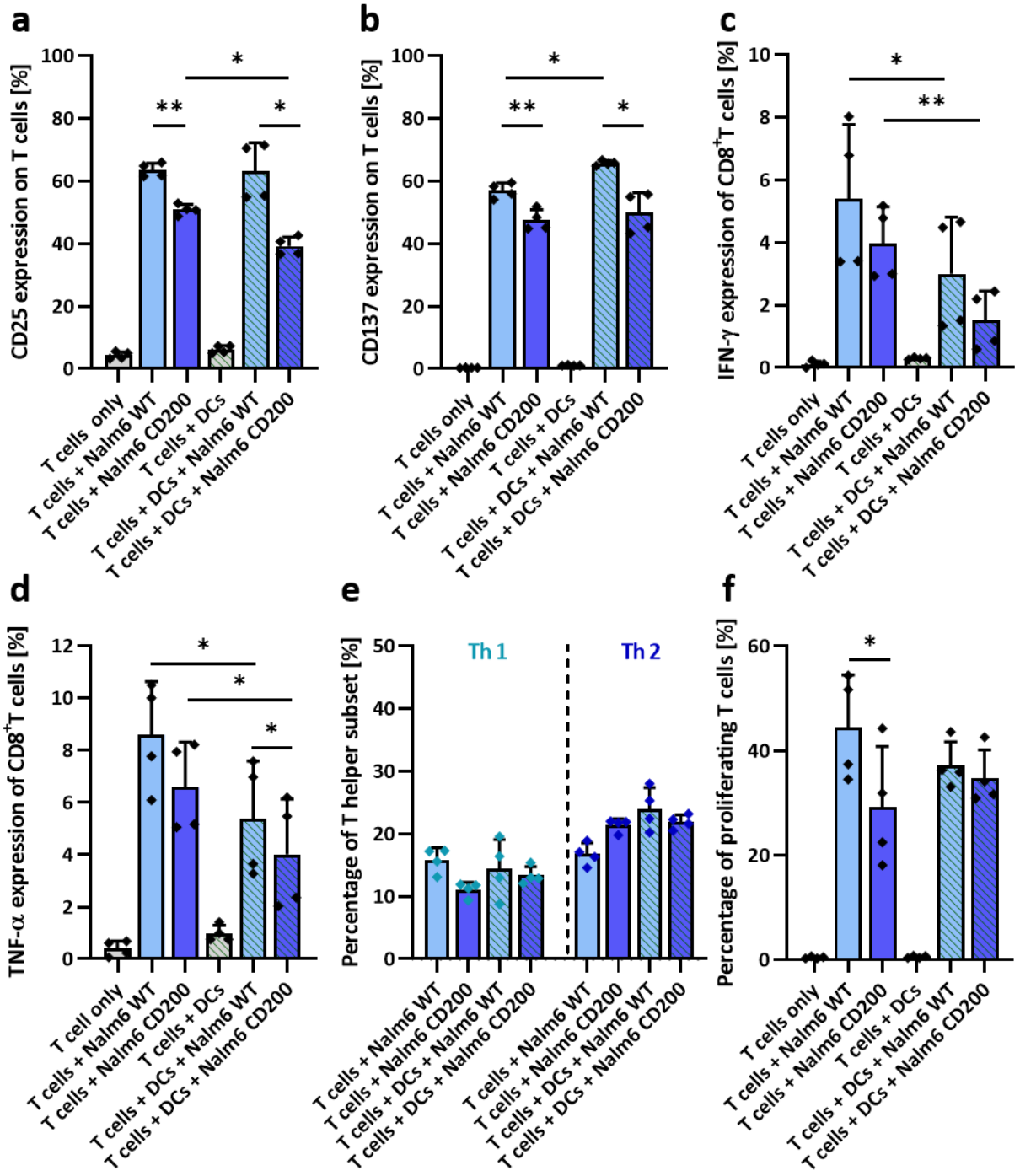

Figure 12: CD200 on ALL reduces T cell functionality independent of presence of dendritic cells mediated through BiTE.

Functionality of T cells was assessed by flow cytometry based analysis of activation markers, cytokines, T helper cell subsets and proliferation of T cells co-cultured with target cells in presence or absence of dendritic cells. Nalm6 WT and Nalm6 CD200 cells were used as target cells. Co-cultures were performed in presence of blinatumomab. **a** Percentage of CD25 and **b** CD137 of T cells after 24 hours of co-culture. **c** IFN-γ and **d** TNF-α expression of T cells co-cultured for 24 hours. **e** Percentage of Th1 and Th2 T helper cells after 72 hours of co-culture. **f** Percentage of proliferating T cells after 72 hours of co-culture. Data represent the mean ± SD of two donors performed in duplicates. P-values were determined using RM one way ANOVA. WT = Wild type. IFN-γ = Interferon gamma. TNF-α = Tumour necrosis factor alpha. FC = Fold change. DC = Dendritic cells. BiTE = Bi-specific T cell engager Blinatumomab.

Addition of DCs led to significant lower levels of IFN-γ and TNF-α independent on the target cell line. In presence of DCs, T cells co-cultured with Nalm6 WT or Nalm6 CD200 cells showed a mean IFN-γ expression of 3.0 ± 1.8 % vs. 1.5 ± 0.9 % and TNF-α expression of 5.4 ± 2.2 % vs. 4.0 ± 2.1 %. Despite a trend towards a reduction of cytokine expression in presence of CD200, significant decrease was only detectable for TNF-α secretion in presence of DCs ($p = 0.0122$). T cells co-cultured with Nalm6 WT or Nalm6 CD200 cells shared a comparable proportion of Th1 (15.8 ± 2.0 % vs. 11.1 ± 1.2%) and Th2 (16.7 ± 1.8 % vs. 21.4 ± 1.1 %) cells measured after 72 hours of co-culture (Figure 12e). DCs did not alter frequencies of Th1 (14.4 ± 4.6 % vs. 13.4 ± 1.4 %) or Th2 (24.0 ± 3.4 % vs. 21.9 ± 1.1 %) subsets when co-cultured with Nalm6 WT or Nalm6 CD200 cells. Lastly, proliferative capacity of T cells was assessed after 72 hours of co-culture (Figure 12f). While 44.5 ± 10.0 % of T cells proliferated upon contact with Nalm6 WT cells, expression of CD200 resulted in a significant reduction of T cell proliferation to 29.2 ± 11.6 % ($p = 0.0188$). In presence of DCs, proliferation profile of T cells co-cultured with Nalm6 WT or Nalm6 CD200 cells was similar (37.2 ± 4.5 % vs. 34.8 ± 5.4 %).

All in all, CD200 mediated T cell dysfunction regarding activation, cytokine release and proliferation was detected. Presence of DCs led to diminished cytokine release and enhanced CD139 expression of T cells.

5.6 CD200 on ALL reduces T cell functionality mediated through BiTE

To further characterize the effect of CD200 on T cells, freshly isolated T cells were co-cultured with Nalm6 WT or Nalm6 CD200 cells in presence of blinatumomab. Supernatant was collected after 48 hours of co-culture and analysed using LEGENDplex™. Despite inter-individual differences, each donor showed a decrease in several tested cytokines and cytolytic proteins when co-cultured with Nalm6 CD200 compared to Nalm6 WT cells (Figure 13a-f). CD200 expression on Nalm6 cells reduced the mean concentrations of interleukin 2 (IL-2) (188.2 pg/ml vs. 55.7 pg/ml, $p = 0.0195$), IFN-γ (6464.8 pg/ml vs. 1939.0 pg/ ml, $p = 0.0161$), TNF-α (362.4 pg/ml vs. 118.4 pg/ml, $p = 0.0446$), FasL (165.0 pg/ml vs. 89.6 pg/ml, $p = 0.0313$), granzyme A (568.2 pg/ml vs. 264.4 pg/ml, $p = 0.1554$) and perforin (113.5 pg/ml vs. 70.2 pg/ml, $p = 0.0088$). Additionally, proliferative ability was assessed after 72 hours of co-culture (Figure 13g). While 44.2 ± 9.1 % of T cells co-cultured with Nalm6 WT cells did not proliferate upon ligation, this fraction was significantly increased in presence of CD200 (60.1 ± 4.4 %, $p = 0.0070$). In absence of CD200 on Nalm6 cells, T cells showed a bigger fraction of cells in first and second generation of proliferation (1st generation: 19.5 ± 4.1% vs. 13.8 ± 3.8 %, $p = 0.0334$, 2nd generation: 23.3 ± 4.0 % vs. 14.9 ± 2.3 %, $p = 0.0053$). Regarding third generation of proliferation, T cells co-cultured with Nalm6 WT or Nalm6 CD200 cells exhibit a similar mean percentage of 12.9 ± 8.1 % and 10.7 ± 6.8 %.

All in all, T cells co-cultured with Nalm6 CD200 cells exhibited significant reduced concentrations of proinflammatory and lytic cytokines, as well as reduced proliferation.

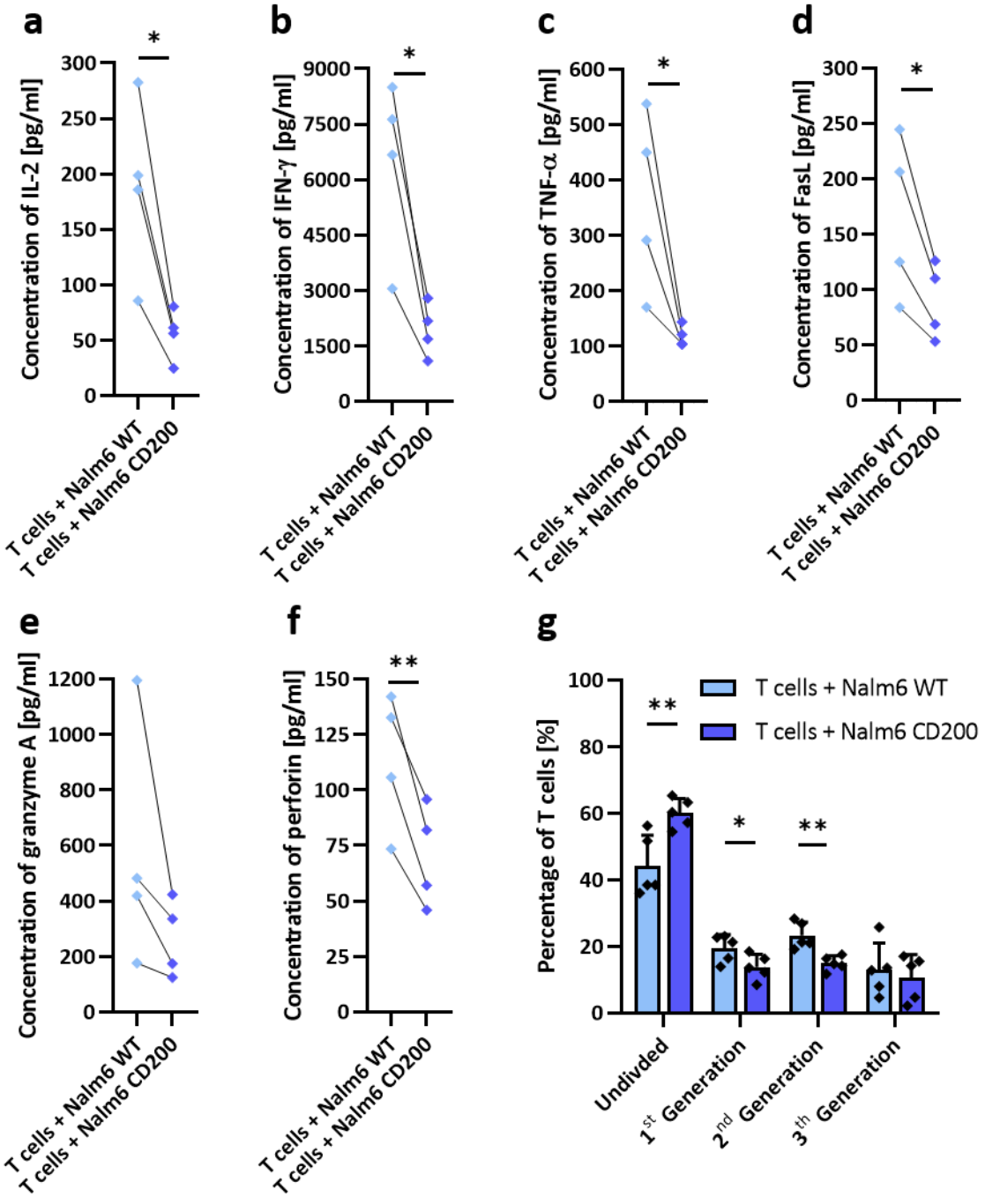

Figure 13: CD200 on ALL reduces T cell functionality mediated through BiTE.
Functionality of T cells were assessed by flow cytometry based analysis of cytokines secretion and proliferative capacity of T cells co-cultured with Nalm6 WT or Nalm6 CD200 target cells. Co-cultures were performed in presence of blinatumomab. **a** Concentration of IL-2, **b** IFN-γ, **c** TNF-α, **d** FasL, **e** granzyme A, and **f** perforin detected in the supernatant of T cells after 48 hours of co-culture with target cells. **g** Percentage of proliferating T cells after 72 hours of co-culture divided into the different generations of proliferation. Data represent the mean ± SD of four donors performed in singlets. P-values were determined using paired Student's t-test. WT = Wild type. IFN-γ = Interferon gamma. TNF-α = Tumour necrosis factor alpha. MΦ = Macrophages. BiTE = Bi-specific T cell engager blinatumomab. Th = T helper cell. FasL = Fas ligand. IL-2 = Interleukin 2.

5.7 Successful generation of CD200R overexpressing T cells and CD200R knock-out T cells with high purity and favourable phenotype

To further investigate the role of CD200R on T cells within the CD200/CD200R axis, overexpression of CD200R was performed in primary human T cells from healthy donors. Additionally, knock-out of CD200R was performed in T cells as an attempt of overcoming CD200 mediated T cell dysfunction (Figure 14a). Retroviral transduction was used to generate either CD200R isoform 1 ($_{RV}$CD200R-Iso1^{OE}) or CD200R isoform 4 ($_{RV}$CD200R-Iso4^{OE}) overexpressing T cells. CD200R isoform 4 represents the full-length protein, while CD200R isoform 1 is missing exon 2. Because potential functional differences of these isoforms are yet to be characterized, both isoforms were used for experiments. Additionally, CRISPR/Cas9 genome editing - using a CD200R-gRNA targeting exon 1 - was performed to knock-out the CD200 receptor on primary human T cells ($_{CR}$CD200R^{KO}). Control T cells were generated using CRISPR/Cas9 genome editing with a non-binding gRNA ($_{CR}$Control).

T cells were cultured for twelve days after transduction or knock-out. Cell count and viability were assessed regularly. After expansion period, $_{RV}$CD200R-Iso1^{OE} T cells and $_{RV}$CD200R-Iso4^{OE} T cells showed 60.4 ± 24.0 -fold and 69.3 ± 19.8 -fold expansion, respectively, with no significant differences to untransduced T cells (69.7 ± 25.1 -fold) (Figure 14b). $_{CR}$CD200R^{KO} T cells grew continuously from day two after electroporation and showed 19.6 ± 10.3 -fold expansion twelve days later. No significant difference in growth was found in comparison to $_{CR}$Control T cells (25.2 ± 14.8 -fold) (Figure 14c). Viability of all T cells remained stable during expansion with no significant differences within different T cell conditions. The mean viability on day twelve for $_{RV}$CD200R-Iso1^{OE} T cells and $_{RV}$CD200R-Iso4^{OE} T cells were 91.9 ± 2.9 % and 92.0 ± 4.7 %, respectively (Figure 14d). $_{CR}$CD200R^{KO} T cells showed a mean viability of 87.9 ± 9.0 % (Figure 14e).

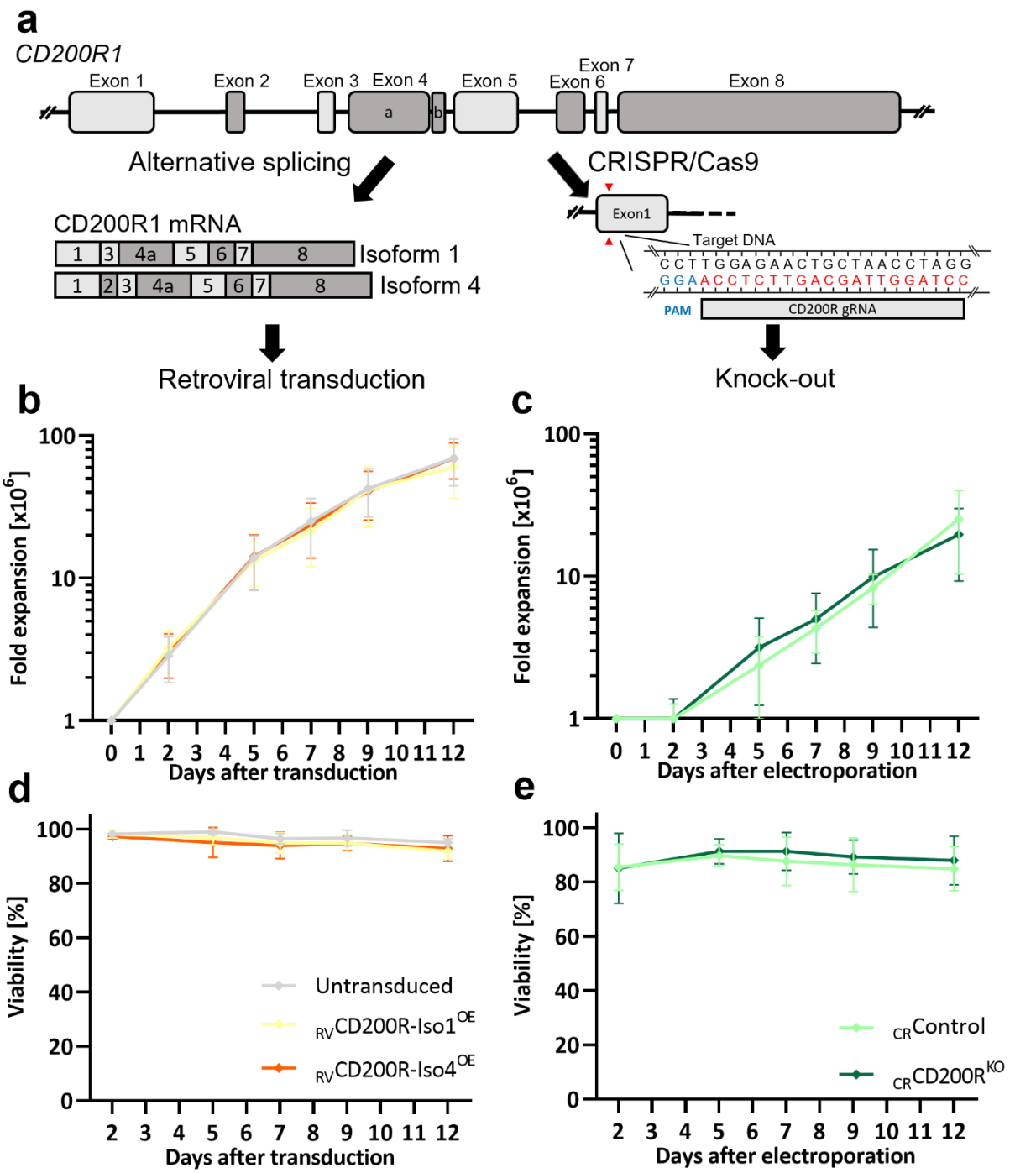

Figure 14: T cells with CD200R overexpression or CD200 knock-out maintain their proliferative capacity and viability during expansion.
Expansion and viability of T cells were determined regularly by counting using the Neubauer haemocytometer during twelve days of expansion. **a** Schematic overview over different T cell conditions. Retroviral transduction of either CD200R isoform 1 or CD200R isoform 4, were used to induce CD200R overexpression on T cells. CRISPR/Cas9 mediated knock-out of CD200R was performed in T cells to generate CD200R negative T cells. **b** Logarithmic presentation of fold expansion of CD200R overexpressing T cells and **c** CD200R knock-out T cells and their respective controls. **d, e** Viability for each T cell condition during the expansion period. Viability was defined as ratio between vital cell count and total cell count. Data represent the mean ± SD of four donors. P-values were determined using (b, d) RM one way ANOVA and (c, e) paired Student's t-test.

The final T cell product was characterised after expansion period of twelve days. While untransduced T cells showed an endogenous CD200R expression of 14.0 ± 3.5 %, a mean transduction rate of 59.5 ± 18.3 % and 65.9 ± 13.0 % could be reached for $_{RV}$CD200R-Iso1^{OE} T cells and $_{RV}$CD200R-Iso4^{OE} T cells (Figure 15a, c). $_{CR}$CD200R^{KO} T cells showed a reduced CD200R expression of 1.5 ± 1.7 % in comparison to $_{CR}$Control T cells (11.7 ± 2.3 %). To quantify the editing efficacy of the CRISPR/Cas9 mediated knock-out of CD200R, Sanger sequencing of $_{CR}$CD200R^{KO} T cells and $_{CR}$Control T cells was performed and analysed using TIDE analysis (Figure 15b, c). The calculated knock-out rate for $_{CR}$CD200R^{KO} T cells (90.6 ± 1.9 %) on DNA level was significantly higher than for $_{CR}$Control T cells (1.4 ± 0.8 %, p = 0.0003). To define the cellular composition of the final product, T cells were stained for lineage markers (Figure 15d). $_{RV}$CD200R-Iso1^{OE} T cells, $_{RV}$CD200R-Iso4^{OE} T cells and $_{CR}$CD200R^{KO} T cells shared a similar proportion of CD4^{+} T cells (45.8 ± 10.7 %, 45.6 ± 11.8 % and 52.3 ± 7.7 %), CD8^{+} T cells (29.5 ± 5.2 %, 29.7 ± 6.2 % and 27.7 ± 4.7 %) and natural killer T cells (22.0 ± 9.7 %, 21.7 ± 8.5 % and 17.3 ± 4.5 %), with no significant alterations to their respective controls. Less than 3 % of other cells including B cells, NK cells and monocytes were found in all conditions. Addressing the question if CD200R overexpression or CD200R knock-out has an impact on the phenotype of T cells, a phenotypic characterisation based on CD45RO, CD62L and CD95 was performed at the end of expansion period (Figure 15e). For evaluation of flow cytometry data of phenotype, T cells were gated according to the gating strategy for the different T cell conditions (see Table 9). Analysis revealed a central memory-predominant phenotype for all T cells. $_{RV}$CD200R-Iso1^{OE} T cells, $_{RV}$CD200R-Iso4^{OE} T cells and $_{CR}$CD200R^{KO} T cells consisted of 60.7 ± 7.8 %, 61.9 ± 10.8 % and 71.1 ± 11.6 % central memory T cells (T_{CM}). Stem cell-like memory T cells (T_{SCM}) represented the second largest population with a mean of 30.8 ± 12.0 %, 30.2 ± 14.4 % and 23.2 ± 9.9 % for $_{RV}$CD200R-Iso1^{OE}, $_{RV}$CD200R-Iso4^{OE} and $_{CR}$CD200R^{KO} T cells. Only a few cells (< 1.1 %) were fully differentiated into effector T cells (T_{EFF}). $_{RV}$CD200R-Iso1^{OE} T cells, $_{RV}$CD200R-Iso4^{OE} T cells and $_{CR}$CD200R^{KO} T cells showed no significant differences to untransduced T cells or $_{CR}$Control T cells.

All in all, CD200R overexpressing T cells and CD200R knock-out T cells were successfully generated. The cellular composition revealed a high purity of all T cell products and a low differentiated phenotype.

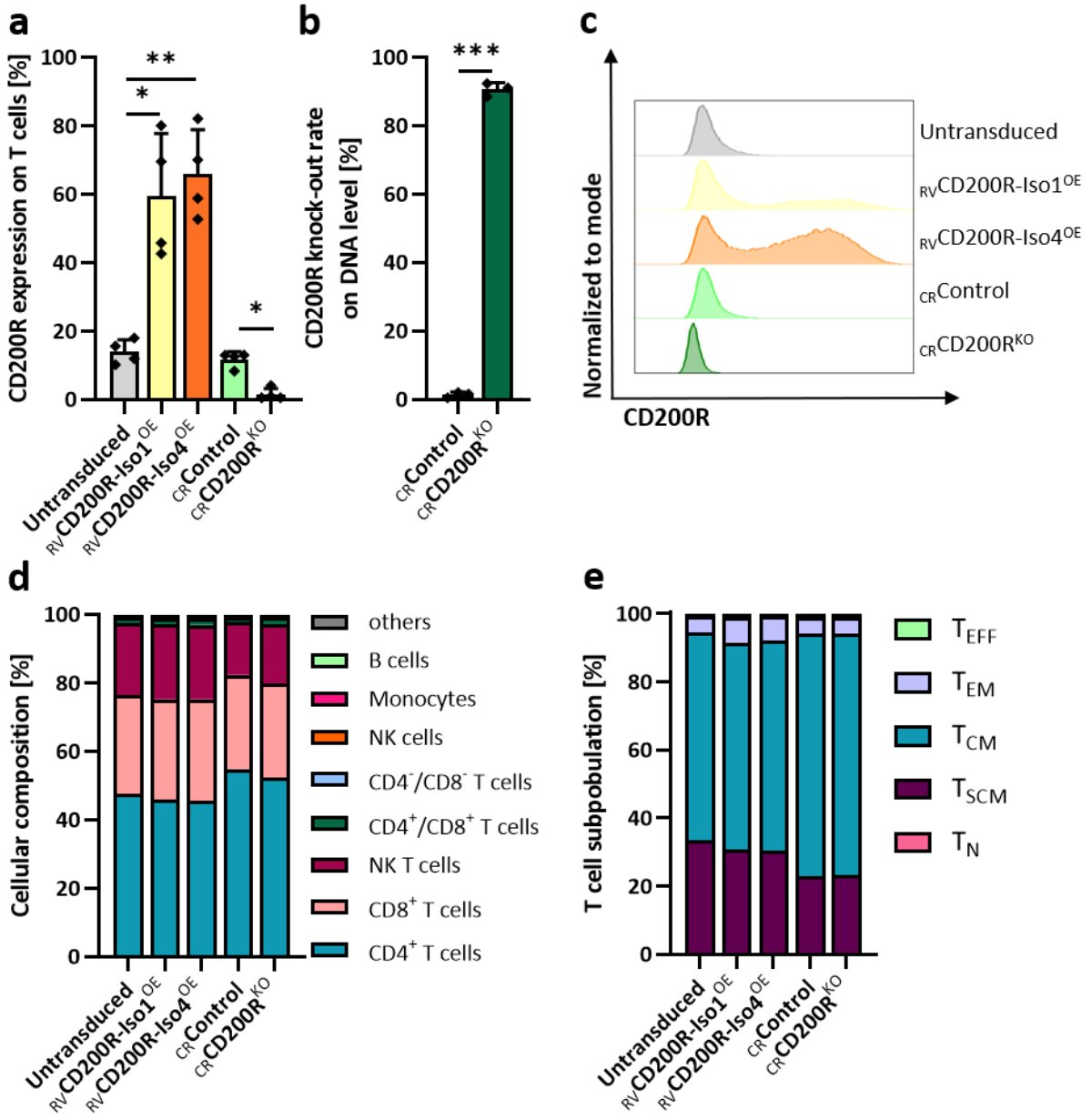

Figure 15: T cell product of CD200R overexpressing T cells and CD200R knock-out T cells shows high purity and favourable phenotype.

T cells were characterized by flow cytometry-based analysis of transduction rate, cellular composition and phenotype after expansion period of twelve days. **a** Percentage of CD200R expression of CD200R overexpressing T cells and CD200R knock-out T cells and their respective controls. **b** Calculated CD200R knock-out rate on DNA level assessed by TIDE analysis. **c** Representative flow cytometry histograms of the different T cell conditions. **d** Cellular composition of the final T cell product. **e** Percentage of T cell subpopulations after expansion. Data represent the mean (d, e) ± SD (a, b) ≥ three donors. P-values were determined using (a, d, e) RM one way ANOVA and (b) paired Student's t-test. NK = natural killer. T_{EFF} = Effector T cells; T_{EM} = Effector memory T cells; T_{CM} = Central memory T cells; T_{SCM} = Stem cell-like memory T cells; T_N = Naive T cells.

5.8 CD200R knock-out protects T cells against CD200 expressing target cells

To assess the functionality of $_{RV}$CD200R-Iso1^{OE} T cells, $_{RV}$CD200R-Iso4^{OE} T cells, $_{CR}$CD200R^{KO} T cells and their respective controls, cytotoxicity, activation, cytokine release and proliferation were measured after co-culture with either Nalm6 WT or Nalm6 CD200 target cell. Blinatumomab was added to induce an interaction between T cells and target cells. For assessment of flow cytometry data, T cells were gated according to the gating strategy for the different T cell conditions (see Table 9).

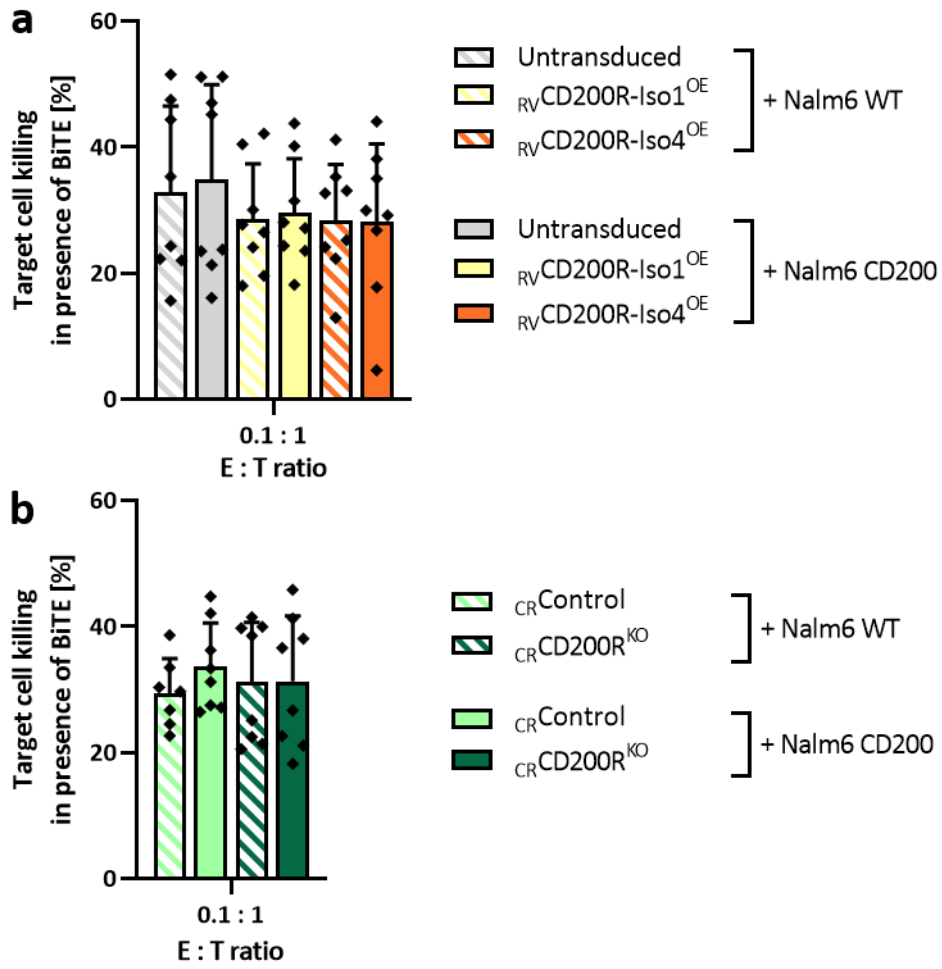

Figure 16: CD200R overexpressing and CD200R knock-out T cells kill target cells efficiently.
Cytotoxicity of T cells were assessed by flow cytometry based analysis of T cells co-cultured with Nalm6 WT and Nalm6 CD200 target cell line in presence of BiTE for 48 hours. **a** Cytotoxicity of CD200R overexpressing T cells and **b** CD200R knock-out T cells and their respective controls at an E:T ratio of 0.1:1. Percentage of killing was determined according to methods. Data represent the mean ± SD of four donors performed in duplicates. P-values were determined using RM one way ANOVA. WT = Wild type. E:T ratio = Effector to target ratio. BiTE = Bi-specific T-cell engager blinatumomab.

To determine cytotoxicity, T cells were co-cultured with target cells for 48 hours. All T cell conditions revealed a similar killing of both Nalm6 WT and Nalm6 CD200 target cells. Significant differences were neither found between the different T cell conditions nor due presence of CD200 on leukaemic cell line. At an E:T ratio of 0.1:1, $_{RV}$CD200R-Iso1^{OE} T cells killed

28.6 ± 8.8 % Nalm6 WT cells and 29.6 ± 8.6 % Nalm6 CD200 cells, and $_{RV}$CD200R-Iso4^{OE} T cells killed 28.4 ± 8.9 % and 28.2 ± 12.4 % (Figure 16a). In the CRISPR/Cas9 edited T cells comparable results were found. At an E:T ratio of 0.1:1, $_{CR}$CD200R^{KO} T cells killed 31.2 ± 9.5 % of Nalm6 WT cells and 31.3 ± 10.4 % of Nalm6 CD200 cells (Figure 16b).

Further, T cells were co-cultured for 48 hours with Nalm6 WT or Nalm6 CD200 cells and then stained for CD25 to elucidate their activation potential (Figure 17a). All T cell conditions displayed a similar CD25 expression upon co-culture with Nalm6 WT target cells, ranging from 63.0 % to 93.6 %. Upon contact with Nalm6 CD200 cells, untransduced T cells, $_{RV}$CD200R-Iso1^{OE}, $_{RV}$CD200R-Iso4^{OE} and $_{CR}$Control T cells showed a tendency towards a slight reduction in CD25 expression (67.2 ± 6.5 %, p = 0.1757; 62.1 ± 7.1 %, p < 0.0001; 68.2 ± 8.7 %, p= 0.1038; 68.3 ± 8.7 %, p = 0.0027), while this could not be seen for $_{CR}$CD200R^{KO} (77.7 ± 11.3 % vs. 75.9 ± 6.4 %). Next, cytokine production was captured by intracellular staining of IFN-γ and TNF-α after 24 hours of co-culture (Figure 17b, c). $_{RV}$CD200R-Iso1^{OE} T cells and $_{RV}$CD200R-Iso4^{OE} T cells displayed a significant lower percentage of IFN-γ positive T cells in presence of CD200 on target cells (7.8 ± 2.8 %, p = 0.0044 and 6.3 ± 1.7 %, p = 0.0482), than upon contact to Nalm6 WT target cells (12.6 ± 4.0 % and 10.6 ± 2.9 %). For untransduced T cells and $_{CR}$Control T cells a non-significant tendency towards decreased IFN-γ levels in presence of CD200 was seen. $_{CR}$CD200R^{KO} T cells demonstrated similar IFN-γ expression after co-culture with Nalm6 WT or Nalm6 CD200 cells (10.8 ± 2.6 % vs. 10.8 ± 3.5 %). For TNF-α, comparable results were found. In comparison to co-culture with Nalm6 WT cells, $_{RV}$CD200R-Iso1^{OE} T cells and $_{RV}$CD200R-Iso4^{OE} T cells co-cultured with Nalm6 CD200 cells displayed a significant decrease of TNF-α positive cells (5.1 ± 1.0 % vs. 2.7 ± 0.6 %, p = 0.0033 and 4.0 ± 0.9 % vs. 2.3 ± 0.3 %, p = 0.0482). For $_{CR}$CD200R^{KO} T cells no significant differences were found (4.0 ± 1.1 % vs. 3.7 ± 1.3 %). Proliferation was measured after 72 hours of co-culture (Figure 17d). T cells varied strongly in their intrinsic state of proliferation in the unstimulated control. Therefore, fold changes were calculated as described in the methods to make values more comparable. Untransduced T cells, $_{RV}$CD200R-Iso1^{OE} and $_{RV}$CD200R-Iso4^{OE} T cells revealed a reduction in proliferation after contact with Nalm6 CD200 target cells (0.091 ± 0.05 -fold, 0.82 ± 0.1 -fold and 0.85 ± 0.09 -fold). $_{CR}$CD200R^{KO} T cells showed a slightly enhanced proliferation (0.97 ± 0.02 -fold, p = 0.0289) in presence of CD200 than $_{CR}$Control T cells (0.93 ± 0.03 -fold).

Taken together, the CD200R overexpressing T cell conditions $_{RV}$CD200R-Iso1^{OE} and $_{RV}$CD200R-Iso4^{OE} showed reduced functionality in presence of CD200 on target cells. Despite statistically significant reductions through CD200, the biological relevance of these results remains to be further investigated. No differences in functionality between $_{RV}$CD200R-Iso1^{OE}

and $_{RV}$CD200R-Iso4^{OE} T cells could be detected. $_{CR}$CD200R^{KO} T cells remained fully functional and killed target cells efficiently even in presence of CD200.

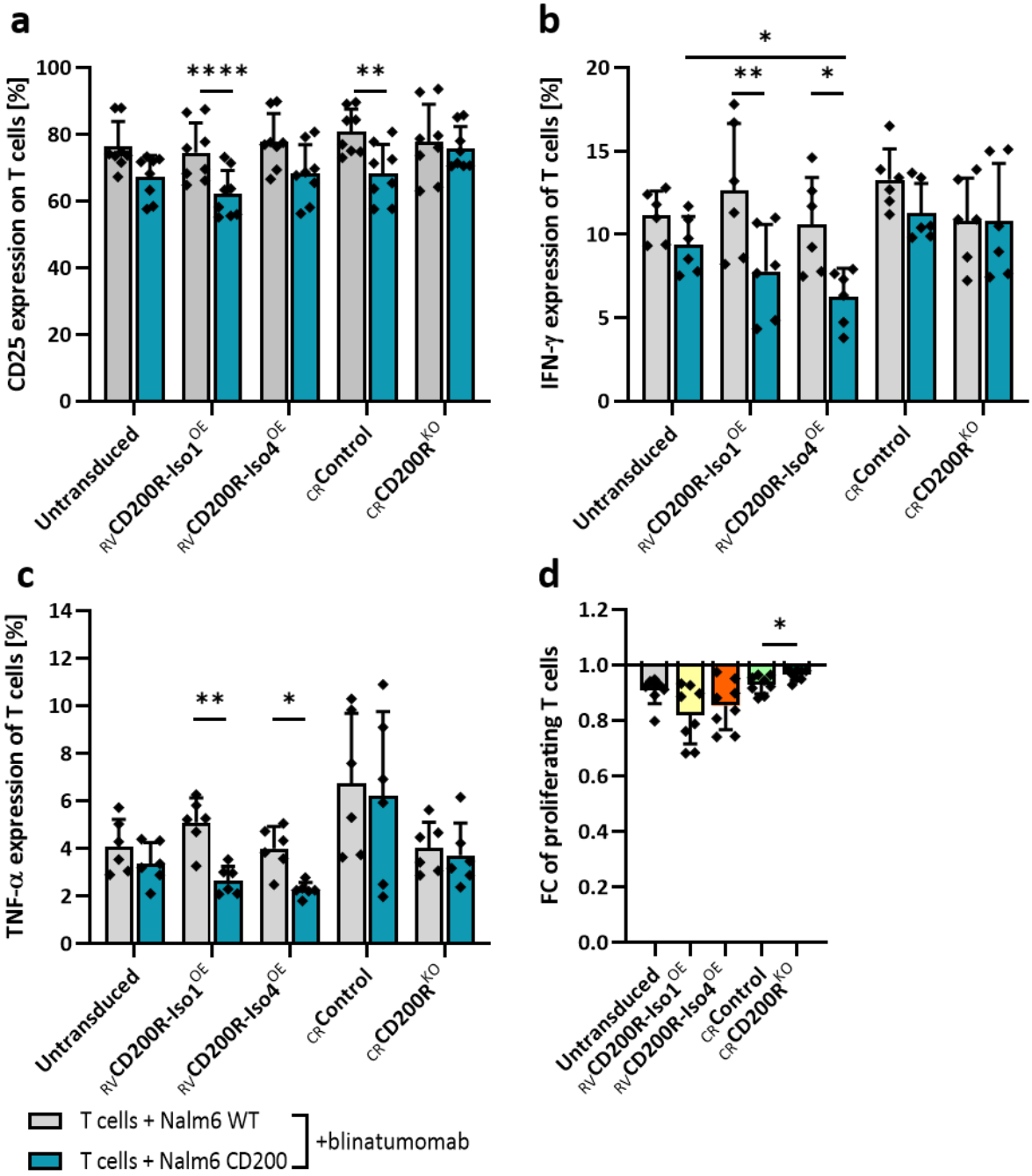

Figure 17: CD200R overexpressing T cells show reduced functionality in presence of CD200, while CD200R knock-out T cells remain fully functional.
Functionality of T cells was assessed by flow cytometry-based analysis of activation marker, cytokines and proliferation of T cells co-cultured with Nalm6 WT and Nalm6 CD200 target cell lines in presence of blinatumomab. **a** Percentage of CD25 positive T cells after 48 hours of co-culture. **b** Percentage of IFN-γ positive and **c** TNF-α positive T cells measured by intracellular staining after 24 hours of co-culture. **d** Fold change of proliferating T cells after 72 hours of co-culture. Data represent the mean ± SD of ≥ three donors performed in duplicates. P-values were determined using RM one way ANOVA. The biologic relevance of statistic significant changes, shown here, will be discussed subsequently. WT = Wild type. IFN-γ = Interferon gamma. TNF-α = Tumour necrosis factor alpha. FC = Fold change. BiTE = Bi-specific T-cell engager blinatumomab.

5.9 Successful generation of CD200R overexpressing and CD200R knock-out CAR T cells with high purity and favourable phenotype

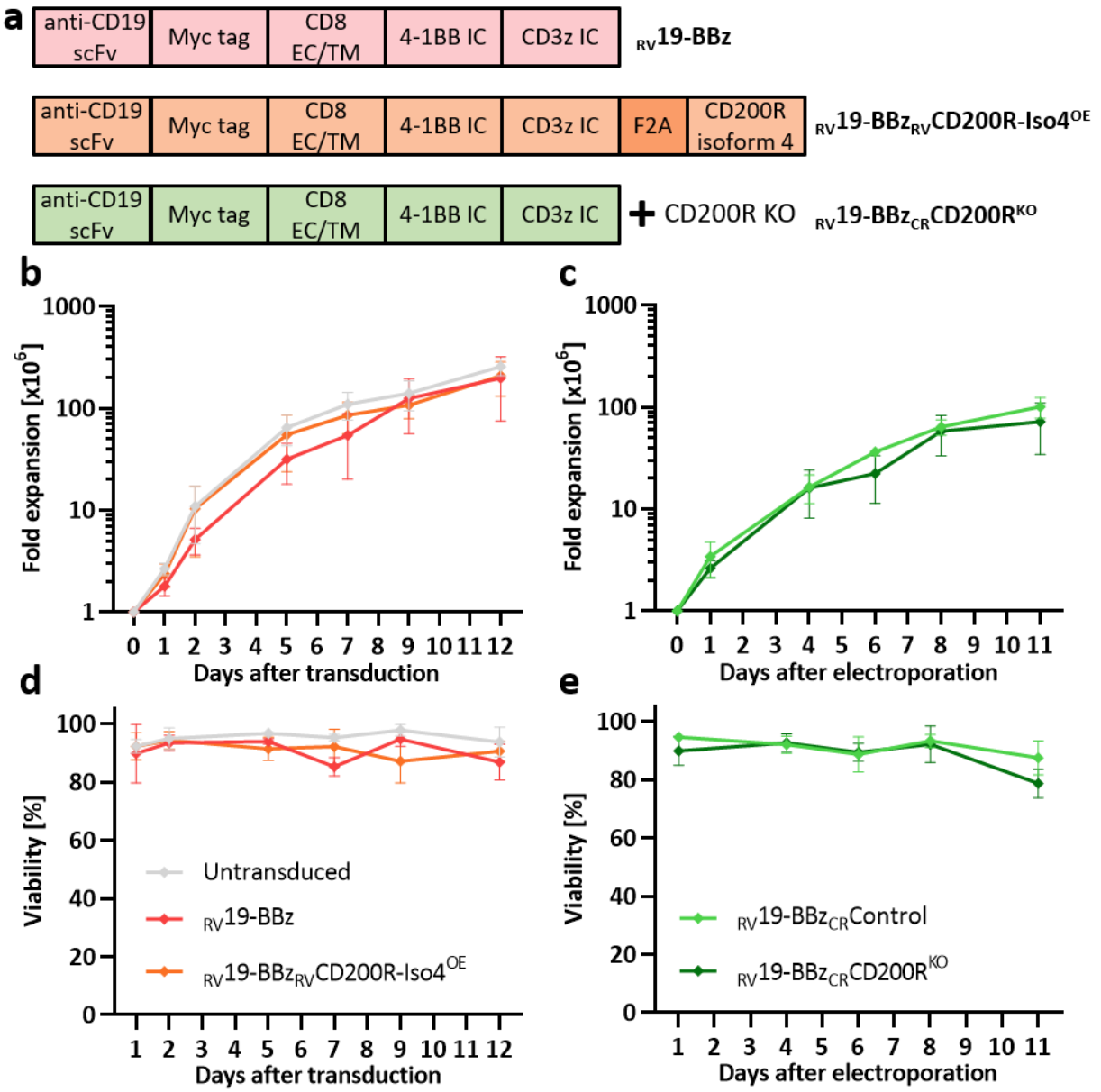

Figure 18: CD200R overexpressing CAR T cells, and CD200R knock-out CAR T cells maintain their proliferative capacity and viability during expansion.
Expansion and viability of CAR T cells were determined regularly by counting using the Neubauer haemocytometer during expansion period. **a** Schematic depiction of the design of the different CAR T cell conditions. **b** Logarithmic presentation of fold expansion of CD200R overexpressing CAR T cells and **c** CD200R knock-out CAR T cells and their respective controls. **d, e** Viability for each CAR T cell condition over the expansion period. Viability was defined as ratio between vital cell count and total cell count. Data represent the mean ± SD of four donors. P-values were determined using (b, d) RM one way ANOVA and (c, e) paired t test. ScFv = Single chain variable fragment. EC = Extracellular. TM = Transmembrane. IC = Intracellular.

In the next experiments, the influence of CD200/CD200R axis on CAR T cells was investigated. Therefore, second generation CAR T cells with CD200R overexpression ($_{RV}$19-BBz$_{RV}$CD200R-Iso4^{OE}) were produced by retroviral transduction of primary human T cells from healthy donors. The used second generation CAR construct consisted of an anti-CD19 scFV as antigen-binding domain, a myc tag to enable detection by flow cytometry, a CD8 extracellular and transmembrane spacer domain as well as a CD3ζ intracellular domain. 4-1BB served as costimulatory intracellular domain. The second generation CAR construct was linked by a F2A linker to the isoform 4 of the CD200R to ensure co-expression. Conventional second generation CAR T cells ($_{RV}$19-BBz) and untransduced T cells served as controls. At the same time, a part of the $_{RV}$19-BBz CAR T cells underwent CRISPR/Cas9 mediated knock-out of CD200R 24 hours after transduction to generate second generation CAR T cells carrying a CD200R knock-out ($_{RV}$19-BBz$_{CR}$CD200R^{KO}). Control CAR T cells were generated using CRISPR/Cas9 genome editing with a non-binding gRNA ($_{RV}$19-BBz$_{CR}$Control) (Figure 18a).

T cells were compared in their expansion capacity and viability. On day twelve after transduction, $_{RV}$19-BBz$_{RV}$CD200R-Iso4^{OE} CAR T cells showed a similar expansion of 209.1 ± 77.1 -fold compared to untransduced T cells and conventional $_{RV}$19-BBz CAR T cells (258.3 ± 49.0 -fold and 198.0 ± 122.5 -fold) (Figure 18b). $_{RV}$19-BBz$_{CR}$CD200R^{KO} and $_{RV}$19-BBz$_{CR}$Control CAR T cells revealed equal continuous growth during expansion (72.1 ± 37.9 -fold vs. 100.9 ± 23.2 -fold) (Figure 18c). Each T cell condition displayed high mean viabilities on day twelve ranging from 74.0 - 96.5 % (Figure 18d, e).

After expansion period, T cells were further characterised. Transduction rate was measured by staining for CD200R and c-myc to detect CARs (Figure 19a). $_{RV}$19-BBz$_{RV}$CD200R-Iso4^{OE} CAR T cells exhibited a high transduction rate of the CAR (67.9 ± 9.8 %). Since $_{RV}$19-BBz, $_{RV}$19-BBz$_{CR}$CD200R^{KO}, and $_{RV}$19-BBz$_{CR}$Control CAR T cells were generated from the same CAR T cell pool, all conditions showed comparable CAR expression of 36.8 ± 8.4 %, 33.1 ± 10.5 % and 33.3 ± 10.2 % (Figure 19b). Untransduced T cells, $_{RV}$19-BBz and $_{RV}$19-BBz$_{CR}$Control CAR T cells revealed an endogenous CD200R expression of less than 15 %, while $_{RV}$19-BBz$_{RV}$CD200R-Iso4^{OE} CAR T cells reached a mean transduction rate of CD200R of 76.4 ± 10.2 %. Co-expression of CD200R and CAR could be proven (Figure 19a). $_{RV}$19-BBz$_{CR}$CD200R^{KO} CAR T cells showed a reduced CD200R expression of 0.5 ± 0.3 % in comparison to $_{RV}$19-BBz$_{CR}$Control CAR T cells (7.4 ± 5.6 %) (Figure 19c). To quantify the editing efficacy of the CRISPR/Cas9 mediated knock-out of CD200R, sanger sequencing data of $_{RV}$19-BBz$_{CR}$CD200R^{KO} CAR T cells and $_{RV}$19-BBz$_{CR}$Control CAR T cells were compared to untransduced T cells using TIDE analysis. The calculated knock-out rate for $_{RV}$19-BBz$_{CR}$CD200R^{KO} CAR T cells was significantly higher than for $_{RV}$19-BBz$_{CR}$Control CAR T cells (79.5 ± 6.0 % vs. 2.9 ± 1.6 %, p = 0.0002) (Figure 19d). To determine T cell subsets in the final product, T cells were stained for several lineage markers. $_{RV}$19-BBz$_{RV}$CD200R-Iso4^{OE} CAR T cells

were composed of a mean of 53.6 ± 9.9 % $CD4^+$ T cells, 33.4 ± 8.1 % $CD8^+$ T cells and 8.7 ± 2.2 % natural killer T cells. No significant differences to untransduced T cells or $_{RV}$19-BBz CAR T cells were detectable. $_{RV}$19-$BBz_{CR}$$CD200R^{KO}$ CAR T cells had a comparable composition to $_{RV}$19-BBz_{CR}Control CAR T cells and consisted of a mean of 48.6 ± 7.4 % $CD4^+$ T cells, 36.4 ± 6.2 % $CD8^+$ T cells and 9.7 ± 2.2 % natural killer T cells. Less than 5 % of other cells including B cells, NK cells and monocytes were found within the different T cell conditions (Figure 19e). At the end of expansion, CAR T cells underwent phenotype characterisation in order to disclose potential impact through CD200R overexpression or CD200R knock-out. For evaluation, T cells were gated according to the gating strategy for the different T cell conditions (see Table 9). All T cells showed a stem cell-like memory-predominated phenotype. High interindividual differences were observed. $_{RV}$19-BBz_{RV}CD200R-$Iso4^{OE}$ CAR T cells and $_{RV}$19-$BBz_{CR}$$CD200R^{KO}$ CAR T cells consisted of less than 1 % of T_N, 37.7 ± 24.1 % and 45.2 ± 20.7 % of T_{SCM} and 12.3 ± 4.9 % and 10.2 ± 4.1 % T_{CM}. 26.7 ± 20.9 % and 22.7 ± 14.0 % were effector memory T cells and 23.1 ± 8.5 % and 21.7 ± 5.3 % were fully differentiated into effector T cells. $_{RV}$19-BBz_{RV}CD200R-$Iso4^{OE}$ CAR T cells and $_{RV}$19-$BBz_{CR}$$CD200R^{KO}$ CAR T cells showed no significant differences to their respective controls (Figure 19f).

All in all, CD200R overexpressing and CD200R knock-out CAR T cells could be successfully generated. The cellular composition revealed a high purity of all T cell products including an early differentiated phenotype.

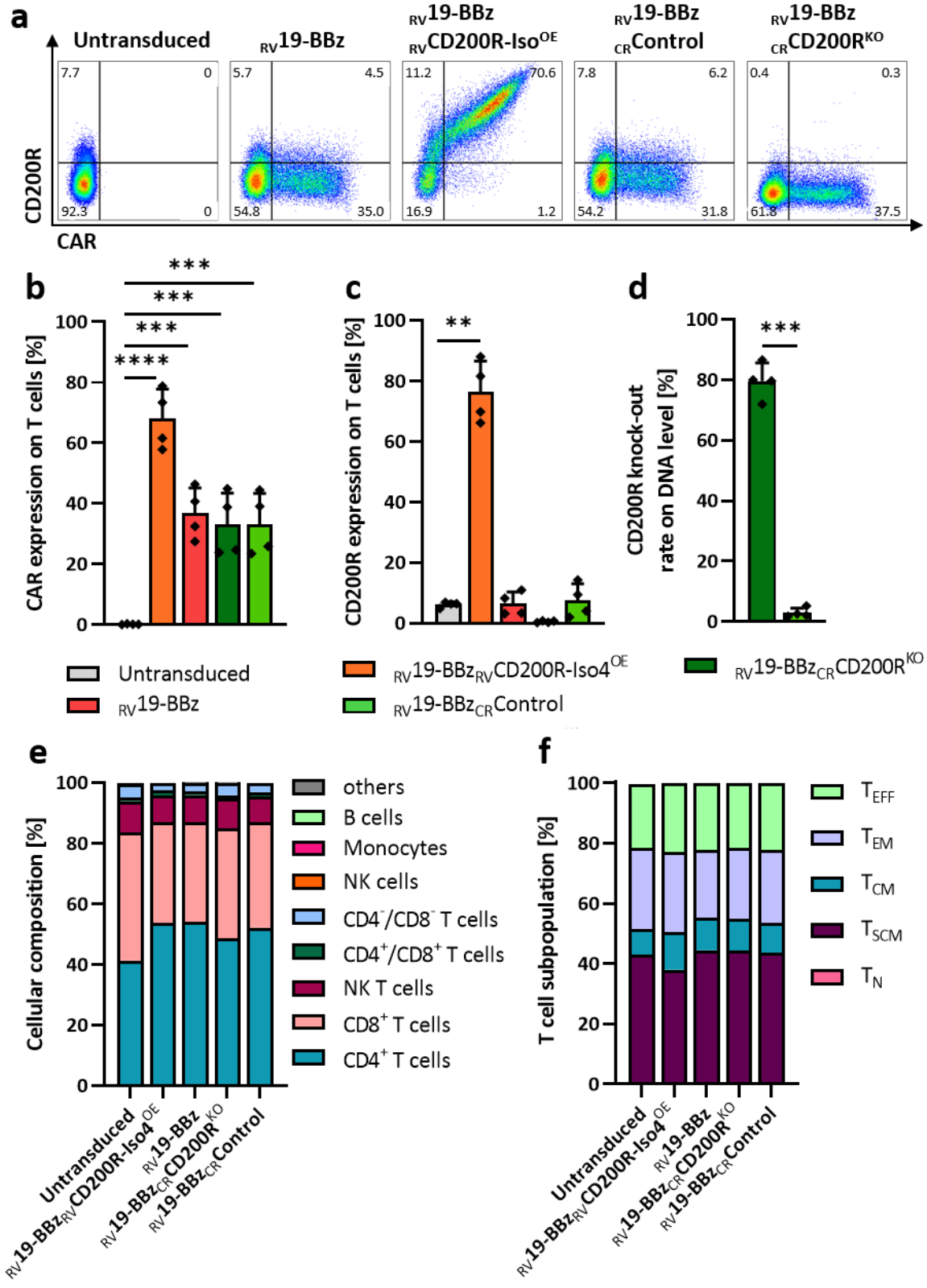

Figure 19: CAR T cell product shows high purity and Tscm dominating phenotype.
CAR T cells were characterized by flow cytometry based analysis of transduction rate, cellular composition and phenotype after expansion period. **a** Representative flow cytometry dot plots of the different CAR T cell conditions. **b** Expression of the CAR construct detected by c-myc staining and **c** CD200R. **d** Calculated CD200R knock-out rate on DNA level assessed by TIDE analysis. **e** Cellular composition of final T cell product. **f** Percentage of CAR T cell subpopulations. Data represent the (d, e) mean (a, b) ± SD of four donors. P-values were determined using RM one way ANOVA. NK = Natural killer. T_{EFF} = Effector T cells; T_{EM} = Effector memory T cells; T_{CM} = Central memory T cells; T_{SCM} = Stem cell-like memory T cells; T_N = Naïve T cells.

5.10 CD200R knock-out attenuates the inhibitory effect of CD200 on CAR T cells

To assess the functionality of $_{RV}$19-BBz$_{RV}$CD200R-Iso4^{OE} CAR T cells and $_{RV}$19-BBz$_{CR}$CD200R^{KO} CAR T cells as well as of their respective controls, cytotoxicity, activation markers, cytokine production and proliferation were measured using flow cytometry after co-culturing T cells with either Nalm6 WT or Nalm6 CD200 target cells. For evaluation of flow cytometry data, T cells were gated according to the gating strategy for different T cell conditions (see Table 9).

Elucidating cytotoxicity, T cells were co-cultured with target cell lines for 48 hours in 1:1, 0.1:1 and 0.01:1 E:T ratios. Killing of target cells was calculated as described in the methods. All T cells showed a dose-dependent killing. At an E:T ratio of 0.1:1, $_{RV}$19-BBz$_{RV}$CD200R-Iso4^{OE} CAR T cells and $_{RV}$19-BBz CAR T cells displayed similar killing of Nalm6 WT cells. In the presence of CD200 on target cells, $_{RV}$19-BBz$_{RV}$CD200R-Iso4^{OE} CAR T cells showed a significantly reduced killing capacity (79.6 ± 9.1 % vs. 48.6 ± 10.4 %, $p < 0.0001$) (Figure 20a).

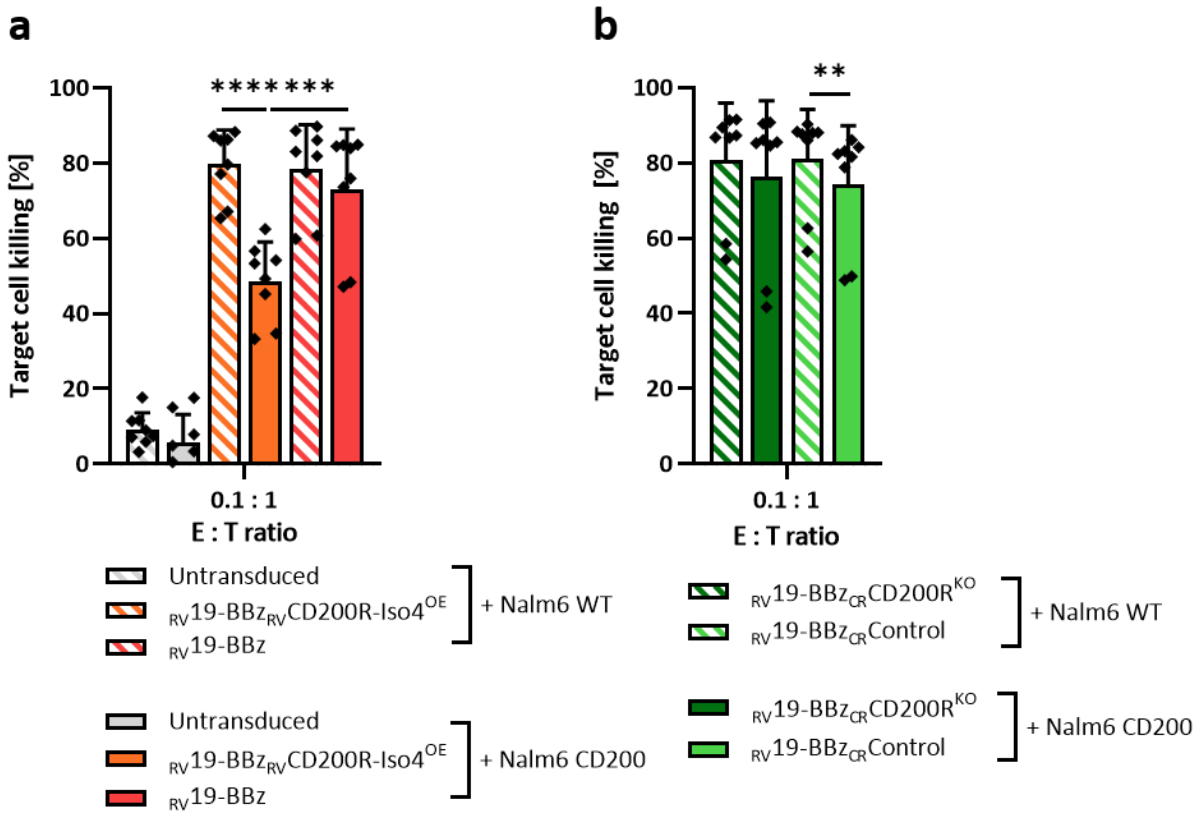

Figure 20: CD200R overexpression reduces killing capacity of CAR T cells in presence of CD200, while CD200R knock-out CAR T cells remain highly effective.
Killing capacity of CAR T cells was assessed by flow cytometry based analysis of CAR T cells co-cultured with either Nalm6 WT or Nalm6 CD200 target cells for 48 hours. **a** Cytotoxicity of CD200R overexpressing and **b** CD200R knock-out T cells as well as their respective controls at an E:T ratio of 0.1:1. Data represent the mean ± SD of four donors performed in duplicates. P-values were determined using RM one way ANOVA. The biologic relevance of statistic significant changes, shown here, will be discussed subsequently. WT = Wild type. E:T ratio = Effector to target ratio.

$_{RV}$19-BBz$_{CR}$CD200R^{KO} CAR T cells yielded comparable cytotoxicity against Nalm6 WT or Nalm6 CD200 cells (80.7 ± 15.1 % vs. 76.2 ± 20.2 %), while $_{RV}$19-BB$_{CR}$Control CAR T cells showed a significant reduction of cytotoxicity in presence of CD200 (80.9 ± 13.3 % vs. 74.3 ± 15.6 %, p = 0.0076) which biological relevance needs to be discussed (Figure 20b).

Activation of T cells was assessed by staining for CD25 and CD69 after 48 hours of co-culture (Figure 21a, b). All CAR T cell conditions presented comparable induction of CD25 after co-culture with Nalm6 WT cells and significant reduced expression after contact with Nalm6 CD200 cells. $_{RV}$19-BBz$_{RV}$CD200R-Iso4^{OE}, $_{RV}$19-BBz and $_{RV}$19-BBz$_{CR}$Control CAR T cells showed a strong reduction of CD25 expression upon contact to CD200 expressing target cells (66.7 ± 10.0 % vs. 7.7 ± 3.1 %, p < 0.0001, 68.5 ± 10.1 % vs. 37.5 ± 15.3 %, p = 0.0002 and 71.9 ± 11.1 % vs. 39.7 ± 16.4 %, p < 0.0001). This effect was diminished in $_{RV}$19-BBz$_{CR}$CD200R^{KO} CAR T cells (68.8 ± 9.3 % vs. 52.3 ± 12.6 %, p = 0.0013). Comparable results were found regarding CD69 expression. $_{RV}$19-BBz$_{RV}$CD200R-Iso4^{OE}, $_{RV}$19-BBz, $_{RV}$19-BBz$_{CR}$CD200R^{KO} and $_{RV}$19-BBz$_{CR}$Control CAR T cells revealed similar expression of CD69 after co-culture with Nalm6 WT cells (71.3 ± 5.4 %, 76.5 ± 10.3 %, 76.1 ± 10.5 % and 75.6 ± 12.3 %) and significantly reduced expression after co-culture with Nalm6 CD200 cells (49.1 ± 11.8 %, p = 0.0034; 64.3 ± 12.3 %, p = 0.0112; 68.8 ± 11.6 %, p = 0.0053 and 62.4 ± 13.1 %, p = 0.0325). To investigate the release of proinflammatory cytokines upon target engagement, T cells were intracellularly stained for IFN-γ and TNF-α after 24 hours of co-culture (Figure 21c). Percentage of IFN-γ positive T cells ranged from 1.0 % to 3.2 % for $_{RV}$19-BBz$_{RV}$CD200R-Iso4^{OE} CAR T cells co-cultured with Nalm6 WT cells, while CD200 decreased IFN-γ expression significantly to levels ranging from 0.3 % to 0.9 % (p = 0.0059). In $_{RV}$19-BBz CAR T cells (range 1.1 % to 5.9 % vs. 0.5 % to 3.9 %) a tendency towards a downregulation of IFN-γ was observable. $_{RV}$19-BBz$_{CR}$CD200R^{KO} CAR T cells displayed a stable expression of IFN-γ after co-culture with Nalm6 WT or Nalm6 CD200 cells (range 0.9 % to 4.2 % vs. 0.9 % to 4.6 %) in contrast to $_{RV}$19-BBz$_{CR}$Control CAR T cells, which showed a significant reduction (range 1.6 % to 5.6 % vs. 0.8 % to 5.3 %; p = 0.002). Results were comparable for TNF-α expression (data not shown). Lastly, proliferative capacity of the T cells was measured after 72 hours of co-culture (Figure 21d). CD200 expression on target cells led to a 0.55 ± 0.31 -fold decrease of $_{RV}$19-BBz$_{RV}$CD200R-Iso4^{OE} CAR T cells compared to Nalm6 WT co-culture, which displays a significantly higher reduction of proliferation than compared to $_{RV}$19-BBz CAR T cells, that remained stable after contact to CD200 expressing target cells (1.03 ± 0.06 -fold, p = 0.0056). Same holds true for $_{RV}$19-BBz$_{CR}$CD200R^{KO} and $_{RV}$19-BBz$_{CR}$Control CAR T cells, where proliferation was not influenced by CD200 expression as well (1.03 ± 0.11 -fold vs. 0.95 ± 0.04 -fold).

Conclusively, presence of CD200 on target cells led to reduced CAR T cell function in terms of activation, cytokine production and proliferation. This effect could be observed especially in CD200R overexpressing CAR T cells and was rescued by performing a CD200R knock-out.

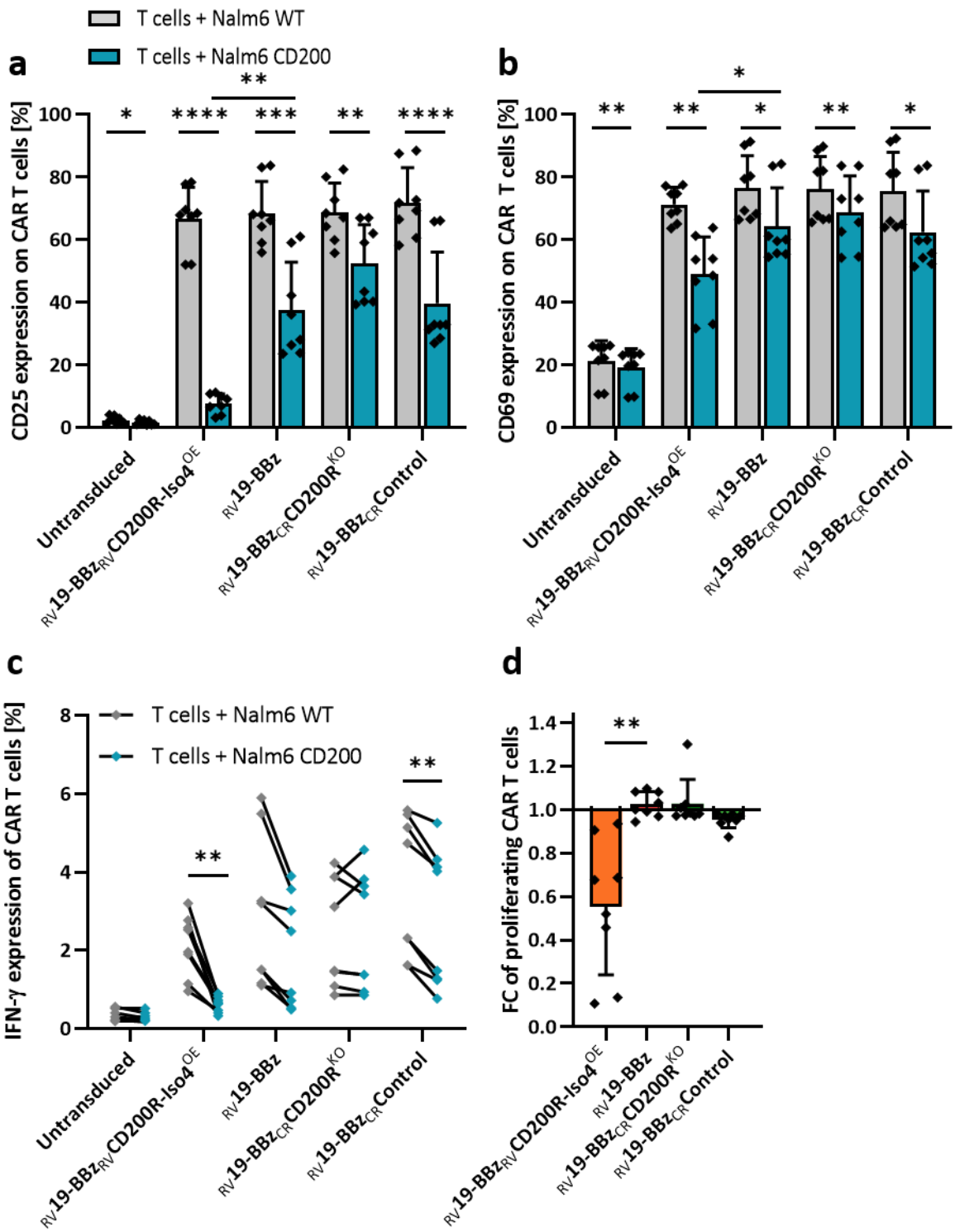

Figure 21: CD200R knock-out protects CAR T cells against inhibitory effects of CD200 expressing Nalm6 cells.

Functionality of CAR T cells was assessed by flow cytometry based analysis of activation markers, cytokines and proliferation of CAR T cells co-cultured with Nalm6 WT or Nalm6 CD200 target cells. **a** Percentage of CD25 and **b** CD69 positive CAR T cells after 48 hours of co-culture. **c** IFN-γ expression measured by intracellular staining after 24 hours of co-culture. **d** Fold change of proliferating CAR T cells after 72 hours of co-culture. Data represent the mean ± SD of four donors performed in duplicates. P-values were determined using RM one way ANOVA. WT = Wild type. IFN-γ = Interferon gamma.

5.11 Successful generation of CD200R-CD28 fusion receptor CAR T cells with high purity and favourable phenotype

To take advantage of CD200 expression on ALL blasts, a CD200R-CD28 fusion receptor was designed to switch the inhibitory signal of CD200R into a stimulating one. Therefore, the extracellular domain of CD200R isoform 4 was fused to parts of extracellular, transmembrane and intracellular domain of CD28. The CD200R-CD28 fusion receptor design is based on the model of Oda, et al. [91]. The fusion receptor was tested in combination with first or second generation CAR T cells. Primary human T cells from healthy donors were retrovirally transduced with either a first or second generation CAR linked by a F2A linker to the CD200R-CD28 fusion receptor ($_{RV}$19-z$_{RV}$CD200R-CD28 and $_{RV}$19-BBz$_{RV}$CD200R-CD28). Untransduced T cells, conventional first ($_{RV}$19-z) and second generation CAR T cells ($_{RV}$19-BBz) served as controls (Figure 22a).

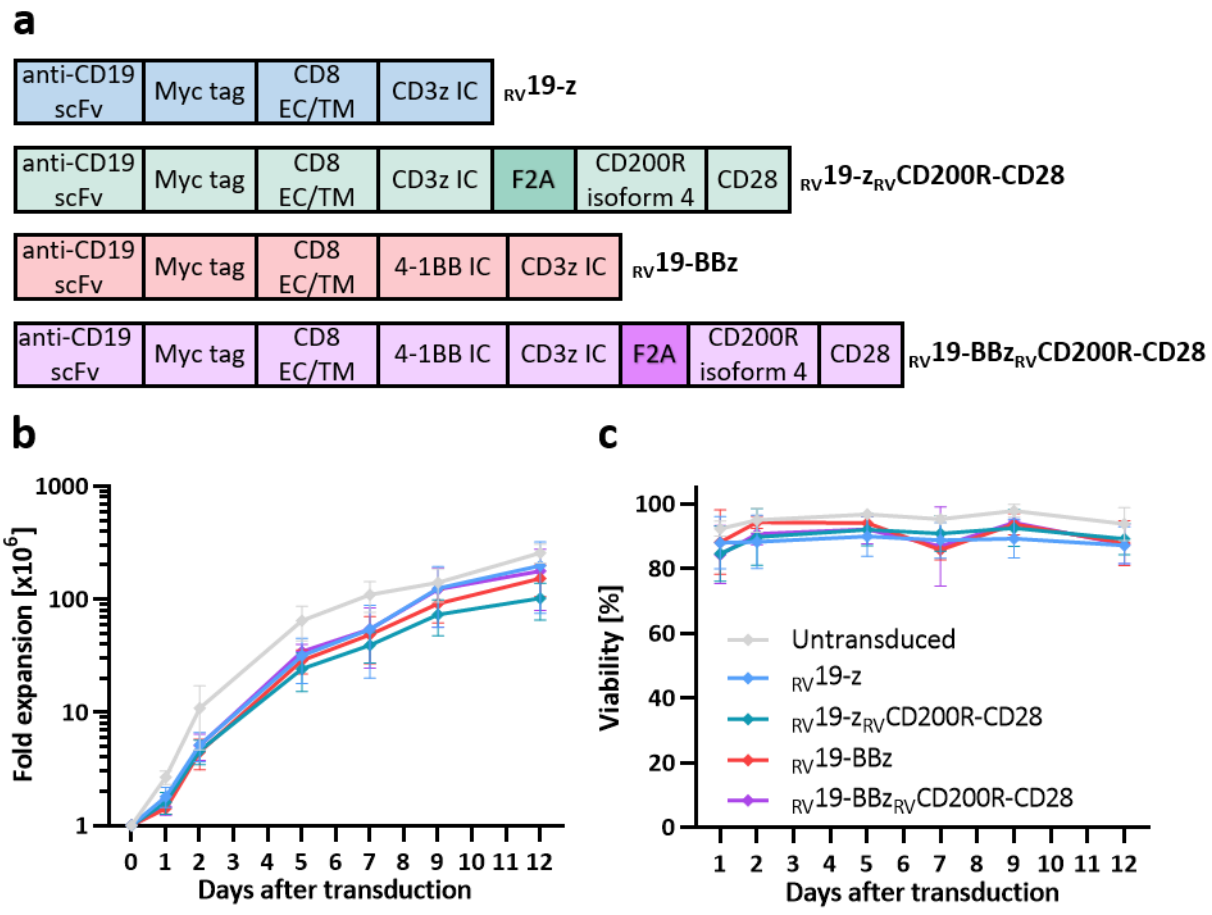

Figure 22: Fusion receptor CAR T cells maintain their proliferative capacity and viability during expansion.

Expansion and viability of CAR T cells were determined regularly by counting using the Neubauer haemocytometer during expansion period. **a** Schematic depiction of different CAR T cell designs. **b** Logarithmic presentation of fold expansion. **c** Viability for each CAR T cell condition during the expansion period. Viability was defined as ratio between vital cell count and total cell count. Data represent the mean ± SD of four donors. P-values were determined using RM one way ANOVA. ScFv = Single chain variable fragment. EC = Extracellular. TM = Transmembrane. IC = Intracellular.

To reduce the amount of blood donations and blood volumes taken from healthy donors, experiments were performed in parallel and same controls were used for different experiments. Thus, values of untransduced T cells and $_{RV}$19-BBz CAR T cells in Figure 22 and Figure 23 are the same as in Figure 18 and Figure 19.

T cells were cultured for twelve days after transduction. Cell count and viability were assessed regularly. After expansion period, $_{RV}$19-z$_{RV}$CD200R-CD28 CAR T cells showed a slightly reduced fold expansion of 102.2 ± 36.3 -fold to untransduced T cells (258.3 ± 40.0 -fold), but with no significant difference to $_{RV}$19-z CAR T cells (198.0 ± 122.5 -fold). $_{RV}$19-BBz$_{RV}$CD200R-CD28 CAR T cells revealed 177.9 ± 98.0 -fold expansion, with no significant differences to untransduced T cells or $_{RV}$19-BBz CAR T cells (153.4 ± 47.9 -fold) (Figure 22b). The overall mean viability on day twelve for $_{RV}$19-z$_{RV}$CD200R-CD28 and $_{RV}$19-BBz$_{RV}$CD200R-CD28 CAR T cells was 89.1 ± 4.9 % and 87.5 ± 6.0% with no significant differences to controls, respectively (Figure 22c).

After the expansion period, T cells were subsequently characterised. Co-expression of CD200R and c-myc could be observed for fusion receptor CAR T cells only (Figure 23a). $_{RV}$19-z$_{RV}$CD200R-CD28 and $_{RV}$19-BBz$_{RV}$CD200R-CD28 CAR T cells showed CAR transduction rates of 18.1 ± 3.3 % and 25.6 ± 5.4 % (Figure 23b). Untransduced T cells, $_{RV}$19-z CAR T cells and $_{RV}$19-BBz CAR T cells had an endogenous CD200R expression of less than 10 %, while $_{RV}$19-z$_{RV}$CD200R-CD28 and $_{RV}$19-BBz$_{RV}$CD200R-CD28 CAR T cells were highly positive for CD200R due to the CD200R-CD28 fusion receptor (39.7 ± 2.2 % and 42.5 ± 7.5 %) (Figure 23c). Analysis for cellular composition revealed that, less than 5 % of other cells including B cells, NK cells and monocytes were found within all T cell conditions (Figure 23d). $_{RV}$19-z$_{RV}$CD200R-CD28 CAR T cells consisted of 46.9 ± 6.5 % CD4$^+$, 41.4 ± 5.7 % CD8$^+$ and 7.9 ± 1.9 % NK T cells. In the $_{RV}$19-BBz$_{RV}$CD200R-CD28 CAR T cell product 47.4 ± 6.3 % CD4$^+$, 40.0 ± 5.0 % CD8$^+$ and 8.5 ± 2.0 % NK T cells were detected. No significant differences to their respective controls were observable. Lastly, the phenotype of the T cells was determined (Figure 23e) and thus gated according to the gating strategy for the different T cell conditions (see Table 9). All T cells showed a T_{SCM}-predominated phenotype with high interindividual differences. $_{RV}$19-z$_{RV}$CD200R-CD28 CAR T cells consisted of less than 1 % of T_N, 54.6 ± 20.0 % of T_{SCM}, 11.3 ± 4.8 % of T_{CM} and 16.5 ± 12.0 % were T_{EM}. 17.5 ± 7.4 % were fully differentiated into T_{EFF}. Significant differences were found in comparison to untransduced T cells (T_{EM}: 16.5 ± 12.0 % vs. 26.9 ± 11.6 %, p = 0.0254) and $_{RV}$19-z T cells (T_{SCM}: 54.6 ± 20.0 % vs. 43.0 ± 19.3 %, p = 0.0461). $_{RV}$19-BBz$_{RV}$CD200R-CD28 CAR T cells consisted of less than 1 % T_N, 51.4 ± 18.1 % T_{SCM}, 11.5 ± 5.9 % T_{CM}, 18.0 ± 10.6 % T_{EM} and 19.1 ± 6.9 % T_{EFF}. Significant differences were observable between $_{RV}$19-BBz$_{RV}$CD200R-CD28 CAR T cells and untransduced T cells (T_{EM}: 18.0 ± 10.6 % vs. 26.9 ± 11.6 %, p = 0.0145).

All in all, first and second generation CAR T cells with CD200R-CD28 fusion receptor could be successfully generated, including a high purity and an early differentiated phenotype.

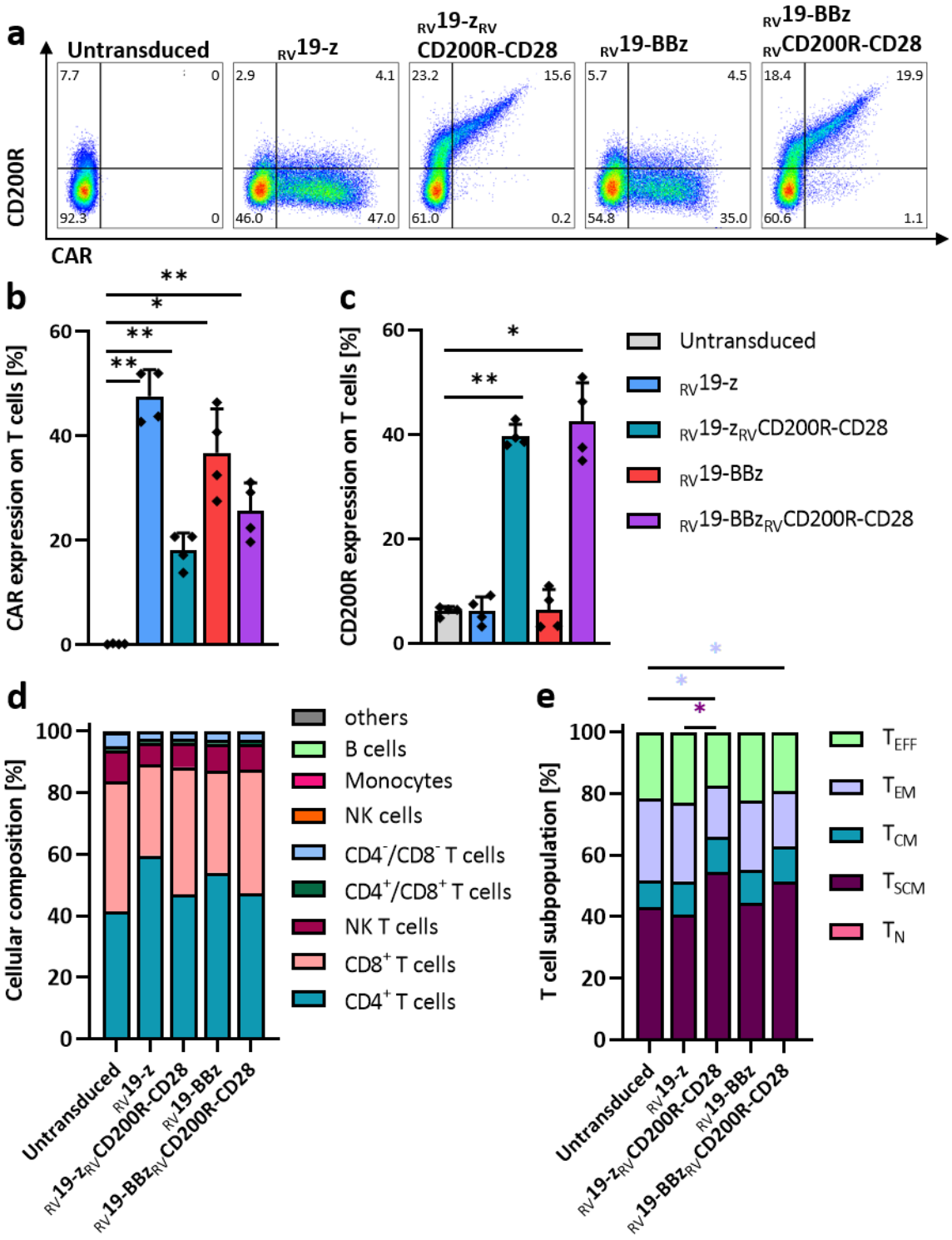

Figure 23: Fusion receptor CAR T cell product shows high purity and Tscm dominating phenotype. CAR T cells were characterized by flow cytometry based analysis of transduction rate, cellular composition and phenotype after expansion period. **a** Representative flow cytometry dot plots of the different CAR T cell conditions. **b** Expression of the CAR construct detected by c-myc staining, and **c** CD200R. **d** Cellular composition of the final T cell product. **e** Percentage of CAR T cell subpopulations. Data represent the (d, e) mean (a, b) ± SD of four donors. P-values were determined using RM one way ANOVA. NK = Natural killer. T_{EFF} = Effector T cells; T_{EM} = Effector memory T cells; T_{CM} = Central memory T cells; T_{SCM} = Stem cell-like memory T cells; T_N = Naive T cells.

5.12 CD200R-CD28 fusion receptor shows high activation upon contact with CD200 expressing target cells

To assess the functionality of first and second generation CD200R-CD28 CAR T cells as well as of their respective controls, cytotoxicity, activation markers, cytokine release and proliferation were measured after co-culture with either Nalm6 WT or Nalm6 CD200 target cells. For evaluation of flow cytometry data, T cells were gated according to the gating strategy for the different T cell conditions (see Table 9). The values for untransduced T cells and $_{RV}$19-BBz CAR T cells in Figure 24 and Figure 25 are the same used for Figure 20 and Figure 21 since these T cells served as controls for both scenarios.

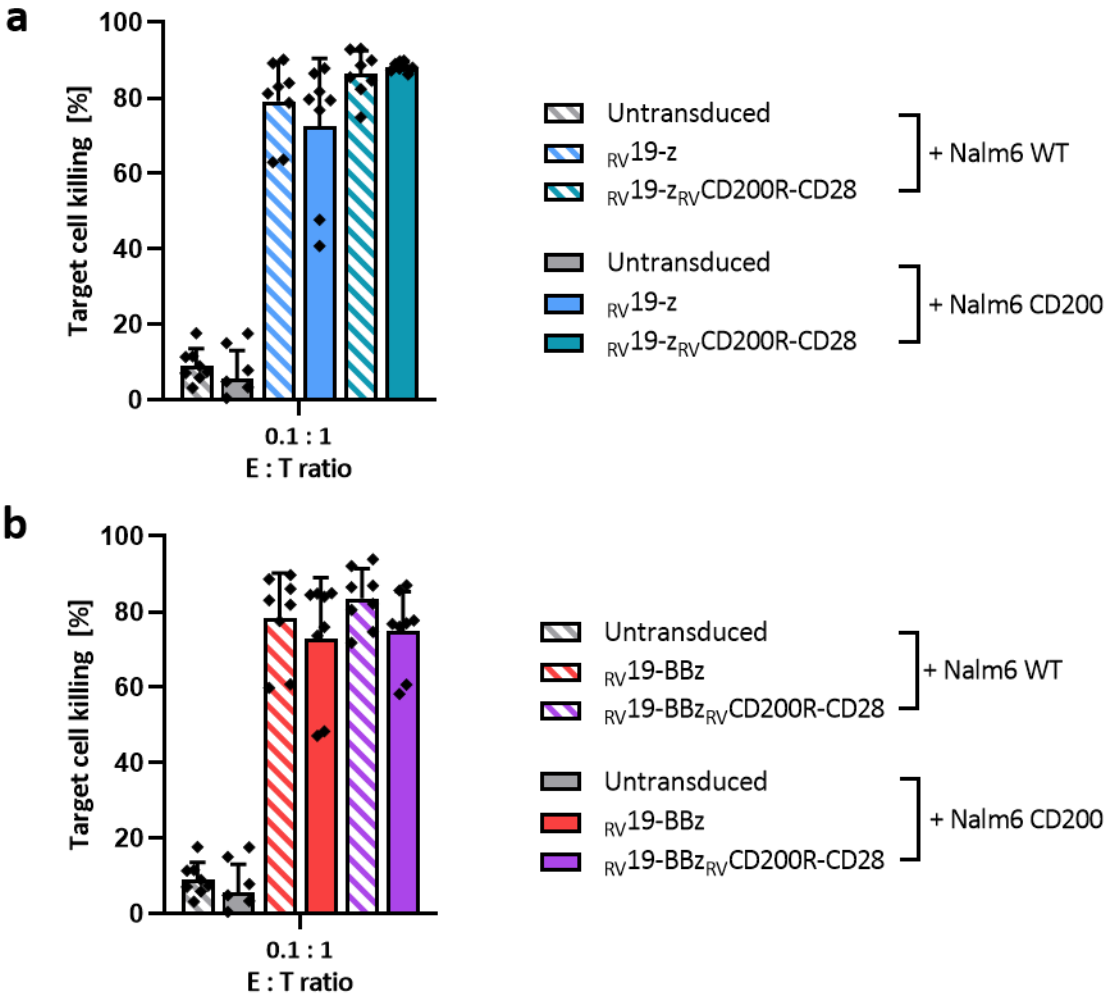

Figure 24: Fusion receptor CAR T cells kill target cell line efficiently.
Cytotoxicity of CAR T cells was assessed by flow cytometry based analysis after co-culturing CAR T cells with either Nalm6 WT or Nalm6 CD200 target cells for 48 hours. **a** Cytotoxicity of first generation and **b** second generation CAR T cells at an E:T ratio of 0.1:1. Data represent the mean ± SD of four donors performed in duplicates. P-values were determined using RM one way ANOVA. WT = Wild type. E:T ratio = Effector to target ratio.

Cytotoxicity was determined 48 hours after co-culture of T cells and target cells (Figure 24a, b). At an effector to target ratio of 0.1:1, $_{RV}$19-z$_{RV}$CD200R-CD28 CAR T cells demonstrated comparable killing of Nalm6 WT and Nalm6 CD200 target cells (86.5 ± 6.1 % vs. 88.3 ± 1.2 %). Furthermore, $_{RV}$19-BBz$_{RV}$CD200R-CD28 CAR T cells displayed similar percentages of killing (83.6 ± 7.8 % vs. 74.9 ± 10.4 %). No significant differences to the respective conventional CAR T cells were found.

Activation of T cells was assessed by staining for CD25 and CD137 after 48 hours of co-culture (Figure 25a, b). $_{RV}$19-z CAR T cells and $_{RV}$19-BBz CAR T cells showed significantly lower CD25 expression after co-culture with Nalm6 CD200 compared to Nalm6 WT cells (53.0 ± 14.6 % vs. 23.1 ± 9.1 %, $p < 0.0001$ and 68.5 ± 10.1 % vs. 37.5 ± 15.3 %, $p = 0.0002$). In contrast, $_{RV}$19-z$_{RV}$CD200R-CD28 and $_{RV}$19-BBz$_{RV}$CD200R-CD28 CAR T cells revealed significant increase in expression of CD25 upon CD200 contact (32.6 ± 7.3 % vs. 89.1 ± 4.9 %, $p < 0.0001$ and 43.7 ± 12.1 % vs. 84.9 ± 4.2 %, $p = 0.0002$). For CD137 similar results were found. $_{RV}$19-z CAR T cells and $_{RV}$19-BBz CAR T cells showed a comparable expression of CD137 after co-culture with Nalm6 WT or Nalm6 CD200 cells (24.9 ± 2.4 % vs. 28.5 ± 10.5 % and 29.8 ± 9.3 % vs. 23.9 ± 8.1 %), whereas $_{RV}$19-z$_{RV}$CD200R-CD28 CAR T cells and $_{RV}$19-BBz$_{RV}$CD200R-CD28 CAR T cells showed significantly elevated percentages (26.3 ± 5.6 % vs. 64.7 ± 8.2 %, $p = 0.004$ and 20.4 ± 4.8 % vs. 57.4 ± 10.2 %, $p = 0.0005$). Analysis of CD69 expression revealed comparable results (data not shown). Next, cytokine expression of T cells was captured by intracellular staining of IFN-γ after 24 hours of co-culture (Figure 25c). IFN-γ expression was significantly elevated after co-culture with Nalm6 CD200 cells for $_{RV}$19-z$_{RV}$CD200R-CD28 and $_{RV}$19-BBz$_{RV}$CD200R-CD28 CAR T cells, in comparison to co-culture with Nalm6 WT cells (1.9 ± 1.1 % vs. 10.2 ± 1.3 %, $p < 0.0001$ and 2.1 ± 1.4 % vs. 7.9 ± 3.0 %, $p = 0.0002$). In contrast, $_{RV}$19-z and $_{RV}$19-BBz CAR T displayed a tendency towards a reduction of IFN-γ (1.9 ± 0.7 % vs. 1.5 ± 0.7 % and 2.8 ± 2.0 % vs. 2.0 ± 1.4%). Similar results were found for TNF-α expression (data not shown). Last, proliferation capacity was measured after 72 hours of co-culture according to methods (Figure 25d). Since T cells varied greatly in their intrinsic state of proliferation in the unstimulated control, fold changes were calculated as described in the methods to make values more comparable. $_{RV}$19-z$_{RV}$CD200R-CD28 and $_{RV}$19-BBz$_{RV}$CD200R-CD28 CAR T cells showed a 1.2 to 3.4 -fold and 1.0 to 1.7 -fold increased proliferation upon contact with Nalm6 CD200 target cells, which resulted in significant higher fold changes of proliferating T cells than $_{RV}$19-z or $_{RV}$19-BBz CAR T cells (mean 1.0 ± 0.0 -fold, $p = 0.0159$ and mean 1.0 ± 0.1 -fold, $p = 0.0352$).

Taken together, in presence of CD200, first and second generation CAR T cells with CD200R-CD28 fusion receptor showed significantly higher activation, cytokine release and proliferation capacity than conventional first and second generation CAR T cells.

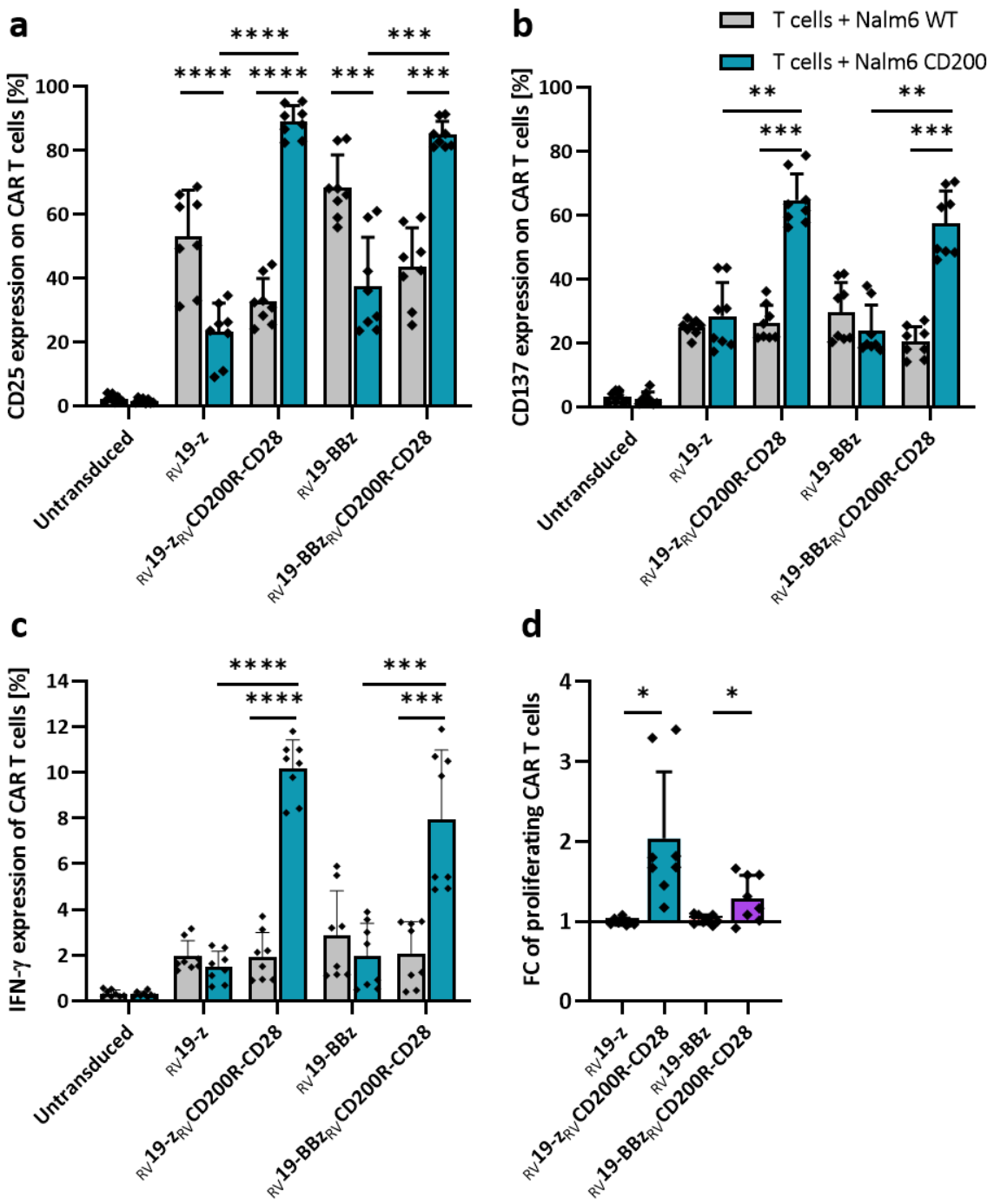

Figure 25: Fusion receptor CAR T cells show enhanced activation, cytokine production and proliferation capacity in presence of CD200 expressing Nalm6 cells.
Functionality of CAR T cells was assessed by flow cytometry based analysis of activation markers, cytokines and proliferation of CAR T cells co-cultured with Nalm6 WT or Nalm6 CD200 target cells. **a** Percentage of CD25 and **b** CD137 positive CAR T cells after 48 hours of co-culture. **c** Percentage of IFN-γ positive CAR T cells assessed by intracellular staining after 24 hours of co-culture. **d** Fold change of proliferating CAR T cells after 72 hours of co-culture. Data represent the mean ± SD of four donors performed in duplicates. P-values were determined using RM one way ANOVA. WT = Wild type. IFN-γ = Interferon gamma.

6 Discussion

B cell acute lymphoblastic leukaemia is the most common malignancy of childhood [1, 2]. Even though the majority of children can be cured nowadays [1, 5], therapy of relapsed or refractory ALL still represents a challenge [10-13]. Here we elucidated the role of the immunoregulatory axis of CD200/CD200R in ALL. CD200 is a glycoprotein found abundantly on B-ALL blasts [61, 87]. It is considered to mediate immunodeficiency in cancer and is associated with a worse outcome [73].

6.1 Assessing the way of CD200 mediated immunosuppression

Cancer cells have the potential to directly interact with T cells through the expression of surface markers or the release of soluble factors [38]. In addition, they can manipulate bystander cells, like APCs, and thus create an immunosuppressive tumour microenvironment (TME) [41, 42], which indirectly inhibit T cell function. In terms of B-ALL, it is not yet clarified if CD200 mediated immunosuppression results from the direct or indirect way, since T cells express the respective receptor as well as APCs. Addressing this question and to determine the functional importance of CD200 expression on B-ALL blasts, co-culture experiments of APCs (macrophages and dendritic cells), leukaemic B-ALL cell lines and T cells were conducted.

6.1.1 Macrophages enhance T cell functionality independent of CD200 *in vitro*

Macrophages are important APCs expressing the CD200R. Depending on the local microenvironment, macrophages can either support tumour progression or supress tumour growth by polarisation towards an immunosuppressive or inflammatory phenotype [49, 51].

To investigate the impact of the leukaemic microenvironment on macrophages through the CD200/CD200R axis, we co-cultured monocyte derived macrophages with a $CD200^{+}$ leukaemic cell line. We observed a decreased expression of CD200R on macrophages upon contact with CD200 expressing cells, indicating that an interaction between both cell types took place which led to a downregulation of the receptor. In this study, macrophages co-cultured with leukaemic cells exhibited a phenotype with only low expression of the characteristic M1 or M2 markers. At this point it is worth noting that a strict classification into M1 and M2 is difficult since it does not meet the complexity of macrophage polarisation. Rather than distinct populations, M1 and M2 should be gathered as two extremes in a spectrum of possible phenotypes [50, 103]. Significant, but only minor differences were found in the expression of CD86 on macrophages in presence of CD200 expressed on leukaemic cells. CD86 is a co-stimulatory molecule needed for T cell activation [47] and therefore represents a marker of M1 polarisation [56]. But due to the low quantity of difference, a biological relevance on T cell activation is improbable here. In line with above mentioned results, CD200 did not alter cytokine release of IFN-γ, TNF-α, IL-6 or IL-10 of macrophages. These results lie in contradiction with the current opinion. Hoeck et al. and Jenmalm et al. observed dysfunction

of macrophages due to CD200 exposure [70, 80]. In addition, leukaemic cells are considered to direct macrophages towards an immunosuppressive phenotype [60], which could not be confirmed in this study. Discrepancy to the literature because of the used methods seems unlikely since macrophages showed changes in phenotype towards M1-like or M2-like macrophages and cytokine release upon stimulation by cytokines but not by tumour cells. CD200 on ALL blasts had no effect on macrophages in our experiments. An explanation could be found in the low immunogenicity of paediatric ALL [104]. Due to the absent immune response *in vitro*, the stimulation of the macrophages might be to week for the effect of CD200 to appear. This would implicate that the impact of CD200 depends on activation.

The presence of CD200 on blasts attenuated activation, cytokine release, cytotoxicity and proliferation of T cells mediated by blinatumomab, while addition of macrophages induced a strong Th1 inflammatory immune response in T cells. Simultaneously, presence of macrophages led to a more pronounced effect of CD200 mediated reduction of activation and cytokine release of T cells. In contrast to the upregulation of Th2 responses found before in mixed lymphocyte reactions with macrophages and CD200 expressing CLL cells [74], no CD200 mediated effect on Th1 or Th2 differentiation was observed in this project. As macrophages were not affected by CD200 on leukaemic cells in our experiments, this did not mediate a shift towards Th2 response in T cells, consequently.

Based on these results, macrophages seem not to be the major mediator of the inhibitory effect of CD200 on leukaemic blasts on T cell functionality.

6.1.2 Dendritic cells influence CD200 mediated dysfunction of T cells

As part of the adaptive immune system, dendritic cells collect and process antigens and present them to T cells [44]. To prevent autoimmunity, besides the specific antigen, a second signal in form of co-stimulation is needed for T cell activation. Only matured DCs, which highly express surface markers like CD80 or CD86, are able to prime naïve T cells. In contrast, presentation of antigens on immature DCs lead to T cell anergy [47]. Thus, DCs are not only important for clearance of bacterial or viral infections but also for anti-tumour response by attracting and activating tumour-specific T cells [43].

DCs showed high initial CD200R expression, which was decreased in presence of CD200 on leukaemic cells, suggesting that an interaction took place. As CD200 is considered to play an important role in mediating immune tolerance, we investigated its effect on DC maturation. We found CD83 slightly higher expressed on DCs in presence of $CD200^+$ leukaemic cells, but due to the marginal difference to co-culture with $CD200^-$ blasts, we deemed this effect as negligible. The result that CD200 had no influence on maturation are consistent with the findings of Jenmalm et al. [80]. The low immunogenicity of paediatric ALL could be responsible here too.

In contrast to experiments with macrophages, DCs did not alter the T cell function mediated by blinatumomab. Nevertheless, CD200 mediated impairment of T cells was detectable in presence and absence of DCs, indicating that CD200 most likely inhibits T cell function directly. In presence of CD200, the addition of DCs led to a stronger reduction of CD25 reduction and proliferative capacity of T cells, indicating that DCs have the potential to amplify the effect of CD200 on T cells.

In conclusion, our data indicates that DCs do not mediate the immunosuppressive effect of CD200 in ALL even though they eventually influence it.

6.1.3 CD200 on leukaemia directly inhibit T cell functionality

In presence of CD200, T cells demonstrated reduced cytokine release of pro-inflammatory (IL-2, IFN-γ, TNF-α) and lytic cytokines (FasL, granzyme A, perforin), as well as reduced proliferation. Our results indicate that the CD200 mediated T cell dysfunction results of direct interaction between T cells and B cell leukaemic blasts, which can be shaped by bystander cells like macrophages or dendritic cells. Direct inhibition through CD200 was found before in AML against natural killer cells [105]. But for T cells opposing views can be found in the literature whether CD200 induced T cell dysfunction results of direct or indirect inhibition through myeloid cells. Most studies elucidating the effect of CD200 on immunoregulation are conducted in MLR, thus no definitive statement can be made [74, 86, 106]. Indirect inhibition was shown in experiments of Jenmalm et al., where the inhibition of antigen-induced cytokine secretion was dependent upon stimulating the CD200R on myeloid cells but not on T cells [80]. Also, Wang et al. showed that CD200 on plasmacytoma had no direct negative effect on proliferation, cytokine secretion or cytotoxicity of cytotoxic T cells but indirectly through the inhibition of cytokine secretion of TAMs [107]. In contrast, Coles et al. found the function of memory T cells directly inhibited by CD200 expressing AML, supporting our hypothesis [84].

We observed a correlation between hight of T cell activation and weight of the inhibitory effect through CD200. The higher the activation, the higher the restriction through CD200/CD200R. This could be regarded as negative feedback loop, which underlines the importance of CD200/CD200R as immunoregulatory axis that protect healthy tissue from excessive immune response [65]. Since T cell function is crucial for effective anti-tumour response, targeting the CD200/CD200R axis represents an auspicious approach in anti-leukaemia therapy.

However, our efforts mirror only an attempt to mimic the complexity of the bone morrow. Here, *in vitro*, leukaemic blasts had no impact on macrophages or dendritic cells, but these results need to be verified *in vivo*. It is quite possible that *in vivo* the leukaemic microenvironment is more complex and immunosuppressive as further cells and extracellular proteins are implicated, and thus CD200 might influence macrophages or DCs differently. In

addition, it must be considered that macrophages as well as DCs display a highly heterogeneous group in terms of functionality and phenotype. Therefore, other subtypes of macrophages or DCs, like conventional or plasmacytoid DCs, might play an important role as well.

6.2 CD200 induced T cell inhibition correlates with CD200R expression

Next, the role of the CD200 receptor within the CD200/CD200R axis was further investigated. Two different isoforms of the transmembrane CD200R exist. Isoform 4 represents the full length isoform, while isoform 1 misses exon 2. Apart from the structure, little is known about the functional differences of both isoforms [67]. Addressing this question, retroviral transduction was used to induce CD200R overexpression of isoform 1 or 4 in primary human T cells from healthy donors. In addition, CD200R overexpressing second generation CAR T cells were generated to rule out biological relevant restrictions through CD200 in the therapy of B-ALL. Therefore, a second generation CAR construct was linked to the full length isoform 4 of CD200R using an F2A linker to ensure equimolar expression of the CAR and the CD200R as two separate proteins.

CD200R overexpression did not alter expansion capacity, viability, cellular composition or phenotype of T cells or CAR T cells during and after expansion. Although CD200R overexpression did not result in less efficient cytotoxic capacity in presence of CD200 on target cells, diminished activation of T cells could be observed. CD200R overexpressing T cells in general did not display any disadvantages in activation potential. Nevertheless, upon contact with CD200 expressing target cells activation, cytokine release and proliferation of CD200R overexpressing T cells were reduced. This tendency could also be observed to a lower extent for T cells expressing physiological levels of CD200R. No significant differences in terms of functionality between CD200R isoform 1 or isoform 4 overexpressing T cells were detectable. Thus, functional differences need to be addressed in further studies. Interestingly, CAR T cells were more affected by CD200 exposure. CD200R overexpressing CAR T cells showed decreased killing capacity in presence of $CD200^{+}$ target cells. Even conventional second generation CAR T cells with physiological expression of CD200R showed slightly, but significantly, reduced killing in presence of CD200. Further, conventional CAR T cells showed mild declines in terms of activation and cytokine release when co-cultured with CD200 positive target cells, while CD200R overexpressing CARs displayed drastic effects. These data suggest, a positive correlation of CD200R expression levels and inhibitory effect on T cells. In accordance with our data, Jenmalm et al. found that the inhibition of cytokine release of macrophages through the CD200/CD200R axis correlates with the CD200R level of the macrophages [80].

Collectively, our results indicate that CD200R has no relevant influence on phenotype and cytotoxic functionality of T cells itself but mediates an expression level-dependent functional

inhibition in presence of CD200. A biological relevance of these effect for T cells and CARs *in vivo* is questionable, because of marginal endogenous expression of CD200R, resulting in only slight T cell dysfunction through CD200. CAR T cells are more affected by CD200 than primary T cells probably based on their enhanced intrinsic activation provided by the CAR. This lies in accordance with our previous results that higher activation results in higher inhibition due to the negative feedback loop. It is tempting to speculate that, CAR T cells *in vivo*, because of activation through bystanders, are even more affected by CD200 than *in vitro*. To verify this, *in vivo* tests will be required in the future.

6.3 CD200R knock-out prevent T cells and CAR T cells from CD200 mediated dysfunctionality

Second generation CARs are already in clinical use for therapy of refractory or relapsing ALL [15, 16], but issues addressing persistence and tumour evasion through checkpoint inhibition limit the outcome of CAR T cell therapy [108, 109]. As a strategy to overcome T cell dysfunctionality caused by CD200 expressing leukaemic blasts, we tested CRISPR/Cas9 mediated knock-out of CD200R on primary human T cells and second generation CAR T cells.

T cells revealed higher CD200R knock-out rates on DNA level than CAR T cells. This is likely due to the different time points of electroporation. The T cell and CAR T cell product demonstrated a high purity with a favourable early differentiated phenotype. As low differentiated T cells show enhanced proliferation capacity and better *in vivo* persistence, adoptive T cell transfer of low differentiated T cells are considered to be more efficient [110-113]. All in all, characterisation at the end of expansion revealed no differences in growth, cellular composition and phenotype of T cells or CAR T cells, when CD200R is knocked-out. In accordance with our prior results, these data indicate that CD200R expression levels on T cells or CAR T cells have no impact on the properties of the final T cell product.

CD200R knock-out T cells showed a comparable killing of ALL cells in absence or presence of CD200. Nevertheless, T cells lacking CD200R, seemed to be protected from inhibition of activation, cytokine release and proliferation when CD200 was expressed. As previously described, CAR T cells killed $CD200^+$ target cells less efficiently than $CD200^-$ ALL cells. This effect could be prevented by performing a CD200R knock-out in CAR T cells. CD200R knock-out was also able to protect CAR T cells partly from inhibition regarding activation, cytokine release and proliferation when CD200 was present on target cells. As there were $CD200R^+$ T cells remaining in the CD200R knock-out T cell pool, because of the knock-out rates, the effect might not be fully rescued. Pre-sorting of CD200R knock-out T cells should be consider for further experiments. High activation levels of CAR T cells might induce susceptibility to inhibition through CD200 at already low expression of CD200R as previously described.

Nevertheless, our results suggest that CD200R knock-out is feasible to overcome T cell dysfunction through CD200. Further *in vivo* tests will be essential to verify the *in vitro* effects.

6.4 Fusion receptor CAR T cells exceed conventional CAR T cells in presence of CD200 on leukaemic blasts

First and second generation CAR T cells expressing a CD200R-CD28 fusion receptor were generated as a second approach for overcoming CD200 mediated T cell dysfunction. Fusion receptors are supposed to switch the negative signal generated through CD200/CD200R interaction into a stimulating signal by exchanging the intracellular part of CD200R. Therefore, based on the model of Oda et al. [91], the extracellular domain of the isoform 4 of CD200R was fused to parts of the extracellular, transmembrane, and intracellular domain of CD28. Even though CD200R-CD28 fusion receptors are already tested on leukaemia-specific T cells, the combination of CD200/CD200R blockade and CAR T cells harnesses general advantages of CAR T cells, like independence from MHC complexes, increased reservoir of potential targets, and tumour specificity [19-21], and enhanced T cell function in presence of CD200. The construct of the CD200R-CD28 fusion receptor was linked to the CAR construct using an F2A linker to ensure equimolar co-expression.

Co-expression of the CD200R-CD28 fusion receptor had no negative effect on expansion and viability of the CAR T cells. Characterisation at the end of expansion period revealed different transductions rates of the CAR. This is most likely because of non-standardized virus titers used for retroviral transduction. In addition, analysis revealed high purity and a T_{SCM}-predominant phenotype of the CAR T cell product. Fusion receptor CAR T cells showed a slightly more undifferentiated phenotype than conventional CAR T cells, indicating an even more preferable phenotype [110-113]. As the base line killing capacity of the CARs used in this study is already very high, no further improvements could be detected using CD200R-CD28 fusion receptor CAR T cells. Fusion receptor CAR T cells and conventional CAR T cells shared comparable activation, cytokine release and proliferative capacity upon co-culture with $CD200^-$ target cells, proofing that the intracellular CD28 domain by itself led to no improvements. Nonetheless, fusion receptor CAR T cells displayed strongly enhanced activation, cytokine release and proliferation in presence of CD200 on target cells.

Conclusively, both, first and second generation CAR T cells with CD200R-CD28 fusion receptor, outperform conventional first and second generation CAR T cells in the presence of CD200. Notable, the second generation CAR T cell with fusion receptor represent a third generation CAR in the proper sense. But even though, some publications suggested that third generation CARs had no advantage over second generation CARs [14], here *in vitro* second generation CAR T cells with fusion receptor outcompeted conventional second generation CAR T cells.

6.5 Interfering the CD200/CD200R axis is an attractive alternative to PD-L1/PD-1 in paediatric B-ALL

CD200/CD200R represents a promising target for checkpoint blockage, as CD200 exclusively binds CD200R [68]. In contrast to other checkpoint receptors, like TIM-3 [114], there are no other endogenous ligands for CD200R. There are encouraging indications that interfering the CD200/CD200R axis through CD200R knock-out or CD200R-CD28 fusion receptor will be saver than PD-1 or CTLA-4 blockage. CD200R knock-out and CD200R-CD28 fusion receptor on T cells and CAR T cells had no negative effect on expansion, phenotype and functionality, while Odorizzi et al. found out that genetic deletion of PD-1 resulted in the development of terminally differentiated and exhausted T cells [115]. Moreover, CTLA-4 depletion in mice disrupted T cell homeostasis leading to accumulation of high reactive and fragile T cell blasts in multiple organs resulting in tissue destruction [116, 117]. CD200 antibodies, like samalizumab and TTI-CD200, might be better tolerated than PD-1 or CTLA-4 checkpoint inhibitors. Both antibodies proofed to be safe and TTI-CD200 led to prolonged survival of low risk ALL in mice models but not of high risk ALL cases [89, 90]. Here combination with CAR T cells could improve the outcome especially for high risk cases. Nevertheless, breaking the CD200/CD200R axis on CAR T cells is more attractive than combining CAR T cells with CD200 antibodies. Systemic adverse effects are diminished through the target specificity of CARs. General block of CD200/CD200R may result in higher susceptibility of autoimmune diseases and excessive immune response upon viral or bacterial infections [118, 119]. Regarding the expression pattern of PD-L1, CD200R knock-out or CD200R-CD28 fusion receptor CAR T cells demonstrate another crucial advantage. Since PD-L1 shows huge inter-individual differences and on average rather low expression on paediatric B-ALL blasts [61], a screening would be necessary to identify patients who will benefit from PD-L1/PD-1 blockage. The same applies to the other checkpoint molecules. CD200 can be found on the surface of nearly all B-ALL blasts [61, 87]. Thus, almost all patients could profit from CD200R knock-out or CD200R-CD28 fusion receptor CAR T cells, making screenings ahead of therapy redundant which subsequently results in reduced efforts and costs.

Conclusively, CD200R knock-out and CD200R-CD28 fusion receptor CAR T cells show various advantages over PD-1 or other checkpoint blockages including a specific ligand, which is abundantly expressed on B-ALL blasts, tumour specificity and diminished systemic side effects.

6.6 Clinical application of novel CAR T cells requires a safety management

CD200R knock-out CAR T cells and CD200R-CD28 fusion receptor CAR T cells proved to be fully functional *in vitro* and were capable of overcoming CD200 mediated T cell dysfunction. Both mechanisms might have the potential to prolong CAR T cell persistence and therefore help to achieve durable tumour surveillance. Nevertheless, there are risks to be considered. Increased CAR T cell activation lead to extended persistence and better cancer control, but also increase

the risk of adverse effects [23]. The literature described this connection as the “double-edged sword of CAR T cell therapy” [14]. Side effects of CAR T cell therapy include neurotoxicity, cytokine release syndrome (CRS) and B cell aplasia. CRS describes a systemic inflammatory response, which can lead to hypotension, respiratory failure and coagulopathy due to elevated cytokine levels especially interleukin 6 (Il-6). CRS and neurotoxicity occurred in 77 % and 40 % of children enrolled in the phase II study of tisagenlecleucel. Fortunately, adverse effects were reversible and not lethal [120]. CAR T cells represent a living drug and should be handled carefully. Especially on the end of CAR T cell therapy, when the cancer is defeated, aplasia of healthy B cells, which also express CD19, could lead to life threatening infections and require replacement of immunoglobulins [22]. To minimize toxicities of CAR T cell therapy, besides specific drugs like the Il-6 antibody tocilizumab [22], implementation of an “off-switch”, for example the iCasp9 cell-suicide system [121], into CAR design should be considered. Additionally, safe and directed implementation of the CAR into the genome should be taken into account. Retroviral transduction is effective, but non targeted implementation of the CAR could lead to mutagenesis. Eyquem et al. (2017) established a CRISPR/Cas9 mediated strategy to target the CAR to a TCR locus, enabling safe and uniform expression [122].

The future of CAR T cell therapy may incorporate various modification of CAR T cells personalized to the individual expression pattern of the patient’s ALL blasts. At this end, a CD200R knock-out or a CD200R-CD28 fusion receptor or even a combination, might be considered, since CD200 is abundantly expressed on paediatric B-ALL blasts.

7 Summary

Acute lymphoblastic leukaemia is the most frequent paediatric malignancy [1, 2]. Even though around 90 % of all children with the diagnosis of ALL can be cured, ALL is responsible for more deaths than any other malignancy in childhood [1]. Especially the poor survival of children suffering from primary refractory disease or ≥2nd relapse (r/rALL) is unsatisfying [10-12]. CAR T cell therapy has emerged as an encouraging strategy in the fight of primary refractory or relapsed paediatric B cell leukaemia. Despite impressive initial responds rates of over 80 %, long-term remissions remain between 30 - 40 % [14]. Different intrinsic and extrinsic factors can lead to development of CAR T cell therapy resistance [35]. Here we focused on the immunoregulatory axis of CD200/CD200R. CD200 is abundantly expressed on B cell leukaemic blasts [61, 87], while its receptor is only found on the surface of T cells and myeloid cells like macrophages and dendritic cells [66].

First, we aimed to elucidate if CD200 on leukaemic blasts affects the immune system through direct interaction with T cells or indirectly through bystander cells of the myeloid line. Therefore, we performed co-culture experiments of leukaemic cells lines and immune cells including T cells, macrophages and dendritic cells. We found that CD200 on B-ALL blasts directly inhibit T cell function *in vitro* mediated by blinatumomab. In addition, macrophages and dendritic cells had the power to shape this inhibition. For example, we observed increased activation of T cells, when macrophages were added to the co-culture with leukaemic cells, and thereby the negative effect of CD200 was even higher. We consider this as a negative feed-back loop: the higher the intrinsic activation of the T cells, the higher the restrictions through CD200. In a next step, we noticed a correlation between the density of CD200R and the extend of the CD200 mediated dysfunction, by generating CD200R overexpressing T cells. We extended our results on CAR T cells. There, we found CAR T cells even more affected by CD200 exposure than primary T cells.

As an attempt of overcoming CD200 mediated inhibition, we armed second generation CAR T cells with a CD200R knock-out. In presence of CD200, the CD200R knock-out protected the CAR T cells from inhibition, making them more functional against CD200 positive ALL cell line. Further, we designed a CD200R-CD28 fusion receptor, which switches the negative signal provided by CD200R into a positive one. CAR T cells expressing the CD200R-CD28 fusion receptor outperformed conventional CAR T cells against CD200 positive leukaemic blasts in terms of activation, cytokine release and proliferation.

Collectively, we gained deeper understanding of the interaction between leukaemic blasts and immune cells through the CD200/CD200R axis, allowing us to enhance CAR T cell therapy for primary refractory or relapsed acute lymphoblastic leukaemia.

German Summary

Die akute lymphatische Leukämie (ALL) ist die häufigste kindliche Krebserkrankung [1, 2]. Trotz Heilungsraten von etwa 90 % ist die ALL, auf Grund ihrer Häufigkeit, für mehr Todesfälle verantwortlich als jede andere Krebserkrankung im Kindesalter [1]. Insbesondere das Langzeitüberleben von Kindern und Jugendlichen mit primär refraktären und ≥2. Rezidiven (r/rALL) ist unbefriedigend [10-12]. Hier hat sich die CAR-T-Zelltherapie als vielversprechender Therapieansatz gezeigt. Doch trotz beeindruckender initialer Ansprechraten von über 80 % erreichen viele Patienten keine langfristige Remission [14]. Als Ursachen werden verschiedene intrinsische und extrinsische Faktoren für die Entwicklung einer Therapieresistenz diskutiert [35]. Der Fokus dieser Arbeit liegt auf der immunregulatorischen Achse von CD200/CD200R. CD200 wird in hoher Dichte auf der Oberfläche von B-Zellen und leukämischen Vorläuferzellen exprimiert. Der dazugehörige Rezeptor CD200R findet sich dagegen auf T-Zellen und myeloischen Zellen [66].

Zunächst wurde untersucht, ob CD200 auf Leukämiezellen das Immunsystem direkt, durch Interaktion mit T-Zellen, oder indirekt, durch andere, unmittelbar benachbarte Zellen der myeloischen Reihe, beeinflusst. Hierfür wurden Co-Kultur-Experimente mit leukämischen Zelllinien und Immunzellen wie T-Zellen, Makrophagen und dendritischen Zellen (DCs) durchgeführt. Die Ergebnisse zeigten, dass CD200 auf leukämischen Zellen die T-Zell-Funktion *in vitro* hemmt, welche mithilfe des bispezifischen Antikörpers *Blinatumomab* vermittelt wird. Zusätzlich zeigte sich, dass Makrophagen und Dendritische Zellen diese Hemmung beeinflussen können. Durch Zugabe von Makrophagen zur Co-Kultur mit leukämischen Zellen wurde eine verstärkte Aktivierung von T-Zellen sowie eine verstärkte negative Wirkung von CD200 beobachtet. Dies wurde als Zeichen einer negativen Rückkopplung gewertet: Je höher die intrinsische Aktivierung der T-Zellen, desto höher die Hemmung durch CD200. Des Weiteren wurde mit Hilfe CD200R-überexprimierender T-Zellen eine Korrelation zwischen der Dichte des CD200R und dem Ausmaß der CD200-vermittelten Inhibierung festgestellt. CAR-T-Zellen zeigten eine stärkere Hemmung durch CD200 als primäre T-Zellen. Als Ansatz, die CD200-vermittelte Funktionsstörung zu überwinden, wurden CAR-T-Zellen der zweiten Generation mit einem CD200R-Knock-out ausgestattet. In Anwesenheit von CD200 schützte dieser die CAR-T-Zellen vor der Hemmung, sodass diese besser gegen CD200-positive ALL-Zelllinien wirkten. Des Weiteren wurde ein CD200R-CD28-Fusionsrezeptor entwickelt, der die Inhibierung durch CD200 in eine Aktivierung umwandelt. CAR-T-Zellen, die diesen Rezeptor exprimierten, zeigten eine deutlich höhere Aktivierung und Proliferation nach Kontakt mit CD200-positiven leukämischen Zellen als herkömmliche CAR-T-Zellen

Insgesamt konnten wir ein tieferes Verständnis der Interaktion zwischen leukämischen Zellen und Immunzellen über die CD200/CD200R-Achse erlangen, was einen Beitrag dazu leisten kann, die CAR-T-Zelltherapie für primär refraktäre oder rezidivierende ALL zu verbessern.

Literature

1. Erdmann F, K.P., Grabow D, Spix C., *German Childhood Cancer Registry - Annual Report 2019 (1980-2018)*. 2020: Institute of Medical Biostatistics, Epidemiology and Informatics (IMBEI) at the University Medical Center of the Johannes Gutenberg University Mainz.
2. Howlader N, N.A., Krapcho M, et al *Childhood cancer. SEER Cancer Statistics Review, 1975-2010*. 2013.
3. Gortner L and M. S, *Duale Reihe Pädiatrie*. Vol. 5. Auflage. 2018, Stuttgart: Thieme.
4. Chessells, J.M., *Pitfalls in the diagnosis of childhood leukaemia.* British Journal of Haematology, 2001. **114**(3): p. 506-511.
5. Hunger, S.P. and C.G. Mullighan, *Acute Lymphoblastic Leukemia in Children.* N Engl J Med, 2015. **373**(16): p. 1541-52.
6. Escherich G, S.M., Creutzig U, *S1 Leitlinie: Akute lymphoblastische Leukämie – ALL - im Kindesalter*. 2016: AWMF online.
7. Rivera, G.K., et al., *Bone marrow recurrence after initial intensive treatment for childhood acute lymphoblastic leukemia.* Cancer, 2005. **103**(2): p. 368-376.
8. Schrappe, M., et al., *Outcomes after Induction Failure in Childhood Acute Lymphoblastic Leukemia.* New England Journal of Medicine, 2012. **366**(15): p. 1371-1381.
9. Reismüller, B., et al., *Long-term outcome of initially homogenously treated and relapsed childhood acute lymphoblastic leukaemia in Austria--a population-based report of the Austrian Berlin-Frankfurt-Münster (BFM) Study Group.* Br J Haematol, 2009. **144**(4): p. 559-70.
10. Chessells, J.M., et al., *Long-term follow-up of relapsed childhood acute lymphoblastic leukaemia.* British Journal of Haematology, 2003. **123**(3): p. 396-405.
11. Einsiedel, H.G., et al., *Long-Term Outcome in Children With Relapsed ALL by Risk-Stratified Salvage Therapy: Results of Trial Acute Lymphoblastic Leukemia-Relapse Study of the Berlin-Frankfurt-Münster Group 87.* Journal of Clinical Oncology, 2005. **23**(31): p. 7942-7950.
12. Roy, A., et al., *Outcome after first relapse in childhood acute lymphoblastic leukaemia – lessons from the United Kingdom R2 trial.* British Journal of Haematology, 2005. **130**(1): p. 67-75.
13. Raetz, E.A. and T. Bhatla, *Where do we stand in the treatment of relapsed acute lymphoblastic leukemia?* ASH Education Program Book, 2012. **2012**(1): p. 129-136.
14. Anagnostou, T., et al., *Anti-CD19 chimeric antigen receptor T-cell therapy in acute lymphocytic leukaemia: a systematic review and meta-analysis.* The Lancet Haematology, 2020. **7**(11): p. e816-e826.
15. FDA, *FDA approval brings first gene therapy to the United States*. 2017, FDA news release. p. www.fda.gov.
16. EMA, *Kymriah: tisagenlecleucel*. 2018, European Medicines Agency. p. https://www.ema.europa.eu.
17. Albinger, N., J. Hartmann, and E. Ullrich, *Current status and perspective of CAR-T and CAR-NK cell therapy trials in Germany.* Gene Therapy, 2021.
18. Hartmann, J., et al., *Clinical development of CAR T cells—challenges and opportunities in translating innovative treatment concepts.* EMBO Molecular Medicine, 2017. **9**(9): p. 1183-1197.

19. Maus, M.V., et al., *Antibody-modified T cells: CARs take the front seat for hematologic malignancies.* Blood, 2014. **123**(17): p. 2625-2635.
20. Sadelain, M., R. Brentjens, and I. Rivière, *The Basic Principles of Chimeric Antigen Receptor Design.* Cancer Discovery, 2013. **3**(4): p. 388-398.
21. Srivastava, S. and S.R. Riddell, *Engineering CAR-T cells: Design concepts.* Trends in Immunology, 2015. **36**(8): p. 494-502.
22. Maude, S.L., et al., *Chimeric Antigen Receptor T Cells for Sustained Remissions in Leukemia.* New England Journal of Medicine, 2014. **371**(16): p. 1507-1517.
23. Gardner, R.A., et al., *Intent-to-treat leukemia remission by CD19 CAR T cells of defined formulation and dose in children and young adults.* Blood, 2017. **129**(25): p. 3322-3331.
24. Shah, N.N. and T.J. Fry, *Mechanisms of resistance to CAR T cell therapy.* Nature Reviews Clinical Oncology, 2019. **16**(6): p. 372-385.
25. Sotillo, E., et al., *Convergence of Acquired Mutations and Alternative Splicing of CD19 Enables Resistance to CART-19 Immunotherapy.* 2015. **5**(12): p. 1282-1295.
26. Orlando, E.J., et al., *Genetic mechanisms of target antigen loss in CAR19 therapy of acute lymphoblastic leukemia.* Nature Medicine, 2018. **24**(10): p. 1504-1506.
27. Jacoby, E., et al., *CD19 CAR immune pressure induces B-precursor acute lymphoblastic leukaemia lineage switch exposing inherent leukaemic plasticity.* Nature Communications, 2016. **7**(1): p. 12320.
28. Gardner, R., et al., *Acquisition of a CD19-negative myeloid phenotype allows immune escape of MLL-rearranged B-ALL from CD19 CAR-T-cell therapy.* Blood, 2016. **127**(20): p. 2406-2410.
29. Aparicio-Pérez, C., et al., *Failure of ALL recognition by CAR T cells: a review of CD 19-negative relapses after anti-CD 19 CAR-T treatment in B-ALL.* Frontiers in Immunology, 2023. **14**.
30. Fry, T.J., et al., *CD22-targeted CAR T cells induce remission in B-ALL that is naive or resistant to CD19-targeted CAR immunotherapy.* Nature medicine, 2018. **24**(1): p. 20-28.
31. Fergusson, N.J., et al., *A systematic review and meta-analysis of CD22 CAR T-cells alone or in combination with CD19 CAR T-cells.* Frontiers in Immunology, 2023. **14**.
32. Qin, H., et al., *Preclinical Development of Bivalent Chimeric Antigen Receptors Targeting Both CD19 and CD22.* Mol Ther Oncolytics, 2018. **11**: p. 127-137.
33. Liu, S., et al., *Combination of CD19 and CD22 CAR-T cell therapy in relapsed B-cell acute lymphoblastic leukemia after allogeneic transplantation.* Am J Hematol, 2021.
34. Shiqi, L., et al., *Durable remission related to CAR-T persistence in R/R B-ALL and long-term persistence potential of prime CAR-T.* Mol Ther Oncolytics, 2023. **29**: p. 107-117.
35. Labanieh, L., R.G. Majzner, and C.L. Mackall, *Programming CAR-T cells to kill cancer.* Nature Biomedical Engineering, 2018. **2**(6): p. 377-391.
36. Hamanishi, J., M. Mandai, and I. Konishi, *Immune checkpoint inhibition in ovarian cancer.* International Immunology, 2016. **28**(7): p. 339-348.
37. Brahmer, J.R. and D.M. Pardoll, *Immune checkpoint inhibitors: making immunotherapy a reality for the treatment of lung cancer.* Cancer immunology research, 2013. **1**(2): p. 85-91.
38. Pardoll, D.M., *The blockade of immune checkpoints in cancer immunotherapy.* Nature Reviews Cancer, 2012. **12**: p. 252.
39. Dong, H., et al., *Tumor-associated B7-H1 promotes T-cell apoptosis: A potential mechanism of immune evasion.* Nature Medicine, 2002. **8**(8): p. 793-800.

40. Lipson, E.J. and C.G. Drake, *Ipilimumab: an anti-CTLA-4 antibody for metastatic melanoma.* Clin Cancer Res, 2011. **17**(22): p. 6958-62.
41. Whiteside, T.L., *The tumor microenvironment and its role in promoting tumor growth.* Oncogene, 2008. **27**(45): p. 5904-5912.
42. Quail, D.F. and J.A. Joyce, *Microenvironmental regulation of tumor progression and metastasis.* Nature Medicine, 2013. **19**(11): p. 1423-1437.
43. Wculek, S.K., et al., *Dendritic cells in cancer immunology and immunotherapy.* Nature Reviews Immunology, 2020. **20**(1): p. 7-24.
44. O'Keeffe, M., W.H. Mok, and K.J. Radford, *Human dendritic cell subsets and function in health and disease.* Cell Mol Life Sci, 2015. **72**(22): p. 4309-25.
45. Alshamsan, A., *Induction of tolerogenic dendritic cells by IL-6-secreting CT26 colon carcinoma.* Immunopharmacology and Immunotoxicology, 2012. **34**(3): p. 465-469.
46. Tang, M., et al., *Toll-like Receptor 2 Activation Promotes Tumor Dendritic Cell Dysfunction by Regulating IL-6 and IL-10 Receptor Signaling.* Cell Rep, 2015. **13**(12): p. 2851-64.
47. Kenneth Murphy, C.W., *Janeway's Immunobiology - 9th Edition*. 2016, W.W Norton & Company: United States of America.
48. Chen, S.-Y., et al., *Organ-Specific Microenvironment Modifies Diverse Functional and Phenotypic Characteristics of Leukemia-Associated Macrophages in Mouse T Cell Acute Lymphoblastic Leukemia.* The Journal of Immunology, 2015. **194**(6): p. 2919-2929.
49. Stout, R.D. and J. Suttles, *Functional plasticity of macrophages: reversible adaptation to changing microenvironments.* Journal of Leukocyte Biology, 2004. **76**(3): p. 509-513.
50. Martinez, F.O. and S. Gordon, *The M1 and M2 paradigm of macrophage activation: time for reassessment.* F1000prime reports, 2014. **6**: p. 13-13.
51. Sica, A. and A. Mantovani, *Macrophage plasticity and polarization: in vivo veritas.* The Journal of Clinical Investigation, 2012. **122**(3): p. 787-795.
52. Pollard, J.W., *Tumour-educated macrophages promote tumour progression and metastasis.* Nature Reviews Cancer, 2004. **4**(1): p. 71-78.
53. Leek, R.D., et al., *Association of Macrophage Infiltration with Angiogenesis and Prognosis in Invasive Breast Carcinoma.* Cancer Research, 1996. **56**(20): p. 4625-4629.
54. Bingle, L., N.J. Brown, and C.E. Lewis, *The role of tumour-associated macrophages in tumour progression: implications for new anticancer therapies.* The Journal of Pathology, 2002. **196**(3): p. 254-265.
55. C. O'Sullivan, P., et al., *Secretion of epidermal growth factor by macrophages associated with breast carcinoma.* The Lancet 1993. **342**: p. 148-149.
56. Duluc, D., et al., *Tumor-associated leukemia inhibitory factor and IL-6 skew monocyte differentiation into tumor-associated macrophage-like cells.* Blood, 2007. **110**(13): p. 4319-4330.
57. Mantovani, A., et al., *Role of tumor-associated macrophages in tumor progression and invasion.* Cancer and Metastasis Reviews, 2006. **25**(3): p. 315-322.
58. Yang, X., et al., *Repolarizing heterogeneous leukemia-associated macrophages with more M1 characteristics eliminates their pro-leukemic effects.* Oncoimmunology, 2017. **7**(4): p. e1412910-e1412910.
59. Colmone, A., et al., *Leukemic Cells Create Bone Marrow Niches That Disrupt the Behavior of Normal Hematopoietic Progenitor Cells.* Science, 2008. **322**(5909): p. 1861-1865.
60. Mussai, F., et al., *Acute myeloid leukemia creates an arginase-dependent immunosuppressive microenvironment.* Blood, 2013. **122**(5): p. 749-758.

61. Feucht Judith , et al., *T-cell responses against CD19+ pediatric acute lymphoblastic leukemia mediated by bispecific T-cell engager (BiTE) are regulated contrarily by PD-L1 and CD80/CD86 on leukemic blasts.* Oncotarget, 2016. **7**: p. 76902-76919.
62. Poorebrahim, M., et al., *Counteracting CAR T cell dysfunction.* Oncogene, 2021. **40**(2): p. 421-435.
63. McCaughan, G.W., M.J. Clark, and A. Neil Barclay, *Characterization of the human homolog of the rat MRC OX-2 membrane glycoprotein.* Immunogenetics, 1987. **25**(5): p. 329-335.
64. Clark, M.J., et al., *MRC OX-2 antigen: a lymphoid/neuronal membrane glycoprotein with a structure like a single immunoglobulin light chain.* The EMBO Journal, 1985. **4**(1): p. 113-118.
65. Wright, G.J., et al., *The unusual distribution of the neuronal/lymphoid cell surface CD200 (OX2) glycoprotein is conserved in humans.* Immunology, 2001. **102**(2): p. 173-179.
66. Wright, G.J., et al., *Characterization of the CD200 Receptor Family in Mice and Humans and Their Interactions with CD200.* The Journal of Immunology, 2003. **171**(6): p. 3034-3046.
67. Vieites, J.M.a., et al., *Characterization of human cd200 glycoprotein receptor gene located on chromosome 3q12-13.* Gene, 2003. **311**: p. 99-104.
68. Hatherley, D., et al., *Recombinant CD200 Protein Does Not Bind Activating Proteins Closely Related to CD200 Receptor.* The Journal of Immunology, 2005. **175**(4): p. 2469.
69. Mihrshahi, R., A.N. Barclay, and M.H. Brown, *Essential roles for Dok2 and RasGAP in CD200 receptor-mediated regulation of human myeloid cells.* Journal of immunology (Baltimore, Md. : 1950), 2009. **183**(8): p. 4879-4886.
70. Hoek, R.M., et al., *Down-Regulation of the Macrophage Lineage Through Interaction with OX2 (CD200).* Science, 2000. **290**(5497): p. 1768-1771.
71. Broderick, C., et al., *Constitutive Retinal CD200 Expression Regulates Resident Microglia and Activation State of Inflammatory Cells during Experimental Autoimmune Uveoretinitis.* The American Journal of Pathology, 2002. **161**(5): p. 1669-1677.
72. Walker, D.G., et al., *Decreased expression of CD200 and CD200 receptor in Alzheimer's disease: a potential mechanism leading to chronic inflammation.* Exp Neurol, 2009. **215**(1): p. 5-19.
73. Moreaux, J., et al., *CD200: A putative therapeutic target in cancer.* Biochemical and Biophysical Research Communications, 2008. **366**(1): p. 117-122.
74. McWhirter, J.R., et al., *Antibodies selected from combinatorial libraries block a tumor antigen that plays a key role in immunomodulation.* 2006. **103**(4): p. 1041-1046.
75. Tiribelli, M., et al., *High CD200 expression is associated with poor prognosis in cytogenetically normal acute myeloid leukemia, even in FlT3-ITD-/NPM1+ patients.* Leuk Res, 2017. **58**: p. 31-38.
76. Siva, A., et al., *Immune modulation by melanoma and ovarian tumor cells through expression of the immunosuppressive molecule CD200.* Cancer Immunology, Immunotherapy, 2008. **57**(7): p. 987-996.
77. Chen, J.X., et al., *Over-expression of CD200 predicts poor prognosis in MDS.* Leuk Res, 2017. **56**: p. 1-6.
78. Daniela Damiani, et al., *Clinical impact of CD200 expression in patients with acute myeloid leukemia and correlation with other molecular prognostic factors.* Oncotarget, 2015. **6**.

79. Tonks, A., et al., *CD200 as a prognostic factor in acute myeloid leukaemia.* Leukemia, 2007. **21**(3): p. 566-568.
80. Jenmalm, M.C., et al., *Regulation of Myeloid Cell Function through the CD200 Receptor.* The Journal of Immunology, 2006. **176**(1): p. 191-199.
81. Herbrich, S., et al., *Overexpression of CD200 is a stem cell-specific mechanism of immune evasion in AML.* Journal for ImmunoTherapy of Cancer, 2021. **9**(7): p. e002968.
82. Petermann, K.B., et al., *CD200 is induced by ERK and is a potential therapeutic target in melanoma.* The Journal of Clinical Investigation, 2007. **117**(12): p. 3922-3929.
83. Fallarino, F., et al., *Murine Plasmacytoid Dendritic Cells Initiate the Immunosuppressive Pathway of Tryptophan Catabolism in Response to CD200 Receptor Engagement.* The Journal of Immunology, 2004. **173**(6): p. 3748-3754.
84. Coles, S.J., et al., *Expression of CD200 on AML blasts directly suppresses memory T-cell function.* Leukemia, 2012. **26**: p. 2148.
85. Coles, S.J., et al., *Increased CD200 expression in acute myeloid leukemia is linked with an increased frequency of FoxP3+ regulatory T cells.* Leukemia, 2012. **26**(9): p. 2146-2148.
86. Rygiel, T.P. and L. Meyaard, *CD200R signaling in tumor tolerance and inflammation: A tricky balance.* Current Opinion in Immunology, 2012. **24**(2): p. 233-238.
87. Alapat, D., et al., *Diagnostic usefulness and prognostic impact of CD200 expression in lymphoid malignancies and plasma cell myeloma.* American journal of clinical pathology, 2012. **137**(1): p. 93-100.
88. Blaeschke, F., et al., *Leukemia-induced dysfunctional TIM-3(+)CD4(+) bone marrow T cells increase risk of relapse in pediatric B-precursor ALL patients.* Leukemia, 2020. **34**(10): p. 2607-2620.
89. Mahadevan, D., et al., *Phase I study of samalizumab in chronic lymphocytic leukemia and multiple myeloma: blockade of the immune checkpoint CD200.* J Immunother Cancer, 2019. **7**(1): p. 227.
90. Diamanti, P., et al., *Targeting pediatric leukemia propagating cells using anti-CD200 antibody therapy.* Blood Adv, 2021.
91. Oda, S.K., et al., *A CD200R-CD28 fusion protein appropriates an inhibitory signal to enhance T-cell function and therapy of murine leukemia.* 2017. **130**(22): p. 2410-2419.
92. Apfelbeck, A.J., *Generation and characterization of CD19 CAR T cells with PD-1_CD28 fusion receptor*, in *Medizinische Fakultät*. 2022, LMU Munich.
93. Deisenberger, L., *CRISPR/Cas9-mediated generation and characterization of glucocorticoid-resistant virus-specific T cells*, in *Medizinische Fakultät*. 2022, LMU Munich.
94. Ortner, E., *Induction of T-cell attack against ALL through a TIM-3-CD28 fusion receptor.*, in *Medizinische Fakultät*. 2023, LMU Munich.
95. Ghani, K., et al., *Generation of a high-titer packaging cell line for the production of retroviral vectors in suspension and serum-free media.* Gene Therapy, 2007. **14**(24): p. 1705-1711.
96. Ghani, K., et al., *Efficient Human Hematopoietic Cell Transduction Using RD114- and GALV-Pseudotyped Retroviral Vectors Produced in Suspension and Serum-Free Media.* Human Gene Therapy, 2009. **20**(9): p. 966-974.
97. Brinkman, E.K., et al., *Easy quantitative assessment of genome editing by sequence trace decomposition.* Nucleic Acids Research, 2014. **42**(22): p. e168-e168.

98. Stitz, J., et al., *Lentiviral vectors pseudotyped with envelope glycoproteins derived from gibbon ape leukemia virus and murine leukemia virus 10A1.* Virology, 2000. **273**(1): p. 16-20.
99. Blaeschke, F., et al., *Induction of a central memory and stem cell memory phenotype in functionally active CD4(+) and CD8(+) CAR T cells produced in an automated good manufacturing practice system for the treatment of CD19(+) acute lymphoblastic leukemia.* Cancer Immunol Immunother, 2018. **67**(7): p. 1053-1066.
100. Restifo, N.P., *Big bang theory of stem-like T cells confirmed.* Blood, 2014. **124**(4): p. 476-7.
101. Benner, B., et al., *Generation of monocyte-derived tumor-associated macrophages using tumor-conditioned media provides a novel method to study tumor-associated macrophages in vitro.* Journal for ImmunoTherapy of Cancer, 2019. **7**(1): p. 140.
102. Heusinkveld, M. and S.H. van der Burg, *Identification and manipulation of tumor associated macrophages in human cancers.* Journal of translational medicine, 2011. **9**: p. 216-216.
103. Petty, A.J. and Y. Yang, *Tumor-Associated Macrophages in Hematologic Malignancies: New Insights and Targeted Therapies.* Cells, 2019. **8**(12): p. 1526.
104. Alexandrov, L.B., et al., *Signatures of mutational processes in human cancer.* Nature, 2013. **500**(7463): p. 415-421.
105. Coles, S.J., et al., *CD200 expression suppresses natural killer cell function and directly inhibits patient anti-tumor response in acute myeloid leukemia.* Leukemia, 2011. **25**(5): p. 792-799.
106. Pallasch, C.P., et al., *Disruption of T cell suppression in chronic lymphocytic leukemia by CD200 blockade.* Leuk Res, 2009. **33**(3): p. 460-4.
107. Wang, L., et al., *Tumor expression of CD200 inhibits IL-10 production by tumor-associated myeloid cells and prevents tumor immune evasion of CTL therapy.* European journal of immunology, 2010. **40**(9): p. 2569-2579.
108. Galon, J., et al., *Characterization of anti-CD19 chimeric antigen receptor (CAR) T cell-mediated tumor microenvironment immune gene profile in a multicenter trial (ZUMA-1) with axicabtagene ciloleucel (axi-cel, KTE-C19).* Journal of Clinical Oncology, 2017. **35**(15_suppl): p. 3025-3025.
109. Kochenderfer, J.N., et al., *Chemotherapy-refractory diffuse large B-cell lymphoma and indolent B-cell malignancies can be effectively treated with autologous T cells expressing an anti-CD19 chimeric antigen receptor.* Journal of clinical oncology : official journal of the American Society of Clinical Oncology, 2015. **33**(6): p. 540-549.
110. Sommermeyer, D., et al., *Chimeric antigen receptor-modified T cells derived from defined CD8+ and CD4+ subsets confer superior antitumor reactivity in vivo.* Leukemia, 2016. **30**(2): p. 492-500.
111. Sadelain, M., I. Rivière, and S. Riddell, *Therapeutic T cell engineering.* Nature, 2017. **545**(7655): p. 423-431.
112. Petersen, C.T., et al., *Improving T-cell expansion and function for adoptive T-cell therapy using ex vivo treatment with PI3Kδ inhibitors and VIP antagonists.* Blood Advances, 2018. **2**(3): p. 210-223.
113. Biasco, L., et al., *In vivo tracking of T cells in humans unveils decade-long survival and activity of genetically modified T memory stem cells.* Science Translational Medicine, 2015. **7**(273): p. 273ra13-273ra13.
114. Zhao, L., et al., *TIM-3: An update on immunotherapy.* International Immunopharmacology, 2021. **99**: p. 107933.

115. Odorizzi, P.M., et al., *Genetic absence of PD-1 promotes accumulation of terminally differentiated exhausted CD8+ T cells.* Journal of Experimental Medicine, 2015. **212**(7): p. 1125-1137.
116. Tivol, E.A., et al., *Loss of CTLA-4 leads to massive lymphoproliferation and fatal multiorgan tissue destruction, revealing a critical negative regulatory role of CTLA-4.* Immunity, 1995. **3**(5): p. 541-547.
117. Waterhouse, P., et al., *Lymphoproliferative Disorders with Early Lethality in Mice Deficient in Ctla-4.* Science, 1995. **270**(5238): p. 985-988.
118. Rygiel, T.P., et al., *Lack of CD200 Enhances Pathological T Cell Responses during Influenza Infection.* The Journal of Immunology, 2009. **183**(3): p. 1990-1996.
119. Mukhopadhyay, S., et al., *Immune Inhibitory Ligand CD200 Induction by TLRs and NLRs Limits Macrophage Activation to Protect the Host from Meningococcal Septicemia.* Cell Host & Microbe, 2010. **8**(3): p. 236-247.
120. Maude, S.L., et al., *Tisagenlecleucel in Children and Young Adults with B-Cell Lymphoblastic Leukemia.* New England Journal of Medicine, 2018. **378**(5): p. 439-448.
121. Di Stasi, A., et al., *Inducible Apoptosis as a Safety Switch for Adoptive Cell Therapy.* New England Journal of Medicine, 2011. **365**(18): p. 1673-1683.
122. Eyquem, J., et al., *Targeting a CAR to the TRAC locus with CRISPR/Cas9 enhances tumour rejection.* Nature, 2017. **543**(7643): p. 113-117.

Supplements

Index of appendices

Supp. 1. Sequences of used primers

Supp. 1.1. Verification of correct retroviral transduction

Supplementary table 1: Sequences of primers used for verification of correct retroviral transduction.

Primers used for PCR	
CAR_ident_forw	GCCAAACATTATTACTACGGTGGTA
CAR_ident_rev	TATGGGAATAAATGGCGGTAAGATG
Primers used for Sanger sequencing	
CAR_ident_forw	GCCAAACATTATTACTACGGTGGTA
CAR_ident_rev	TATGGGAATAAATGGCGGTAAGATG
K2A_CD200R_forw	GACGTGGAGTCCAACCCAGGCCCGCTCTGCCCTTGGAGAACTGC
K2A_CD200R_rev	GCAGTTCTCCAAGGGCAGAGCGGGCCTGGGTTGGACTCCACGTC
CD200RK_Seq_forw	GGACGAAGAGAGGAGTACGATGTTTTGGACAAGAG

Supp. 1.2. Verification of 200R knock-out

Supplementary table 2: Sequences of primers used for verification of CD200R knock-out

Primers used for PCR	
STO220_CD200R_f2	TGCTTCAGGGCTTCATACAGGA
STO221_CD200R_r2	CAGGAGGCTGAGTGGGAGGAC T
Primers used for Sanger sequencing	
STO220_CD200R_f2	TGCTTCAGGGCTTCATACAGGA

Supp. 2. Sequences of used T cell constructs

Supp. 2.1. $_{RV}$CD200R-Iso1^{OE}

CTCTGCCCTTGGAGAACTGCTAACCTAGGGCTACTGTTGATTTTGACTATCTTCTTAGTGGCCGCTTCA
AGCAGTTTATGTATGGATGAAAAACAGATTACACAGAACTACTCGAAAGTACTCGCAGAAGTTAACA
CTTCATGGCCTGTAAAGATGGCTACAAATGCTGTGCTTTGTTGCCCTCCTATCGCATTAAGAAATTTG
ATCATAATAACATGGGAAATAATCCTGAGAGGCCAGCCTTCCTGCACAAAAGCCTACAAGAAAGAAA
CAAATGAGACCAAGGAAACCAACTGTACTGATGAGAGAATAACCTGGGTCTCCAGACCTGATCAGA
ATTCGGACCTTCAGATTCGTACCGTGGCCATCACTCATGACGGGTATTACAGATGCATAATGGTAACA
CCTGATGGGAATTTCCATCGTGGATATCACCTCCAAGTGTTAGTTACACCTGAAGTGACCCTGTTTCA
AAACAGGAATAGAACTGCAGTATGCAAGGCAGTTGCAGGGAAGCCAGCTGCGCATATCTCCTGGAT
CCCAGAGGGCGATTGTGCCACTAAGCAAGAATACTGGAGCAATGGCACAGTGACTGTTAAGAGTAC
ATGCCACTGGGAGGTCCACAATGTGTCTACCGTGACCTGCCACGTCTCCCATTTGACTGGCAACAAG
AGTCTGTACATAGAGCTACTTCCTGTTCCAGGTGCCAAAAAATCAGCAAAATTATATATTCCATATATC
ATCCTTACTATTATTATTTTGACCATCGTGGGATTCATTTGGTTGTTGAAAGTCAATGGCTGCAGAAA
ATATAAATTGAATAAAACAGAATCTACTCCAGTTGTTGAGGAGGATGAAATGCAGCCCTATGCCAGC
TACACAGAGAAGAACAATCCTCTCTATGATACTACAAACAAGGTGAAGGCATCTGAGGCATTACAAA
GTGAAGTTGACACAGACCTCCATACTTTATAA

Supp. 2.2. $_{RV}$CD200R-Iso4^{OE}

CTCTGCCCTTGGAGAACTGCTAACCTAGGGCTACTGTTGATTTTGACTATCTTCTTAGTGGCCGAAGC
GGAGGGTGCTGCTCAACCAAACAACTCATTAATGCTGCAAACTAGCAAGGAGAATCATGCTTTAGCT
TCAAGCAGTTTATGTATGGATGAAAAACAGATTACACAGAACTACTCGAAAGTACTCGCAGAAGTTA
ACACTTCATGGCCTGTAAAGATGGCTACAAATGCTGTGCTTTGTTGCCCTCCTATCGCATTAAGAAAT
TTGATCATAATAACATGGGAAATAATCCTGAGAGGCCAGCCTTCCTGCACAAAAGCCTACAAGAAAG
AAACAAATGAGACCAAGGAAACCAACTGTACTGATGAGAGAATAACCTGGGTCTCCAGACCTGATC
AGAATTCGGACCTTCAGATTCGTACCGTGGCCATCACTCATGACGGGTATTACAGATGCATAATGGT
AACACCTGATGGGAATTTCCATCGTGGATATCACCTCCAAGTGTTAGTTACACCTGAAGTGACCCTGT
TTCAAAACAGGAATAGAACTGCAGTATGCAAGGCAGTTGCAGGGAAGCCAGCTGCGCATATCTCCT
GGATCCCAGAGGGCGATTGTGCCACTAAGCAAGAATACTGGAGCAATGGCACAGTGACTGTTAAGA
GTACATGCCACTGGGAGGTCCACAATGTGTCTACCGTGACCTGCCACGTCTCCCATTTGACTGGCAAC
AAGAGTCTGTACATAGAGCTACTTCCTGTTCCAGGTGCCAAAAAATCAGCAAAATTATATATTCCATA
TATCATCCTTACTATTATTATTTTGACCATCGTGGGATTCATTTGGTTGTTGAAAGTCAATGGCTGCAG
AAAATATAAATTGAATAAAACAGAATCTACTCCAGTTGTTGAGGAGGATGAAATGCAGCCCTATGCC
AGCTACACAGAGAAGAACAATCCTCTCTATGATACTACAAACAAGGTGAAGGCATCTGAGGCATTAC
AAAGTGAAGTTGACACAGACCTCCATACTTTATAA

Supp. 2.3. $_{RV}$19-z

ATGCTTCTCCTGGTGACAAGCCTTCTGCTCTGTGAGTTACCACACCCAGCATTCCTCCTGATCCCAGAC
ATCCAGATGACACAGACTACATCCTCCCTGTCTGCCTCTCTGGGAGACAGAGTCACCATCAGTTGCAG
GGCAAGTCAGGACATTAGTAAATATTTAAATTGGTATCAGCAGAAACCAGATGGAACTGTTAAACTC
CTGATCTACCATACATCAAGATTACACTCAGGAGTCCCATCAAGGTTCAGTGGCAGTGGGTCTGGAA
CAGATTATTCTCTCACCATTAGCAACCTGGAGCAAGAAGATATTGCCACTTACTTTTGCCAACAGGGT
AATACGCTTCCGTACACGTTCGGAGGGGGGACTAAGTTGGAAATAACAGGCTCCACCTCTGGATCCG
GCAAGCCCGGATCTGGCGAGGGATCCACCAAGGGCGAGGTGAAACTGCAGGAGTCAGGACCTGGC
CTGGTGGCGCCCTCACAGAGCCTGTCCGTCACATGCACTGTCTCAGGGGTCTCATTACCCGACTATGG
TGTAAGCTGGATTCGCCAGCCTCCACGAAAGGGTCTGGAGTGGCTGGGAGTAATATGGGGTAGTGA
AACCACATACTATAATTCAGCTCTCAAATCCAGACTGACCATCATCAAGGACAACTCCAAGAGCCAAG
TTTTCTTAAAAATGAACAGTCTGCAAACTGATGACACAGCCATTTACTACTGTGCCAAACATTATTACT
ACGGTGGTAGCTATGCTATGGACTACTGGGGTCAAGGAACCTCAGTCACCGTCTCCTCAGAGCAAAA
GCTCATTTCTGAAGAGGACTTGTTCGTGCCGGTCTTCCTGCCAGCGAAGCCCACCACGACGCCAGCG
CCGCGACCACCAACACCGGCGCCCACCATCGCGTCGCAGCCCCTGTCCCTGCGCCCAGAGGCGTGCC
GGCCAGCGGCGGGGGGCGCAGTGCACACGAGGGGGCTGGACTTCGCCTGTGATATCTACATCTGG
GCGCCCTTGGCCGGGACTTGTGGGGTCCTTCTCCTGTCACTGGTTATCACCCTTTACTGCAACCACAG
GAACAGAGTGAAGTTCAGCAGGAGCGCAGACGCCCCCGCGTACCAGCAGGGCCAGAACCAGCTCTA
TAACGAGCTCAATCTAGGACGAAGAGAGGAGTACGATGTTTTGGACAAGAGACGTGGCCGGGACCC
TGAGATGGGGGGAAAGCCGAGAAGGAAGAACCCTCAGGAAGGCCTGTACAATGAACTGCAGAAAG
ATAAGATGGCGGAGGCCTACAGTGAGATTGGGATGAAAGGCGAGCGCCGGAGGGGCAAGGGGCA
CGATGGCCTTTACCAGGGTCTCAGTACAGCCACCAAGGACACCTACGACGCCCTTCACATGCAGGCC
CTGCCCCCTCGCTAA

Supp. 2.4. $_{RV}$19-BBz

ATGCTTCTCCTGGTGACAAGCCTTCTGCTCTGTGAGTTACCACACCCAGCATTCCTCCTGATCCCAGAC
ATCCAGATGACACAGACTACATCCTCCCTGTCTGCCTCTCTGGGAGACAGAGTCACCATCAGTTGCAG
GGCAAGTCAGGACATTAGTAAATATTTAAATTGGTATCAGCAGAAACCAGATGGAACTGTTAAACTC
CTGATCTACCATACATCAAGATTACACTCAGGAGTCCCATCAAGGTTCAGTGGCAGTGGGTCTGGAA
CAGATTATTCTCTCACCATTAGCAACCTGGAGCAAGAAGATATTGCCACTTACTTTTGCCAACAGGGT
AATACGCTTCCGTACACGTTCGGAGGGGGGACTAAGTTGGAAATAACAGGCTCCACCTCTGGATCCG
GCAAGCCCGGATCTGGCGAGGGATCCACCAAGGGCGAGGTGAAACTGCAGGAGTCAGGACCTGGC
CTGGTGGCGCCCTCACAGAGCCTGTCCGTCACATGCACTGTCTCAGGGGTCTCATTACCCGACTATGG
TGTAAGCTGGATTCGCCAGCCTCCACGAAAGGGTCTGGAGTGGCTGGGAGTAATATGGGGTAGTGA
AACCACATACTATAATTCAGCTCTCAAATCCAGACTGACCATCATCAAGGACAACTCCAAGAGCCAAG
TTTTCTTAAAAATGAACAGTCTGCAAACTGATGACACAGCCATTTACTACTGTGCCAAACATTATTACT
ACGGTGGTAGCTATGCTATGGACTACTGGGGTCAAGGAACCTCAGTCACCGTCTCCTCAGAGCAAAA
GCTCATTTCTGAAGAGGACTTGTTCGTGCCGGTCTTCCTGCCAGCGAAGCCCACCACGACGCCAGCG
CCGCGACCACCAACACCGGCGCCCACCATCGCGTCGCAGCCCCTGTCCCTGCGCCCAGAGGCGTGCC

GGCCAGCGGCGGGGGGCGCAGTGCACACGAGGGGGCTGGACTTCGCCTGTGATATCTACATCTGG
GCGCCCTTGGCCGGGACTTGTGGGGTCCTTCTCCTGTCACTGGTTATCACCCTTTACTGCAACCACAG
GAACAAACGGGGCAGAAAGAAACTCCTGTATATATTCAAACAACCATTTATGAGACCAGTACAAACT
ACTCAAGAGGAAGATGGCTGTAGCTGCCGATTTCCAGAAGAAGAAGAAGGAGGATGTGAACTGAG
AGTGAAGTTCAGCAGGAGCGCAGACGCCCCCGCGTACCAGCAGGGCCAGAACCAGCTCTATAACGA
GCTCAATCTAGGACGAAGAGAGGAGTACGATGTTTTGGACAAGAGACGTGGCCGGGACCCTGAGAT
GGGGGGAAAGCCGAGAAGGAAGAACCCTCAGGAAGGCCTGTACAATGAACTGCAGAAAGATAAGA
TGGCGGAGGCCTACAGTGAGATTGGGATGAAAGGCGAGCGCCGGAGGGGCAAGGGGCACGATGG
CCTTTACCAGGGTCTCAGTACAGCCACCAAGGACACCTACGACGCCCTTCACATGCAGGCCCTGCCCC
CTCGCTAA

Supp. 2.5. $_{RV}$19-z$_{RV}$CD200R-CD28

ATGCTTCTCCTGGTGACAAGCCTTCTGCTCTGTGAGTTACCACACCCAGCATTCCTCCTGATCCCAGAC
ATCCAGATGACACAGACTACATCCTCCCTGTCTGCCTCTCTGGGAGACAGAGTCACCATCAGTTGCAG
GGCAAGTCAGGACATTAGTAAATATTTAAATTGGTATCAGCAGAAACCAGATGGAACTGTTAAACTC
CTGATCTACCATACATCAAGATTACACTCAGGAGTCCCATCAAGGTTCAGTGGCAGTGGGTCTGGAA
CAGATTATTCTCTCACCATTAGCAACCTGGAGCAAGAAGATATTGCCACTTACTTTTGCCAACAGGGT
AATACGCTTCCGTACACGTTCGGAGGGGGGACTAAGTTGGAAATAACAGGCTCCACCTCTGGATCCG
GCAAGCCCGGATCTGGCGAGGGATCCACCAAGGGCGAGGTGAAACTGCAGGAGTCAGGACCTGGC
CTGGTGGCGCCCTCACAGAGCCTGTCCGTCACATGCACTGTCTCAGGGGTCTCATTACCCGACTATGG
TGTAAGCTGGATTCGCCAGCCTCCACGAAAGGGTCTGGAGTGGCTGGGAGTAATATGGGGTAGTGA
AACCACATACTATAATTCAGCTCTCAAATCCAGACTGACCATCATCAAGGACAACTCCAAGAGCCAAG
TTTTCTTAAAAATGAACAGTCTGCAAACTGATGACACAGCCATTTACTACTGTGCCAAACATTATTACT
ACGGTGGTAGCTATGCTATGGACTACTGGGGTCAAGGAACCTCAGTCACCGTCTCCTCAGAGCAAAA
GCTCATTTCTGAAGAGGACTTGTTCGTGCCGGTCTTCCTGCCAGCGAAGCCCACCACGACGCCAGCG
CCGCGACCACCAACACCGGCGCCCACCATCGCGTCGCAGCCCCTGTCCCTGCGCCCAGAGGCGTGCC
GGCCAGCGGCGGGGGGCGCAGTGCACACGAGGGGGCTGGACTTCGCCTGTGATATCTACATCTGG
GCGCCCTTGGCCGGGACTTGTGGGGTCCTTCTCCTGTCACTGGTTATCACCCTTTACTGCAACCACAG
GAACAGAGTGAAGTTCAGCAGGAGCGCAGACGCCCCCGCGTACCAGCAGGGCCAGAACCAGCTCTA
TAACGAGCTCAATCTAGGACGAAGAGAGGAGTACGATGTTTTGGACAAGAGACGTGGCCGGGACCC
TGAGATGGGGGGAAAGCCGAGAAGGAAGAACCCTCAGGAAGGCCTGTACAATGAACTGCAGAAAG
ATAAGATGGCGGAGGCCTACAGTGAGATTGGGATGAAAGGCGAGCGCCGGAGGGGCAAGGGGCA
CGATGGCCTTTACCAGGGTCTCAGTACAGCCACCAAGGACACCTACGACGCCCTTCACATGCAGGCC
CTGCCCCCTCGCGTGAAACAGACTTTGAATTTTGACCTTCTCAAGTTGGCGGGAGACGTGGAGTCCA
ACCCAggcccgCTCTGCCCTTGGAGAACTGCTAACCTAGGGCTACTGTTGATTTTGACTATCTTCTTAGT
GGCCGAAGCGGAGGGTGCTGCTCAACCAAACAACTCATTAATGCTGCAAACTAGCAAGGAGAATCA
TGCTTTAGCTTCAAGCAGTTTATGTATGGATGAAAAACAGATTACACAGAACTACTCGAAAGTACTCG
CAGAAGTTAACACTTCATGGCCTGTAAAGATGGCTACAAATGCTGTGCTTTGTTGCCCTCCTATCGCA
TTAAGAAATTTGATCATAATAACATGGGAAATAATCCTGAGAGGCCAGCCTTCCTGCACAAAAGCCT

ACAAGAAAGAAACAAATGAGACCAAGGAAACCAACTGTACTGATGAGAGAATAACCTGGGTCTCCA
GACCTGATCAGAATTCGGACCTTCAGATTCGTACCGTGGCCATCACTCATGACGGGTATTACAGATG
CATAATGGTAACACCTGATGGGAATTTCCATCGTGGATATCACCTCCAAGTGTTAGTTACACCTGAAG
TGACCCTGTTTCAAAACAGGAATAGAACTGCAGTATGCAAGGCAGTTGCAGGGAAGCCAGCTGCGC
ATATCTCCTGGATCCCAGAGGGCGATTGTGCCACTAAGCAAGAATACTGGAGCAATGGCACAGTGAC
TGTTAAGAGTACATGCCACTGGGAGGTCCACAATGTGTCTACCGTGACCTGCCACGTCTCCCATTTGA
CTGGCAACAAGAGTCTGTACATAGAGCTACTTCCTGTTTGTCCAAGTCCCCTATTTCCCGGACCTTCTA
AGCCCTTTTGGGTGCTGGTGGTGGTTGGTGGAGTCCTGGCTTGCTATAGCTTGCTAGTAACAGTGGC
CTTTATTATTTTCTGGGTGAGGAGTAAGAGGAGCAGGCTCCTGCACAGTGACTACATGAACATGACT
CCCCGCCGCCCCGGGCCCACCCGCAAGCATTACCAGCCCTATGCCCCACCACGCGACTTCGCAGCCTA
TCGCTCCTGA

Supp. 2.6. $_{RV}$19-BBz$_{RV}$CD200R-CD28

ATGCTTCTCCTGGTGACAAGCCTTCTGCTCTGTGAGTTACCACACCCAGCATTCCTCCTGATCCCAGAC
ATCCAGATGACACAGACTACATCCTCCCTGTCTGCCTCTCTGGGAGACAGAGTCACCATCAGTTGCAG
GGCAAGTCAGGACATTAGTAAATATTTAAATTGGTATCAGCAGAAACCAGATGGAACTGTTAAACTC
CTGATCTACCATACATCAAGATTACACTCAGGAGTCCCATCAAGGTTCAGTGGCAGTGGGTCTGGAA
CAGATTATTCTCTCACCATTAGCAACCTGGAGCAAGAAGATATTGCCACTTACTTTTGCCAACAGGGT
AATACGCTTCCGTACACGTTCGGAGGGGGGACTAAGTTGGAAATAACAGGCTCCACCTCTGGATCCG
GCAAGCCCGGATCTGGCGAGGGATCCACCAAGGGCGAGGTGAAACTGCAGGAGTCAGGACCTGGC
CTGGTGGCGCCCTCACAGAGCCTGTCCGTCACATGCACTGTCTCAGGGGTCTCATTACCCGACTATGG
TGTAAGCTGGATTCGCCAGCCTCCACGAAAGGGTCTGGAGTGGCTGGGAGTAATATGGGGTAGTGA
AACCACATACTATAATTCAGCTCTCAAATCCAGACTGACCATCATCAAGGACAACTCCAAGAGCCAAG
TTTTCTTAAAAATGAACAGTCTGCAAACTGATGACACAGCCATTTACTACTGTGCCAAACATTATTACT
ACGGTGGTAGCTATGCTATGGACTACTGGGGTCAAGGAACCTCAGTCACCGTCTCCTCAGAGCAAAA
GCTCATTTCTGAAGAGGACTTGTTCGTGCCGGTCTTCCTGCCAGCGAAGCCCACCACGACGCCAGCG
CCGCGACCACCAACACCGGCGCCCACCATCGCGTCGCAGCCCCTGTCCCTGCGCCCAGAGGCGTGCC
GGCCAGCGGCGGGGGGCGCAGTGCACACGAGGGGGCTGGACTTCGCCTGTGATATCTACATCTGG
GCGCCCTTGGCCGGGACTTGTGGGGTCCTTCTCCTGTCACTGGTTATCACCCTTTACTGCAACCACAG
GAACAAACGGGGCAGAAAGAAACTCCTGTATATATTCAAACAACCATTTATGAGACCAGTACAAACT
ACTCAAGAGGAAGATGGCTGTAGCTGCCGATTTCCAGAAGAAGAAGAAGGAGGATGTGAACTGAG
AGTGAAGTTCAGCAGGAGCGCAGACGCCCCCGCGTACCAGCAGGGCCAGAACCAGCTCTATAACGA
GCTCAATCTAGGACGAAGAGAGGAGTACGATGTTTTGGACAAGAGACGTGGCCGGGACCCTGAGAT
GGGGGGAAAGCCGAGAAGGAAGAACCCTCAGGAAGGCCTGTACAATGAACTGCAGAAAGATAAGA
TGGCGGAGGCCTACAGTGAGATTGGGATGAAAGGCGAGCGCCGGAGGGGCAAGGGGCACGATGG
CCTTTACCAGGGTCTCAGTACAGCCACCAAGGACACCTACGACGCCCTTCACATGCAGGCCCTGCCCC
CTCGCGTGAAACAGACTTTGAATTTTGACCTTCTCAAGTTGGCGGGAGACGTGGAGTCCAACCCAggc
ccgCTCTGCCCTTGGAGAACTGCTAACCTAGGGCTACTGTTGATTTTGACTATCTTCTTAGTGGCCGAA
GCGGAGGGTGCTGCTCAACCAAACAACTCATTAATGCTGCAAACTAGCAAGGAGAATCATGCTTTAG

CTTCAAGCAGTTTATGTATGGATGAAAAACAGATTACACAGAACTACTCGAAAGTACTCGCAGAAGT
TAACACTTCATGGCCTGTAAAGATGGCTACAAATGCTGTGCTTTGTTGCCCTCCTATCGCATTAAGAA
ATTTGATCATAATAACATGGGAAATAATCCTGAGAGGCCAGCCTTCCTGCACAAAAGCCTACAAGAA
AGAAACAAATGAGACCAAGGAAACCAACTGTACTGATGAGAGAATAACCTGGGTCTCCAGACCTGA
TCAGAATTCGGACCTTCAGATTCGTACCGTGGCCATCACTCATGACGGGTATTACAGATGCATAATG
GTAACACCTGATGGGAATTTCCATCGTGGATATCACCTCCAAGTGTTAGTTACACCTGAAGTGACCCT
GTTTCAAAACAGGAATAGAACTGCAGTATGCAAGGCAGTTGCAGGGAAGCCAGCTGCGCATATCTC
CTGGATCCCAGAGGGCGATTGTGCCACTAAGCAAGAATACTGGAGCAATGGCACAGTGACTGTTAA
GAGTACATGCCACTGGGAGGTCCACAATGTGTCTACCGTGACCTGCCACGTCTCCCATTTGACTGGC
AACAAGAGTCTGTACATAGAGCTACTTCCTGTTTGTCCAAGTCCCCTATTTCCCGGACCTTCTAAGCCC
TTTTGGGTGCTGGTGGTGGTTGGTGGAGTCCTGGCTTGCTATAGCTTGCTAGTAACAGTGGCCTTTAT
TATTTTCTGGGTGAGGAGTAAGAGGAGCAGGCTCCTGCACAGTGACTACATGAACATGACTCCCCGC
CGCCCCGGGCCCACCCGCAAGCATTACCAGCCCTATGCCCCACCACGCGACTTCGCAGCCTATCGCTC
CTGA

Supp. 2.7. $_{RV}$19-BBz$_{RV}$CD200R-Iso4^{OE}

ATGCTTCTCCTGGTGACAAGCCTTCTGCTCTGTGAGTTACCACACCCAGCATTCCTCCTGATCCCAGAC
ATCCAGATGACACAGACTACATCCTCCCTGTCTGCCTCTCTGGGAGACAGAGTCACCATCAGTTGCAG
GGCAAGTCAGGACATTAGTAAATATTTAAATTGGTATCAGCAGAAACCAGATGGAACTGTTAAACTC
CTGATCTACCATACATCAAGATTACACTCAGGAGTCCCATCAAGGTTCAGTGGCAGTGGGTCTGGAA
CAGATTATTCTCTCACCATTAGCAACCTGGAGCAAGAAGATATTGCCACTTACTTTTGCCAACAGGGT
AATACGCTTCCGTACACGTTCGGAGGGGGGACTAAGTTGGAAATAACAGGCTCCACCTCTGGATCCG
GCAAGCCCGGATCTGGCGAGGGATCCACCAAGGGCGAGGTGAAACTGCAGGAGTCAGGACCTGGC
CTGGTGGCGCCCTCACAGAGCCTGTCCGTCACATGCACTGTCTCAGGGGTCTCATTACCCGACTATGG
TGTAAGCTGGATTCGCCAGCCTCCACGAAAGGGTCTGGAGTGGCTGGGAGTAATATGGGGTAGTGA
AACCACATACTATAATTCAGCTCTCAAATCCAGACTGACCATCATCAAGGACAACTCCAAGAGCCAAG
TTTTCTTAAAAATGAACAGTCTGCAAACTGATGACACAGCCATTTACTACTGTGCCAAACATTATTACT
ACGGTGGTAGCTATGCTATGGACTACTGGGGTCAAGGAACCTCAGTCACCGTCTCCTCAGAGCAAAA
GCTCATTTCTGAAGAGGACTTGTTCGTGCCGGTCTTCCTGCCAGCGAAGCCCACCACGACGCCAGCG
CCGCGACCACCAACACCGGCGCCCACCATCGCGTCGCAGCCCCTGTCCCTGCGCCCAGAGGCGTGCC
GGCCAGCGGCGGGGGGCGCAGTGCACACGAGGGGGCTGGACTTCGCCTGTGATATCTACATCTGG
GCGCCCTTGGCCGGGACTTGTGGGGTCCTTCTCCTGTCACTGGTTATCACCCTTTACTGCAACCACAG
GAACAAACGGGGCAGAAAGAAACTCCTGTATATATTCAAACAACCATTTATGAGACCAGTACAAACT
ACTCAAGAGGAAGATGGCTGTAGCTGCCGATTTCCAGAAGAAGAAGAAGGAGGATGTGAACTGAG
AGTGAAGTTCAGCAGGAGCGCAGACGCCCCCGCGTACCAGCAGGGCCAGAACCAGCTCTATAACGA
GCTCAATCTAGGACGAAGAGAGGAGTACGATGTTTTGGACAAGAGACGTGGCCGGGACCCTGAGAT
GGGGGGAAAGCCGAGAAGGAAGAACCCTCAGGAAGGCCTGTACAATGAACTGCAGAAAGATAAGA
TGGCGGAGGCCTACAGTGAGATTGGGATGAAAGGCGAGCGCCGGAGGGGCAAGGGGCACGATGG
CCTTTACCAGGGTCTCAGTACAGCCACCAAGGACACCTACGACGCCCTTCACATGCAGGCCCTGCCCC

CTCGCGTGAAACAGACTTTGAATTTTGACCTTCTCAAGTTGGCGGGAGACGTGGAGTCCAACCCAGG
CCCGCTCTGCCCTTGGAGAACTGCTAACCTAGGGCTACTGTTGATTTTGACTATCTTCTTAGTGGCCG
AAGCGGAGGGTGCTGCTCAACCAAACAACTCATTAATGCTGCAAACTAGCAAGGAGAATCATGCTTT
AGCTTCAAGCAGTTTATGTATGGATGAAAAACAGATTACACAGAACTACTCGAAAGTACTCGCAGAA
GTTAACACTTCATGGCCTGTAAAGATGGCTACAAATGCTGTGCTTTGTTGCCCTCCTATCGCATTAAG
AAATTTGATCATAATAACATGGGAAATAATCCTGAGAGGCCAGCCTTCCTGCACAAAAGCCTACAAG
AAAGAAACAAATGAGACCAAGGAAACCAACTGTACTGATGAGAGAATAACCTGGGTCTCCAGACCT
GATCAGAATTCGGACCTTCAGATTCGTACCGTGGCCATCACTCATGACGGGTATTACAGATGCATAAT
GGTAACACCTGATGGGAATTTCCATCGTGGATATCACCTCCAAGTGTTAGTTACACCTGAAGTGACCC
TGTTTCAAAACAGGAATAGAACTGCAGTATGCAAGGCAGTTGCAGGGAAGCCAGCTGCGCATATCTC
CTGGATCCCAGAGGGCGATTGTGCCACTAAGCAAGAATACTGGAGCAATGGCACAGTGACTGTTAA
GAGTACATGCCACTGGGAGGTCCACAATGTGTCTACCGTGACCTGCCACGTCTCCCATTTGACTGGC
AACAAGAGTCTGTACATAGAGCTACTTCCTGTTCCAGGTGCCAAAAAATCAGCAAAATTATATATTCC
ATATATCATCCTTACTATTATTATTTTGACCATCGTGGGATTCATTTGGTTGTTGAAAGTCAATGGCTG
CAGAAAATATAAATTGAATAAAACAGAATCTACTCCAGTTGTTGAGGAGGATGAAATGCAGCCCTAT
GCCAGCTACACAGAGAAGAACAATCCTCTCTATGATACTACAAACAAGGTGAAGGCATCTGAGGCAT
TACAAAGTGAAGTTGACACAGACCTCCATACTTTATAA

Supp. 3. Vector maps

Supp. 3.1. Vector map of pMP71

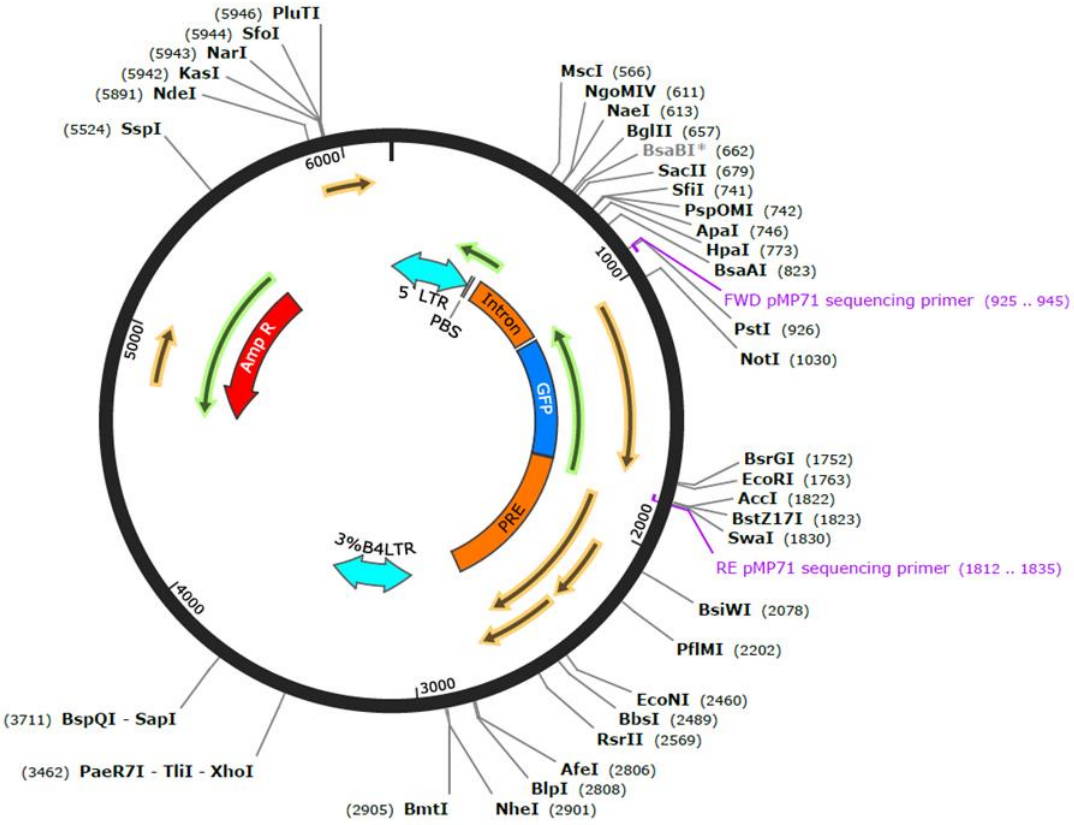

Supplementary figure 1: Vector map of pMP71
CAR constructs were inserted instead of GFP.

Supp. 3.2. Vector map of gag/pol (pcDNA3.1-MLV-g/p)

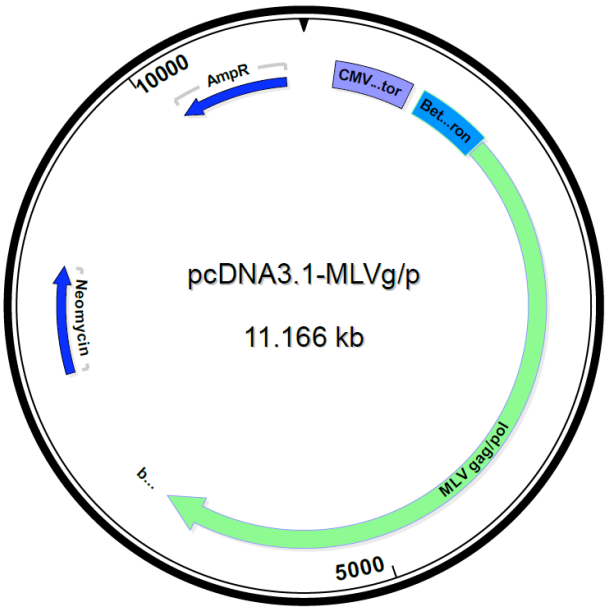

Supplementary figure 2: Vector map of gag/pol (pcDNA3.1-MLV-g/p)

Acknowledgements

First, I like to say thank you to Prof. Dr. Feuchtinger for having me in his work group and for giving me the chance to research in this interesting and important topic. I am very grateful for all of his advices and excellent support.

Further, I would like to express my deep gratitude for Dana Stenger. Thank you for the great support, the many hours spent together on this thesis and the comfort when something didn't work out. Thank you for all the time you provided to teach me how to do things in the lab, to work through my results and to correct this thesis.

I also want to thank my wonderful lab members Dr. Semjon Willier, Tanja Weißer, Nicola Habjan, Dr. Franziska Blaeschke, Dr. Theresa Käuferle, Nadine Stoll, Lena Jablonowski, Annika Peters and Paulina Ferrada Ernst for the great atmosphere in the lab, for many laughers and for all the help and support during the last years.

I am grateful for Julian and Vasil, my two lab partners. A sorrow shared is a sorrow halved.

Moreover, I like to thank all my blood doners, for giving me their blood for my experiments and for trusting in my blood drawing skills.

Additionally, I would like to extend my sincere thanks to Raffaele Conca and Susanne Wullinger for helping with FACS procedure, sorting and for providing all required technical devices.

This work was supported by a doctoral fellowship of the *Bettina Bräu Stiftung*. And I like to express my deep gratitude for the financial support allowing me to focus on this work.

Lastly, I would like to thank my family, my friends and my boyfriend for their emotional support and motivation. I couldn’t write this thesis without you.

Affidavit

Eidesstattliche Versicherung

Mate, Wyona Claire

Name, Vorname

Ich erkläre hiermit an Eides statt, dass ich die vorliegende Dissertation mit dem Titel:

The role of the CD200/CD200 receptor axis on CAR T cells against paediatric acute lymphoblastic B-lineage leukaemia

.

selbständig verfasst, mich außer der angegebenen keiner weiteren Hilfsmittel bedient und alle Erkenntnisse, die aus dem Schrifttum ganz oder annähernd übernommen sind, als solche kenntlich gemacht und nach ihrer Herkunft unter Bezeichnung der Fundstelle einzeln nachgewiesen habe.

Ich erkläre des Weiteren, dass die hier vorgelegte Dissertation nicht in gleicher oder in ähnlicher Form bei einer anderen Stelle zur Erlangung eines akademischen Grades eingereicht wurde.

Heidenheim, 09.12.2025 Wyona Claire Mate

Ort, Datum Unterschrift Wyona Claire Mate